

RECLAMATION

Managing Water in the West

Hexavalent Chromium Treatment Technologies

Research and Development Office
Science and Technology Program
Final Report ST-2018-9085-01



U.S. Department of the Interior
Bureau of Reclamation
Research and Development Office

10/1/2018

Mission Statements

Protecting America's Great Outdoors and Powering Our Future

The Department of the Interior protects and manages the Nation's natural resources and cultural heritage; provides scientific and other information about those resources; and honors its trust responsibilities or special commitments to American Indians, Alaska Natives, and affiliated island communities.

The following form is a Standard form 298, Report Documentation Page. This report was sponsored by the Bureau of Reclamations Research and Development office. For more detailed information about this Report documentation page please contact Miguel Arias-Paic at 303-445-2131. THIS TEXT WILL BE INVISIBLE. IT IS FOR 508 COMPLIANCE OF THE NEXT PAGE.

Disclaimer

Information in this report may not be used for advertising or promotional purposes. The data and findings should not be construed as an endorsement of any product or firm by the Bureau of Reclamation, Department of Interior, or Federal Government. The products evaluated in the report were evaluated for purposes specific to the Bureau of Reclamation mission. Reclamation gives no warranties or guarantees, expressed or implied, for the products evaluated in this report, including merchantability or fitness for a particular purpose.

REPORT DOCUMENTATION PAGE			<i>Form Approved</i> <i>OMB No. 0704-0188</i>	
T1. REPORT DATE: SEPTEMBER 2018		T2. REPORT TYPE: RESEARCH		T3. DATES COVERED
T4. TITLE AND SUBTITLE Hexavalent Chromium Treatment Technologies			5a. CONTRACT NUMBER Z1759, X9085, FA280	
			5b. GRANT NUMBER	
			5c. PROGRAM ELEMENT NUMBER 1541 (S&T)	
6. AUTHOR(S) Julie Korak, Ph.D., P.E. Anthony Kennedy, Ph.D., P.E. Miguel Arias-Paic, Ph.D., P.E.			5d. PROJECT NUMBER ST-2018-0985-01	
			5e. TASK NUMBER	
			5f. WORK UNIT NUMBER 86-68190	
7. PERFORMING ORGANIZATION NAME(S) AND ADDRESS(ES) Miguel Arias-Paic, Water Treatment Group, Technical Service Center, Bureau of Reclamation, mariaspaic@usbr.gov , 303-445-2132			8. PERFORMING ORGANIZATION REPORT NUMBER	
9. SPONSORING / MONITORING AGENCY NAME(S) AND ADDRESS(ES) Research and Development Office U.S. Department of the Interior, Bureau of Reclamation, PO Box 25007, Denver CO 80225-0007			10. SPONSOR/MONITOR'S ACRONYM(S) R&D: Research and Development Office BOR/USBR: Bureau of Reclamation DOI: Department of the Interior	
			11. SPONSOR/MONITOR'S REPORT NUMBER(S) ST-2018-0985-01	
12. DISTRIBUTION / AVAILABILITY STATEMENT Final report can be downloaded from Reclamation's website: https://www.usbr.gov/research/				
13. SUPPLEMENTARY NOTES				
14. ABSTRACT (Maximum 200 words) Naturally occurring hexavalent chromium (Cr(VI)) is found in many groundwaters used as drinking water sources. Depending on concentration and local regulations, contaminant specific water treatment may be needed for potable use. California passed a Cr(VI) regulation in 2014 that was more stringent than the national standard, requiring many decentralized, rural water districts to identify technically feasible and cost-effective solutions. This project investigated two treatment technologies: strong base ion exchange and stannous chloride. For ion exchange, multiple regeneration approaches were tested to determine the impact on regeneration efficiency, waste production and salt use. Waste brine minimization through a hybrid ion exchange – nanofiltration process was developed. Finally, the feasibility of using stannous chloride in a reduction, coagulation, filtration process was evaluated.				
15. SUBJECT TERMS Water treatment, hexavalent chromium, ion exchange, nanofiltration, stannous chloride				
16. SECURITY CLASSIFICATION OF: U			17. LIMITATION OF ABSTRACT U	18. NUMBER OF PAGES 105
a. REPORT U	b. ABSTRACT U	c. THIS PAGE U		
			19b. TELEPHONE NUMBER 303-445-2132	

BUREAU OF RECLAMATION

**Research and Development Office
Science and Technology Program**

Water Treatment Group, 86-68190

Final Report ST-2018-9085-01

Hexavalent Chromium Removal Technologies

Prepared by: Julie Korak, PhD, PE
Assistant Professor, Department of Civil, Environmental and Architectural Engineering
University of Colorado at Boulder

Prepared by: Anthony Kennedy, PhD, PE
Civil Engineer, Water Treatment Group, 86-68190

Checked by / Technical Approval: Miguel Arias-Paic, PhD, PE
Civil Engineer, Water Treatment Group, 86-68190

For Reclamation disseminated reports, a disclaimer is required for final reports and other research products, this language can be found in the peer review policy:

“This information is distributed solely for the purpose of pre-dissemination peer review under applicable information quality guidelines. It has not been formally disseminated by the Bureau of Reclamation. It does not represent and should not be construed to represent Reclamation’s determination or policy.”

Acknowledgements

This work was funded through the Bureau of Reclamation Science and Technology Program for which the project team thanks Yuliana Porras-Mendoza. This project would not have been possible without the support of two water districts, Joshua Basin Water District and City of Norman, who welcomed the installation of pilot equipment, provided in-kind labor to operate treatment systems, and contributed analytical analysis support. At the Joshua Basin Water District, much gratitude is extended to Curt Sauer, Randy Mayes, Randy Little, Steve Corbin, and Bill Kline. At The stannous chloride work was generously supported by the City of Norman, Oklahoma (Chris Mattingly, Geri Wellborn and Rachel Croft) and the Oklahoma-Texas Area Office (Collins Balcombe and Nathan Kuhnert). Lastly, the authors thank Reclamation staff who contributed to both lab and field work – Rick Huggins, Leah Flint, Catherine Hoffman, Matt Hirschbeck, and Dan Gonzalez.

The ion exchange research (Chapter 2 and Chapter 3) was supported by Proposition 50 funding through the California Department of Water Resources (DWR). Many thanks to Robert Thompson, Tallé Lopez, Sophie James, and District Staff at California Water Service; Eugene Leung at the State Water Resources Control Board, Division of Drinking Water; and Steve Giambrone at DWR. We would also like to thank Dr. Chad Seidel, Sarah Plummer, Craig Gorman, and Tarrah Henrie at Corona Environmental Consulting; Dr. Peter Green, Dr. Tom Young, and Nathaniel Homan at the University of California – Davis; and Phil Chandler and Mike Waite at Ionex SG, for contributions to this work.

Acronyms and Abbreviations

ANOVA	Analysis of variance
BV	Bed volume
BV _{avg}	Average bed volume
CA	California
CA-1	California test site 1
CA-2	California test site 2
CaCO ₃	Calcium carbonate
[C _f]	Feed concentration
Cl ₂	Chlorine
CO ₃ ²⁻	Carbonate
CPM	Concentration polarization modulus
[C _p]	Permeate concentration
Cr	Chromium
Cr(III)	Trivalent chromium
Cr(T)	Total chromium
Cr(VI)	Hexavalent chromium
Cr(VI) _t	Hexavalent chromium concentration at time t
Cr(VI) ₀	Initial hexavalent chromium concentration
CrO ₄ ²⁻	Chromate
Cr(OH) ₃ (s)	Chromium hydroxide
Cr ₂ O ₇ ²⁻	Dichromate
DCF	Depth cartridge filter
DI	Deionized water
EDS	Energy dispersive spectroscopy
eqCl ⁻	Equivalents of chloride
eq _{resin}	Equivalents of resin
eq/L	Equivalents per liter
Fe(II)	Ferrous form of iron
Fe(III)	Ferric form of iron
Fe:Cr	Iron to chromium ratio
Fe(OH) ₃ (s)	Ferric hydroxide
GAC	Granular activated carbon
GW	Groundwater
h	Hour
HCl	Hydrochloric acid
HCO ₃	Bicarbonate
HCrO ₄ ⁻	Bichromate
HDPE	High density polyethylene
HLR	Hydraulic loading rate
ICP-AES	Inductively coupled plasma atomic emission spectrometry
ICP-MS	Inductively coupled plasma mass spectrometry
kPa	Kilopascal
L	Liter

L _{H2O}	Liters of water
L _{resin}	Liters of ion exchange resin
L _{waste}	Liters of waste brine
MCL	Maximum contaminant level
meq/L	Milliequivalents per liter
mgd	Million gallons per day
mg/L	Milligrams per liter
min	Minute
mL	Milliliters
MRL	Minimum reporting level
mS/cm	Millisiemens per centimeter
N	Normality
NaCl	Sodium chloride
NaHCO ₃	Sodium bicarbonate
NaOCl	Sodium hypochlorite
Na ₂ SO ₄	Sodium sulfate
ND	Not detected
NF	Nanofiltration
NO ₃	Nitrate
NOM	Natural organic matter
NTU	Nephelometric turbidity units
OK	Oklahoma test site
PCF	Pleated cartridge filter
psi	Pounds per square inch
PVC	Polyvinyl chloride
RCF	Reduction coagulation filtration
Reclamation	Bureau of Reclamation
Rej _{Cl,i}	Rejection of chloride in recovery step <i>i</i>
RO	Reverse osmosis
R _{obs}	Observed membrane rejection
RPD	Relative percent difference
SBA	Strong base ion exchange
SEM	Scanning electron microscope
SnCl ₂	Stannous chloride
Sn(II)	Stannous form of tin
Sn(II):Cr(VI)	Stannous to hexavalent chromium ratio
Sn(IV)	Stannic form of tin
SnO ₂ (s)	Cassiterite
<i>t_i</i>	Total run time in recovery step <i>i</i>
TCLP	Toxicity characteristic leaching procedure
TENORM	Technologically enhanced naturally occurring radioactive material
TMP	Transmembrane pressure
U	Uranium
V	Vanadium
V _{<i>i</i>}	Volume in recovery step <i>i</i>
w/w	Weight percent

WBA	Weak base anion exchange
X_{Cl}	Chloride fraction
$\Delta Cr(VI)$	Change in hexavalent chromium concentration
Δt	Incremental change in time
ΔV	Incremental change in volume
$\mu eq/L$	Microequivalents per liter
μm	Micrometer
$\mu S/cm$	Microsiemens per centimeter

Executive Summary

Hexavalent chromium (Cr(VI)) is present in many groundwater aquifers used as drinking water sources and may be naturally occurring or due to anthropogenic sources. While the US Environmental Protection Agency regulates total chromium (trivalent and hexavalent) concentrations at 100 µg/L, the State of California has set a maximum contaminant level (MCL) for Cr(VI) in drinking water at 10 µg/L. As a result of this new regulation, many drinking water utilities in California now require expanded treatment operations to meet the California MCL. If a nationwide regulation is implemented, it is anticipated that thousands of entry points in public water systems would require additional treatment (Seidel and Corwin, 2013) at a cost of \$0.5-\$5.1 billion per year (Seidel et al., 2013).

Strong base anion exchange is effective for Cr(VI) removal, but efficient resin regeneration and waste minimization are important for operational, economic and environmental considerations. This study compared multiple regeneration methods on pilot-scale columns based on regeneration efficiency, waste production and salt usage. A conventional 1-Stage regeneration using 2 N sodium chloride (NaCl) was compared to 1) a 2-Stage process with 0.2 N NaCl followed by 2 N NaCl and 2) a mixed regenerant solution with 2 N NaCl and 0.2 N sodium bicarbonate. All methods eluted similar cumulative amounts of chromium with 2 N NaCl. The 2-Stage process eluted an additional 20-30% of chromium in the 0.2 N fraction, but total resin capacity is unaffected if this fraction is recycled to the ion exchange headworks. The 2-Stage approach selectively eluted bicarbonate and sulfate with 0.2 N NaCl before regeneration using 2 N NaCl. Regeneration approach impacted the elution efficiency of both uranium and vanadium. Regeneration without co-eluting sulfate and bicarbonate led to incomplete uranium elution and potential formation of insoluble uranium hydroxides that could lead to long-term resin fouling, decreased capacity and render the resin a low-level radioactive solid waste. Partial vanadium elution occurred during regeneration due to co-eluting sulfate suppressing vanadium release. Waste production and salt usage were comparable for the 1- and 2-Stage regeneration processes with similar operational setpoints with respect to chromium or nitrate elution.

Managing waste brine from strong base anion exchange processes used for Cr(VI) removal is an important operational, environmental and economic consideration. This study investigated the use of nanofiltration to recover excess regenerant salt and reduce the waste volume using brine collected from full-scale and pilot-scale installations. Using a 2 N NaCl regeneration solution, divalent anions (i.e., sulfate and chromate) exhibited high rejections (>0.97), and monovalent anions (i.e., chloride and nitrate) exhibited low to negative rejections (-0.2 to 0.05), allowing preferential passage of excess regenerant salt. A batch concentration model was developed for a case study. Waste can be concentrated to 0.6 BV and a significant fraction of the regenerant salt can be recovered. This process would require about 20 m² of membrane area per 1000 L of resin to treat waste in 8 hours, which could be implemented in a mobile treatment unit serving multiple decentralized systems.

While strong base anion exchange is an established best available technology, alternative processes for Cr(VI) removal from drinking water continue to be of interest for utilities due to economic considerations. Stannous chloride (SnCl₂) can reduce Cr(VI) to trivalent chromium, but research has been limited, especially related to the filterability of total chromium (Cr(T))

following reduction. At the pilot scale, SnCl_2 was tested over a range of doses in three groundwaters with naturally occurring Cr(VI) concentrations ranging from 0.020 to 0.090 mg/L. Stannous chloride was found to be effective as a reductant at doses <2 mg/L and contact times <5 min. A tin-to-chromium molar dose ratio of 4 was sufficient for reducing Cr(VI) to below 0.010 mg/L. Cartridge filters were unable to practically remove Cr(T) following reduction, but a standard-design sand filter was able to remove Cr(T) to <0.010 mg/L.

In summary, this project investigated three different treatment technologies to make Cr(VI) more efficient, more effective and cheaper. Improving the efficiency and cost of Cr(VI) is integral for continued of water resources containing Cr(VI). Alternative regeneration approaches can improve resin regeneration by ensuring the complete recovery of trace metals, such as uranium and vanadium. The disposal costs for ion exchange waste brine can be significantly reduced by integrating nanofiltration to reduce waste volume and recover unused regenerant. Finally, alternative reduction-coagulation-filtration using stannous chloride is conceptually a promising technology, but additional work is needed to optimize filtration and understand the fate of tin and chromium in distribution system.

Contents

Acknowledgements.....	v
Acronyms and Abbreviations	vi
Executive Summary	ix
Chapter 1. Introduction.....	9
Chapter 2. Regeneration of Pilot-Scale Columns.....	10
Introduction.....	10
Materials and Methods.....	11
Column Regeneration	14
Batch Regeneration	15
Analytical Methods	15
Mass Balance Assumptions	16
Results.....	16
Raw water quality and column loading	16
Three regeneration approaches	17
Discussion.....	21
Elution efficiency	22
Salt use and waste production	29
Waste production	30
Conclusions.....	30
Chapter 3. Nanofiltration for Waste Brine Management	31
Introduction.....	31
Methods/Materials	33
Waste Brine Generation, Collection and Fractionation	33
Nanofiltration of SBA Waste Brine	35
Sampling and Analytical Methods	37
Results and Discussion	37
Brine characterization	37
Nanofiltration of SBA Regeneration Waste	39
Empirical Relationships	42
Modeling Batch Concentration of Regeneration Brine	44
Feasibility of nanofiltration: Resin regeneration case study	46
Conclusions.....	49
Chapter 4. Chromium removal by Stannous Chloride	51
Introduction.....	51
Materials and Method	53
Waters	53
Pilot Setup and Operation	54
Water quality analysis	55
Microscopy	56
Chlorination	56
Results and Discussion	57
Stannous chloride dose response	57
Cartridge filtration	61

Sand Filtration	65
Trivalent Chromium Reoxidation	67
Conclusions.....	68
Chapter 5. References.....	72

Tables

Table 2.1. Raw water quality analysis for influent samples collected during run	13
Table 2.2. Summary of regeneration approaches conducted on three pilot scale columns on consecutive loading cycles	14
Table 2.3 Comparison of regeneration processes in terms of chromium, uranium and nitrate elution, salt requirements and waste produced.	23
Table 3.1 Operating parameters for the full-scale and pilot-scale SBA treatment plants	33
Table 3.2. Regeneration and nanofiltration operating parameters for the full-scale and pilot-scale SBA processes used to produce brines A-C	34
Table 3.3. Initial and final brine composition.....	38
Table 4.1. Average raw water quality	54
Table 4.2. Cr(VI) concentrations after SnCl ₂ reduction followed by contact with free chlorine for 3 to 4 days	68
Table 4.3. Qualitative summary of testing.....	68
Table A 1. Distribution of Anionic Equivalents relative to total resin capacity for regenerations R1 and R3	A-2
Table A 2. Cumulative elution of chromium, vanadium and uranium during regeneration.....	A-11

Figures

Figure 2.1. Process flow diagram of pilot-scale ion exchange process.	12
Figure 2.2. Hexavalent chromium breakthrough for the first loading cycle.....	17
Figure 2.3. Elution profile from the 1-Stage DI (R1) regeneration and 2-Stage DI (R3) regeneration	18
Figure 2.4. Elution profile from the NaCl/NaHCO ₃ regeneration (R5)	21
Figure 2.5 Comparison of elution curves for a) chromium, b) pH and c) nitrate for all regeneration approaches.....	24
Figure 2.6. Chromium peak aligned chromatograms for uranium and vanadium (top row) and sulfate and bicarbonate (bottom row) for each regeneration approach.....	27
Figure 3.1. Chromium and conductivity regeneration elution profiles and composite brine fractions used for nanofiltration experiments.....	35
Figure 3.2. Schematic of nanofiltration system	36
Figure 3.3. Temperature corrected flux and brine conductivity as a function of water recovery.....	39
Figure 3.4. Nanofiltration membrane rejection as a function of water recovery or flux.	40
Figure 3.5. Empirical relationships for flux and chloride rejection.....	43
Figure 3.6. Verification of batch nanofiltration model for Brine B.....	46
Figure 3.7 Case study coupling nanofiltration with resin regeneration	48
Figure 4.1. Pilot testing schematic.....	54
Figure 4.2. Dissolved Cr(VI) and Cr(T) concentrations in reduced samples after contact with SnCl ₂	58
Figure 4.3. Dissolved Cr(VI) concentrations after contact with SnCl ₂ for all three waters as function of MDR.....	59
Figure 4.4. SEM images of filters tested with OK at SnCl ₂ doses ranging from 1.5 to 1.8 mg/L.....	61
Figure 4.5. Raw, reduced, and filtered Cr(T) and Cr(VI) concentrations during low HLR DCF testing.....	63
Figure 4.6. Raw, reduced, and filtered Cr(T) and Cr(VI) concentrations during high HLR DCF testing.....	64
Figure 4.7. Raw, reduced, and filtered Cr(T) and Sn(T) concentrations during sand filtration testing.....	66
Figure A 1. Elution chromatograph for 1-Stage DI regeneration (R1).....	A-3
Figure A 2. Elution chromatograph for 1-Stage GW regeneration (R4)	A-4
Figure A 3. Elution chromatograph for 2-Stage DI regeneration (R3).....	A-5
Figure A 4. Elution chromatograph for 2-Stage GW regeneration (R6)	A-6
Figure A 5. Elution chromatograph for 2-Stage regeneration (R2) approach	A-7
Figure A 6. Elution chromatograph for NaCl/NaHCO ₃ regeneration (R5)	A-8
Figure A 7. Cumulative mass eluted as a function of regeneration bed volume	A-9
Figure A 8. Fraction of constituents remaining on resin aliquots after the 1 st cycle	A-10
Figure A 9. Cr(VI) breakthrough during second loading cycle.....	A-11

Figure B 1. SEM image of 0.45 μm filter used to filter raw OK.....	B-1
Figure B 2. EDS spectrum for solids depicted in Figure 4b and 4c in main manuscript.....	B-1
Figure B 3. Cutout of a 20 μm PCF filter after testing with OK.	B-2
Figure B 4. Cutout of a 5 μm DCF filter after testing with CA-1.	B-2

Chapter 1. Introduction

Hexavalent chromium (Cr(VI)) is a widely studied drinking water constituent, present naturally in many groundwaters at concentrations ranging from <0.001 up to 0.2 mg/L (Kotaś and Stasicka, 2000; McNeill et al., 2012; Seidel and Corwin, 2013). Hexavalent chromium does not have a specific maximum contaminant level (MCL) regulated by the US Environmental Protection Agency (USEPA), but it is regulated as part of the total chromium (Cr(T)) MCL of 0.100 mg/L. As an area of high occurrence and national focus for Cr(VI) in drinking water (Seidel and Corwin, 2013), California was the only state to specifically regulate Cr(VI) at an MCL of 0.010 mg/L. As a result, most Cr(VI) research targets 0.010 mg/L or lower for treated water. Despite the California MCL recently being rescinded (SWRCB, 2017), there is a continued national interest among utilities to address Cr(VI) in drinking water, especially with ongoing toxicological reviews by USEPA and a requirement to develop a new California MCL (SWRCB, 2017; USEPA, 2014). If a nationwide regulation is implemented, it is anticipated that thousands of entry points in public water systems would require additional treatment (Seidel and Corwin, 2013) at a cost of \$0.5-\$5.1 billion per year (Seidel et al., 2013).

The state-level regulation in California disproportionately affects decentralize, rural water systems that rely on a network of groundwater wells to meet water demands. To implement Cr(VI) treatment, most utilities would have to install treatment systems at each point of entry to the distribution system, further intensifying the economic and operational considerations for compliance. Several treatment technologies have been identified for Cr(VI) treatment, including strong base anion exchange (SBA), weak base anion exchange (WBA), reverse osmosis (RO), and reduction-coagulation-filtration (RCF), each of which have unique benefits and limitations.

This project partnered with two water districts, one in California and one in Oklahoma, to improve process efficiency and reduce cost. In California, a pilot-scale SBA process was installed at one of the system points of entry. Columns with SBA resin were loaded until exhausted for chromium, at which point they were sent back to Bureau of Reclamation (Reclamation) for regeneration and waste minimization process development. A pilot-scale study of stannous chloride RCF was conducted at two wells in California and one well in Oklahoma.

All the results from this project have been published in peer-reviewed journals. This report is divided into three main chapters, where each chapter is a stand-alone study and a reprint of the published articles. The effect of regeneration approach on process efficiency is investigated in Chapter 2. Using brine from the pilot-scale processes and from a full-scale plant, waste minimization using nanofiltration was evaluated in Chapter 3. Finally, the stannous chloride RCF pilot study is presented in Chapter 4.

Chapter 2. Regeneration of Pilot-Scale Columns

This chapter is a reprint of the following peer-reviewed journal article:

Korak, J. A., Huggins, R., & Arias-Paic, M. (2017). Regeneration of pilot-scale ion exchange columns for hexavalent chromium removal. *Water Research*, 118, 141–151.

Introduction

Hexavalent chromium (Cr(VI)) is present in many groundwater aquifers used as drinking water sources and may be naturally occurring or due to anthropogenic sources (Ball and Izbicki, 2004; Seidel and Corwin, 2013). While the US Environmental Protection Agency (USEPA) regulates total chromium (trivalent and hexavalent) concentrations at 100 mg/L, the State of California has set a maximum contaminant level (MCL) for Cr(VI) in drinking water at 10 mg/L. As a result of this new regulation, many drinking water utilities in California now require expanded treatment operations to meet the California MCL. If a nationwide regulation is implemented, it is anticipated that thousands of entry points in public water systems would require additional treatment (Seidel and Corwin, 2013) at a cost of \$0.5-\$5.1 billion per year (Seidel et al., 2013).

Strong base anion exchange (SBA) is one treatment technology that is effective for removing Cr(VI) (Gorman et al., 2016; Li et al., 2016a; McGuire et al., 2006; Seidel et al., 2013; Sengupta and Clifford, 1986a, 1986b). SBA uses an inert polymeric resin activated with surface and interstitial exchangeable functional groups, such as quaternary amines. For a chloride regenerated SBA resin, sulfate, bicarbonate, nitrate, and other anions with greater affinity for the resin functional groups exchange with chloride based on ion selectivity in ratios that maintain charge balance in the system. Divalent anions are generally more selective than monovalent anions (Clifford and Weber, 1983; Subramonian and Clifford, 1988). Additional transformations can occur within the pore structure; weak acids, such as bicarbonate (HCO_3^-), can deprotonate to form a more selective multivalent anion (Horn and Clifford, 1997; Zhang and Clifford, 1994).

Resin exhaustion is operationally-defined based on contaminants of concern and process configuration. In a single pass system, the threshold for Cr(VI) exhaustion may occur when the effluent concentration exceeds a pre-defined concentration either from an individual contactor or the blended effluent from several contactors (e.g., 8 mg/L or 80% of the California MCL). In a lead-lag configuration, the lead (i.e., first) contactor is fully loaded with Cr(VI) at exhaustion, and a second contactor in series (i.e., lag) captures Cr(VI) in the effluent of the lead unit. Upon exhaustion, SBA resin can be regenerated using a concentrated salt solution. In the case of Cr(VI) processes, this waste brine is hazardous, and disposal represents a major operating cost.

Currently, there are two regeneration approaches implemented at full-scale plants. One approach uses a single regenerant solution concentration, while the second uses a staged approach with multiple regenerant solution concentrations. The multi-stage approach includes strategically increasing the regenerant concentration to first elute sulfate and bicarbonate followed by chromium and nitrate (Waite, 2015). While implemented at the full-scale, little

information exists to objectively compare the regeneration approaches to make informed decisions about optimal process operation. At the bench- and pilot-scale, previous work has investigated using sodium bicarbonate in lieu of sodium chloride as an alternative regeneration approach (Li et al., 2016b), but mixed regenerant solutions have not been investigated.

Regeneration efficiency, waste production and salt usage are primary factors governing SBA selection for full-scale treatment of drinking water, but little research has focused on the regeneration efficiency of chromium treatment. In most studies, only chromate, sulfate and/or nitratedata is presented (Li et al., 2016a; Sengupta et al., 1988). The impacts of treatment and regeneration on other trace metals (e.g., uranium, vanadium, arsenic, molybdenum) has not been investigated. An evaluation of regeneration efficiency for chromium and other trace metals, waste production and salt usage is needed to evaluate current approaches and provide a basis for future innovation. The objective of this study was to regenerate parallel loaded pilot-scale SBA columns for drinking water Cr(VI) removal using different regeneration approaches and compare performance in terms of 1) total constituent elution, 2) waste production and 3) regenerant salt requirements.

Materials and Methods

Column Loading

Groundwater from a well in California with naturally-occurring Cr(VI) at concentrations above the California regulatory MCL was used as the source water for the pilot-scale SBA columns (Figure 2.1). Three columns (2 inch diameter polyvinylchloride) were operated in parallel to produce loaded resins of similar exchanger phase composition. Figure 2.1 includes a process flow diagram. Each column was loaded with 2 L of Purolite A600E/9149 resin, which is a Type I quaternary amine, gel polystyrene resin crosslinked with divinyl- benzene and has a minimum capacity of 1.6 eq/L. Columns were operated at a loading rate of 8 gpm/ft² (325 L/min/m²). Samples were collected 2-3 times per week from each column effluent and analyzed for Cr(VI). Columns were operated until full exhaustion with respect to Cr(VI), when equal influent and effluent concentrations were measured. Column pressures, flows and bed height were recorded 3-4 times per week, and flows were adjusted as needed to maintain a constant loading rate.

Hexavalent Chromium Treatment Technologies

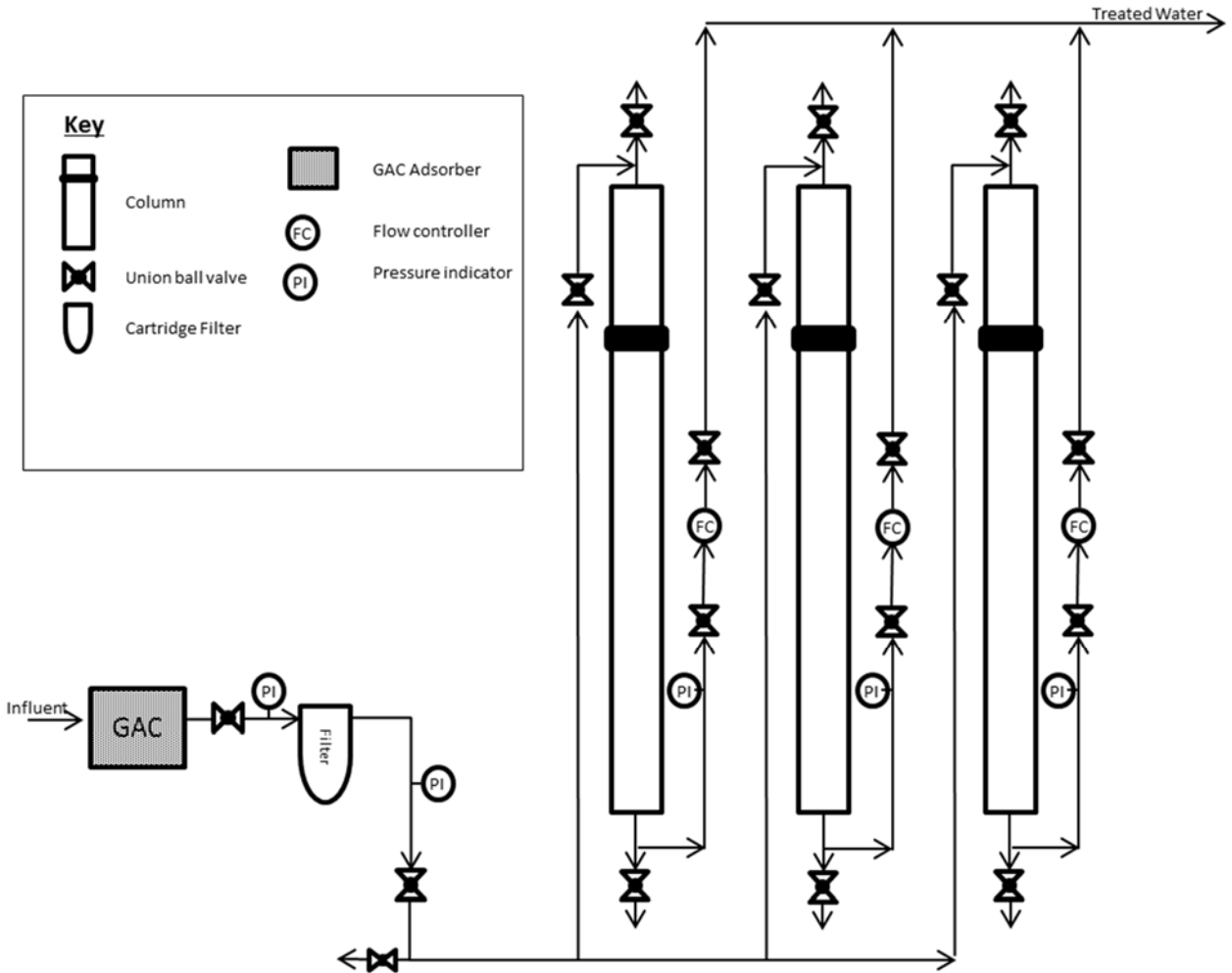


Figure 2.1. Process flow diagram of pilot-scale ion exchange process.

Table 2.1. Raw water quality analysis for influent samples collected during run (n=3). Values reported as Average \pm Standard Deviation, and values below the MRL are reported as ND.

Category	Parameter	Units	Value	MRL	Method
Wet Chemistry	Alkalinity, Total	mg/L as CaCO ₃	94.0 \pm 3.5	5	SM 2320B
	Bicarbonate	mg/L	116.7 \pm 5.8	5	SM 2320B
	Carbonate	mg/L	ND	5	SM 2320B
	Chloride	mg/L	8.0 \pm 0.9	1	EPA 300.0
	Cyanide	μ g/L	ND	100	SM4500CNF
	Specific conductance	μ mhos/cm	240.0 \pm 0	2	SM 2510B
	Fluoride	mg/L	0.6 \pm 0	0.1	EPA 300.0
	Hydroxide	mg/L	ND	5	SM 2320B
	MBAS (LAS Mole Wt. 340)	mg/L	ND	0.1	SM 5540C
	Nitrate as N	mg/L	2.9 \pm 0.1	0.4	EPA 300.0
	Nitrate + Nitrite (as N)	mg/L	2.9 \pm 0.1	0.4	EPA 300.0
	Nitrite as N	mg/L	ND	0.4	EPA 300.0
	Perchlorate	μ g/L	ND	4	EPA 314.0
	pH	SU	8.0 \pm 0.2	0	SM 4500 HB
	Sulfate	mg/L	8.2 \pm 0.5	0.5	EPA 300.0
	TDS	mg/L	146.7 \pm 5.8	5	SM 2540C
TOC	mg/L	ND	0.3	SM 5310B	
Metals	Aluminum	μ g/L	ND	50	EPA 200.7
	Antimony	μ g/L	ND	6	SM 3113B
	Arsenic	μ g/L	5.2 \pm 0.3	2	SM 3113B
	Barium	μ g/L	ND	100	EPA 200.7
	Beryllium	μ g/L	ND	1	EPA 200.7
	Boron	μ g/L	ND	100	EPA 200.7
	Cadmium	μ g/L	ND	1	EPA 200.7
	Calcium	mg/L	11.7 \pm 1.2	1	EPA 200.7
	Chromium (+6)	μ g/L	40	1	EPA 218.6
	Chromium (Total)	μ g/L	39.7 \pm 2.3	10	EPA 200.7
	Copper	μ g/L	ND	50	EPA 200.7
	Iron	μ g/L	ND	100	EPA 200.7
	Lead	μ g/L	ND	5	SM 3113B
	Magnesium	mg/L	1.5 \pm 0.1	1	EPA 200.7
	Manganese	μ g/L	ND	20	EPA 200.7
	Mercury	μ g/L	ND	1	EPA 245.1
	Molybdenum	μ g/L	ND	10	EPA 200.7
	Nickel	μ g/L	ND	10	EPA 200.7
	Potassium	mg/L	1.5 \pm 0.2	1	EPA 200.7
	Selenium	μ g/L	ND	5	SM 3113B
	Silver	μ g/L	ND	10	EPA 200.7
Sodium	mg/L	39.3 \pm 1.5	1	EPA 200.7	
Thallium	μ g/L	ND	1	EPA 200.9	
Vanadium	μ g/L	28.7 \pm 4.7	3	EPA 200.9	
Zinc	μ g/L	ND	50	EPA 200.7	
Calculated Values	Hardness (Total)	mg/L	35.3 \pm 2.3		—
	Total Anions	meq/L	2.5 \pm 0.11		—
	Total Cations	meq/L	2.5 \pm 0.05		—
Uranium	Uranium	pCi/L	ND	1	EPA 908.0

Column Regeneration

After the first water treatment loading cycle, the columns were regenerated following three approaches. As summarized in Table 2.2, the first regeneration method using Column 1 applied a single sodium chloride (NaCl) concentration of 2 N NaCl (1-Stage). The second regeneration method applied to Column 3 used two concentrations of NaCl, 0.2 N NaCl followed by 2 N NaCl (2-Stage). Column 2 was regenerated with a modified 2-Stage approach but was not fully characterized. Deionized water (DI) with a resistivity of at least 16 M Ω -cm was used as the background water for regenerations R1-R3. After regeneration, the columns were put back in service and loaded to Cr(VI) exhaustion. In the second regeneration cycle, Columns 1 and 3 were regenerated with a 1-Stage and 2-Stage approach, respectively. Column 2 was regenerated with a 2 N NaCl brine followed by a mixed 2 N NaCl with 0.2 N sodium bicarbonate (NaHCO₃) brine. The second regeneration cycle used softened well water from the pilot site. Analytical grade NaCl and NaHCO₃ were used in all regeneration tests.

Table 2.2. Summary of regeneration approaches conducted on three pilot scale columns on consecutive loading cycles

Regen. Number	Cycle	Column	Stage 1		Stage 2		Description
			Regenerant	BV	Regenerant	BV	
R1	1	1	2 N NaCl	4	--	--	1-Stage DI
R2 ¹	1	2	0.4 NaCl 0.1 NaCl	1 6	2 N NaCl	2	2-Stage Modified
R3	1	3	0.2 N NaCl	7	2 N NaCl	2	2-Stage DI
R4	2	1	2 N NaCl	4	--	--	1-Stage GW
R5	2	2	2 N NaCl	1.25	2 N NaCl + 0.2 N NaHCO ₃	2.75	NaCl/NaHCO ₃
R6	2	3	0.2 N NaCl	4	2 N NaCl	4	2-Stage GW

DI: Deionized water
 GW: Softened raw groundwater from pilot study site
¹Regeneration R2 was only analyzed for uranium elution and is only presented for context when interpreting the second regeneration cycle of Column 2 (R5)

Each regeneration process was conducted co-current to flow during water treatment. Regeneration loading rate was $49 \pm 4 \text{ L/min/m}^3$ ($0.37 \pm 0.03 \text{ gpm/ft}^3$). The nominal bed volumes of brine used in each regeneration are summarized in Table 1. Actual regenerant solution contact is calculated using elution data and presented in the results section.

During regeneration, effluent from the column was fractionated into high density polyethylene bottles between 250 and 1000 mL depending on required elution resolution. Small sample bottles were used for dynamic segments of the regeneration to better define elution peaks (e.g. initial increase of conductivity after interstitial water is displaced). By collecting entire fractions rather than grab samples, a mass balance could be performed with minimal data interpolation. The mass and volume of each fraction was measured, and the average bed volume (BV_{avg}) was calculated for each fraction collected. BV_{avg} is defined as the average cumulative volume of the fraction divided by the resin bed volume. For example, if a fractionated sample

was collected between 1 L and 1.5 L of cumulative elution from a 2 L resin bed, the BV_{avg} of that fraction would be 0.625 (i.e., average quantity of 1.5 L and 1 L divided by 2 L of resin). The term bed volume (BV) will be used to describe a normalized solution volume relative to resin volume, irrespective of the regeneration elution sequence. BV_{avg} will only be used in the context of the regeneration elution profile regarding the timing of the elution profile.

After the second regeneration cycle, the columns were regenerated with analytical grade hydrochloric acid (HCl) to evaluate the elution efficiency of trace metals. Following manufacturer recommendations, three BVs of 6% (w/w) HCl was prepared. Upon elution of the first HCl BV, the pump was turned off. After a 2 h HCl soaking period, the final 2 bed volumes were eluted from the column before rinsing.

Batch Regeneration

For the first regeneration cycle, aliquots of resin were collected from the top, middle and bottom of the loaded columns and re-generated as a batch experiment to determine the spatial profile of constituents throughout the resin bed. 10 mL resin samples were added to 250 mL Erlenmeyer flasks with 200 mL of 2 N NaCl and agitated for about 70 h. All regenerant solutions were made using DI. A strainer was used to separate the resin from the supernatant, and the supernatant was analyzed for trace metals, sulfate, nitrate and alkalinity.

Analytical Methods

During column loading, raw water quality was monitored using standard methods listed in Table 2.1. Column effluent samples were collected about every 2500 BV to monitor Cr(VI) breakthrough and analyzed using EPA Method 218.6. During regeneration, samples were analyzed for conductivity and pH (HQ40d, Hach, Loveland, CO). Meters were calibrated daily. Total, carbonate and bicarbonate alkalinity was determined using sulfuric acid titration following Standard Method 2320. It was assumed that bicarbonate alkalinity was representative of bicarbonate concentrations, and other alkalinity contributors were negligible.

A suite of elements in the regeneration brine were measured using inductively coupled plasma mass spectrometry (ICP-MS) (7500, Agilent, Santa Clara, CA). Samples were acidified with nitric acid prior to analysis and diluted as needed with 1% nitric acid based on the instrument calibration range. The instrument was calibrated with a multi-element solution (SPEX CertiPrep 2A) between 0.1 mg/L and 1 mg/L and with a chloride standard (Hach, 1000 mg/L as Cl) from 1 mg/L to 200 mg/L. Duplicates and matrix spikes were analyzed every 10 samples, and a NIST 1643f standard was used to verify the calibration curve. In the regeneration brine, total chromium was analyzed as a surrogate for Cr(VI). Negligible concentrations of trivalent chromium were measured in the raw water, and reduction reactions during ion exchange were assumed to be negligible. Total elemental chlorine was used as a surrogate for chloride as no other common sources of elemental chlorine (e.g., perchlorate) were measured in the source water. The average relative percent difference (RPD) between duplicate samples was 2.0% for elemental sodium, chlorine, chromium and uranium. Matrix spike recoveries for chromium and uranium were within an acceptable range (85-109% and 89-97%, respectively).

Nitrate was analyzed using flow injection analysis (QuikChem Method 10-107-04-1-A). The average RPD between nitrate duplicates was 11% (< 0.2 mg-N/L, n = 14), and matrix spike

recoveries ranged from 83 to 111%. Sulfate was also analyzed by flow injection analysis (QuikChem Method 10-116-10-1-A). The average RPD for sulfate duplicates was 5%, and matrix spike recovery ranged from 74 to 101% (n = 11).

Mass Balance Assumptions

To facilitate mass balance calculations during regeneration, several assumptions were made regarding the anionic form of constituents in the exchanger phase. For elements measured by ICP-MS that have a propensity to form oxyanions in aqueous systems, anionic forms were assumed based on oxidation state and pH. It was assumed that the oxidized form would be most abundant since more than 97% of chromium was found in the oxidized, hexavalent form. At a pH of 8, chromium is present as predominantly chromate (CrO_4^{2-}) (Sengupta and Clifford, 1986a). Comparing the reduction potential of chromate with other oxyanions, it would be expected that vanadium, arsenic, selenium, molybdenum and uranium would also be found in an oxidized state. Despite non-detection in the raw water (Table 2.1), selenium, molybdenum and uranium accumulated on the resin and resulted in significant concentrations in the regeneration waste due to the high affinity and high water throughput until chromium exhaustion. The most abundant form of vanadium in oxic groundwater was assumed to be the monovalent oxyanion vanadate (H_2VO_4^-) (Wright et al., 2014). Arsenic and selenium were assumed to be present as divalent arsenate (HAsO_4^{2-}) and selenate (SeO_4^{2-}), respectively (Bissen et al., 2003; Horng and Clifford, 1997; White and Dubrovsky, 1994). Molybdenum was assumed to be present as molybdate (MoO_4^{2-}). Uranium was assumed to be present in its most selective and stable form as a uranyl carbonate complex ($\text{UO}_2(\text{CO}_3)_3^{4-}$) (Langmuir, 1978; Zhang and Clifford, 1994).

The form of polyprotic anions and polynuclear metals within the exchanger phase were also assumed. Although found predominantly as bicarbonate at pH 8 in groundwater, bicarbonate (HCO_3^-) has been shown to deprotonate to form a more selective carbonate (CO_3^{2-}) divalent anion within the resin, increasing the relative selectivity to chromate (Horng and Clifford, 1997). Vanadium may also be present as a divalent anion (HVO_4^{2-}) or polynuclear complex ($\text{HV}_2\text{O}_7^{3-}$) in the exchanger phase (Horng and Clifford, 1997; Rice, 1983). For the purpose of calculations, only the monovalent forms (i.e., HCO_3^- and H_2VO_4^-) were assumed. Chromium and molybdenum can form polynuclear complexes (i.e., $\text{Cr}_2\text{O}_7^{2-}$ and $\text{Mo}_7\text{O}_{24}^{6-}$) within the exchanger phase, but these polynuclear forms were assumed to be absent for mass balance calculations due to the alkaline operating pH (Sengupta, 1986).

Natural organic matter (NOM) can compete in SBA processes due to the negative surface charge of humic substances (Thurman, 1985) but was assumed to be absent for mass balance purposes. Total organic carbon was not detected in the raw water entering the SBA columns (Method Reporting Limit (MRL) = 0.3 mg/L). The majority of NOM present in the groundwater was likely removed by the granular activated carbon pre-filter, which also removed any free chlorine residual from normal well operations. The insignificant effect of NOM is confirmed in Appendix A.

Results

Raw water quality and column loading

The source water for the pilot-scale SBA columns was an operational groundwater well at a municipal water district in California that has Cr(VI) concentrations of 40 mg/L as

summarized in Table 2.1, which is above the California MCL. More than 97% of the total chromium in the raw water was measured as the Cr(VI) form based on paired samples where hexavalent and total chromium were both quantified.

Columns were fully exhausted around 50,000 BV with respect to Cr(VI). Loading until exhaustion is representative of an ion ex-change process operating in a lead-lag configuration. Figure 2.2 shows consistent breakthrough of Cr(VI) from all three columns. The California MCL for Cr(VI) of 10 mg/L was exceeded at $36,000 \pm 850$ BV.

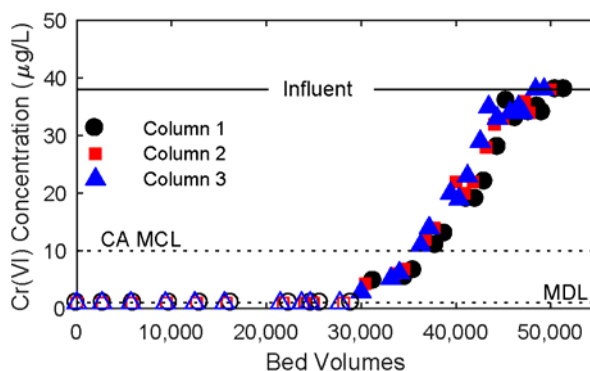


Figure 2.2. Hexavalent chromium breakthrough for the first loading cycle. Dashed lines indicate California (CA) MCL for Cr(VI) and method detection level (MDL). Unfilled markers indicate samples measured at the MDL

The observed run-time is significantly longer than reported data from other studies using the same resin and is due to different concentrations of competing anions (i.e., sulfate). One pilot study with half as much raw water Cr(VI) 0.61-0.65 meq/L (16-17 mg/L) exceeded the California MCL at a similar throughput (30,000-35,000 BV), a difference that can be attributed to higher raw water sulfate concentrations around 0.42 eq/L (20 mg/L) (Seidel et al., 2014). Another pilot study using a raw water with half as much Cr(VI) (0.65 meq/L, 17 mg/L) but six times as much sulfate (1.0 eq/L, 48 mg/L) reached the California MCL at about 13,000 BV (Gorman et al., 2016). These results demonstrate that SBA is well-suited to treat this raw water due to reduced competition from sulfate compared to other reported studies.

Three regeneration approaches

1-Stage regenerations

The 1-Stage regeneration process was designed to model a conventional SBA regeneration process with NaCl at a constant concentration (2 N NaCl). This regeneration was performed on Column 1 after each loading cycle (Table 2.2, Regenerations R1 and R4). In the first regeneration (R1), deionized water used as the background regenerant solution (1-Stage DI), whereas the second cycle (R4) used softened raw water (1-Stage GW).

The elution profiles for regenerations R1 and R4 are shown in Figure 2.3a-d, Figure A 1, and Figure A 2. A mass balance between chloride exchange (Figure 2.3b) and anions eluted (Figure 2.3c) was in good agreement (3% difference) and found that 79% of the active sites exchanged during regeneration. Details are provided in Appendix A. Figure 2.3c illustrates the chromatographic elution of major anions for regeneration R1. Sulfate and bicarbonate began

eluting from the column as soon as it was contacted with regenerant solution ($0.66 \text{ BV}_{\text{avg}}$). Sulfate concentrations peaked around $1.1 \text{ BV}_{\text{avg}}$ and tailed off by $1.9 \text{ BV}_{\text{avg}}$. Bicarbonate and chromium concentrations peaked around $1.4 \text{ BV}_{\text{avg}}$ and tailed off by $2 \text{ BV}_{\text{avg}}$. Nitrate exhibited a broader elution peak centered near $1.9 \text{ BV}_{\text{avg}}$. Without additional data between 2.5 and $4 \text{ BV}_{\text{avg}}$, it is difficult to assess the true breadth of the nitrate elution peak for regeneration R1. Uranium co-eluted with chromium and bicarbonate with a peak between 1.25 and $1.4 \text{ BV}_{\text{avg}}$ and a peak fraction concentration of 1.5 meq/L (92 mg/L). Elution of other trace metals (i.e., arsenic, molybdenum and selenium) is provided in Figure A 1.

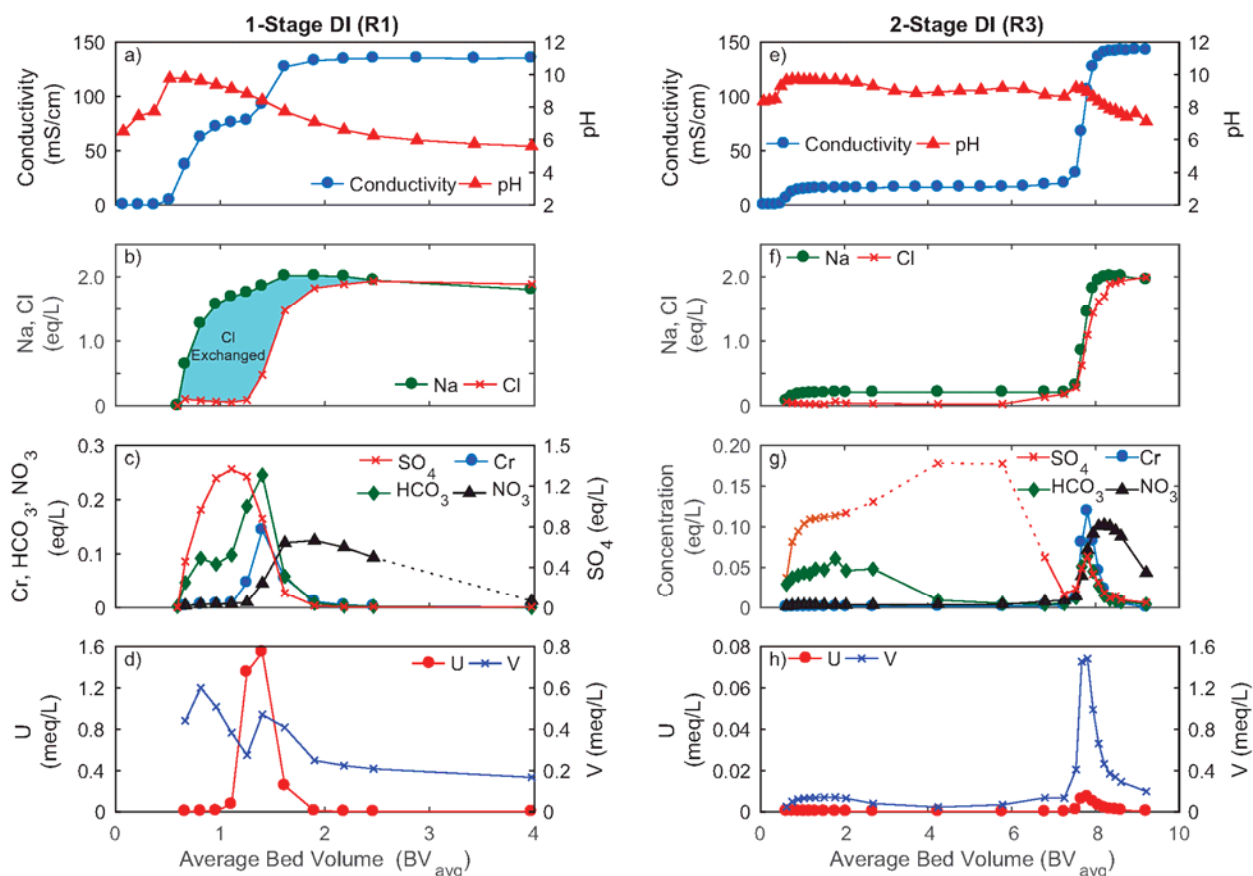


Figure 2.3. Elution profile from the 1-Stage DI (R1) regeneration and 2-Stage DI (R3) regeneration represented as conductivity and pH (a, e), sodium and chloride (b, f), sulfate, bicarbonate, chromium and nitrate (c, g) and uranium and vanadium (d, h). Dashed lines for nitrate and sulfate indicate analysis of non-consecutive sample fractions.

The effects of selectivity reversal on elution order are apparent comparing Figure 2.3c to typical monovalent and divalent selectivity (chromate > sulfate > nitrate > chloride > bicarbonate) in low ionic strength groundwater (Clifford and Weber, 1983). Figure 2.3c, however, shows that nitrate elutes after sulfate. At high ionic strengths, selectivity reversal shifts resin selectivity to favor monovalent an-ions (e.g., nitrate) over divalent anions (Boari et al., 1974). In resin regeneration for nitrate removal, sulfate elutes first and more efficiently than nitrate (Guter, 1995). The retardation of nitrate can also be due its hydrophobic character coupled with the hydrophobicity of the exchanger phase (Clifford and Weber, 1983), which has divinylbenzene crosslinking. The co-elution of bicarbonate and sulfate may also be due to acid-

base reactions, where more selective carbonate molecules present in the exchanger phase have a selectivity similar to sulfate and protonate when released into the bulk solution (Horng and Clifford, 1997). pH increased (Figure 2.3a) as bicarbonate and carbonate eluted from the resin indicating protonation of weak acids in the regeneration solution.

In both regenerations (R1 and R4), the bed volumes of solution required for complete regeneration is governed by nitrate rather than chromium elution. Using sodium as a conservative tracer, a mass balance was used to calculate the total volume of regenerant solution eluted from the column at complete nitrate elution. For the 1-Stage DI regeneration (R1), 3.2 BVs of regenerant solution were passed through the column corresponding to samples collected up to 4 BV_{avg} of total liquid elution (initial interstitial volume plus regenerant solution). In the 1-Stage GW regeneration (R4), additional bed volumes of regenerant solution were used to ensure complete elution, but only data up until complete nitrate elution are shown. To manage leakage and potential chromatographic peaking during the water treatment cycle, complete nitrate elution was defined as effluent concentrations less than 2% of the peak concentration. For regeneration R4, nitrate elution was complete at 4.7 BV_{avg}, which equated to 3.4 BV of regenerant solution (Figure A 2). A mass balance between chloride and other anions was calculated to confirm that the column tests agree with batch tests, and no significant constituents were missing from the analytical suite (Appendix A).

2-Stage regenerations

The 2-Stage regeneration process exposed the resin to a low strength stage with 0.2 N NaCl (0.2 N Stage) followed by a high strength stage with 2 N NaCl (2 N Stage) to control the elution of constituents based on selectivity. This regeneration was performed on Column 3 after each loading cycle (Table 2.2, Regenerations R3 and R6). In regeneration R6, the volume of the 0.2 N Stage was decreased from a nominal 7 BV to 4 BV, and the volume of the high strength stage was increased from 2 BV to 4 BV for complete nitrate elution. The elution profiles for the 2-Stage DI (R3) and 2-Stage GW (R6) regenerations are presented in Figure 2.3e-h and Figure A 4, respectively.

Focusing on the 2-Stage DI regeneration (Figure 2.3e-h), the 0.2 N Stage primarily eluted sulfate, bicarbonate, arsenic, and some vanadium from the resin, and these constituents exhibited elution peaks in the low strength stage. Sulfate concentrations peaked between 4.25 and 5.75 BV_{avg} (Figure 2.3g), but non-consecutive fractions were analyzed (indicated by the dashed line). Chromium and nitrate exhibited increases in concentration throughout this stage. Chromium concentrations increased monotonically from 0.78 meq/L (20 mg/L) at 0.9 BV_{avg} to 2.9 meq/L (75 mg/L) at the end of the stage (7.2 BV_{avg}). A similar trend was observed for nitrate with concentrations increasing monotonically from 2.9 meq/L (40.7 mg-N/L) to 9.1 meq/L (127 mg-N/L) for the same BV_{avg} range. Uranium concentrations were below the method reporting limit (0.1 mg/L). Some vanadium eluted during the 0.2 N Stage shown in Figure 2.3h.

By the end of 0.2 N Stage in regeneration R3, the concentration of both sulfate and bicarbonate decreased, indicating that elution was not limited by the number of 0.2 N bed volumes. Simultaneously, chloride concentrations in the effluent increased eventually equaling sodium concentrations at 7.25 BV_{avg}, prior to the 2 N Stage transition. The increase in eluted chloride at the end of the 0.2 N Stage indicated that active sites in the exchanger phase reached

an equilibrium with respect to major anions (i.e., sulfate, bicarbonate), and chloride in the regenerant solution was not limiting. The 2-Stage GW regeneration (R6), differed by decreasing the bed volumes used in the 0.2 N Stage. As a result, sulfate exchange was not complete before transitioning to the 2 N Stage (Figure A 4).

The 2 N Stage eluted chromium, nitrate, vanadium, molybdenum and some uranium from the column. The delayed elution of nitrate compared to chromium, vanadium and uranium demonstrated selectivity reversal and/or retardation similar to the 1-Stage regenerations. Uranium elution differed between the two 2-Stage regenerations (R3 and R6). In the 2-Stage DI regeneration (R3), the maximum uranium fraction concentration was only 7.2 meq/L (0.4 mg/L) at 7.8 BV_{avg} (Figure 2.3h). In the 2-Stage GW regeneration (R6), the maximum uranium fraction concentration was 2 meq/L (122 mg/L) at 4.9 BV_{avg} (Figure A 4). To confirm the absence of a significant uranium peak in regeneration R3, samples were reanalyzed in the 2 N Stage brine at a lower dilution factor (lower detection limit) and were in good agreement (RPD < 10%). Uranium was also analyzed from regeneration R2 (Table 2.2, Figure A 5), which followed a similar approach, affirming the low uranium concentrations in regeneration R3.

By sodium mass balance, regeneration R3 exposed the resin to a total of 6.7 BV of 0.2 N NaCl followed by 1.6 BV of 2 N NaCl. Complete nitrate elution was not observed in regeneration R3. Regeneration R6 exposed the resin to 3.9 BV of 0.2 N NaCl followed by 3.6 BV of 2 N NaCl for complete nitrate elution.

1-Stage NaCl with NaHCO₃ addition

Based on the elution results from the first regeneration cycle, a hybrid regeneration approach was conducted on Column 2 (Table 2.2, Regeneration R5), which included 2 N NaCl followed by 2 N NaCl buffered with 0.2 N NaHCO₃. The elution profiles for this regeneration are presented in Figure 2.4 and Figure A 6. Up until the addition of NaHCO₃, the elution profiles are similar to those observed during 1-Stage regeneration. Addition of NaHCO₃ increased pH and eluted additional chromium, uranium and vanadium (Figure 2.4). The peak vanadium concentration observed with NaHCO₃ was greater than any regeneration that only used NaCl (Figure 2.4c). At complete nitrate elution, the resin was exposed to 1.1 BV of 2 N NaCl and 2.5 BV of 2 N NaCl/0.2 N NaHCO₃.

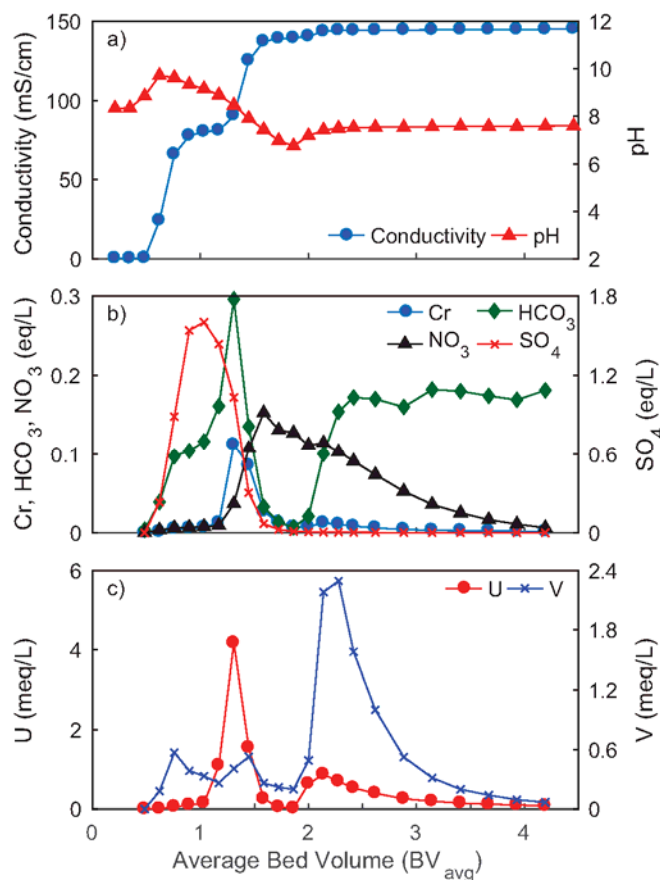


Figure 2.4. Elution profile from the NaCl/NaHCO₃ regeneration (R5) represented as a) conductivity and pH, b) sulfate, bicarbonate, chromium and nitrate and c) uranium and vanadium.

Discussion

The differences between regeneration approaches were evaluated by comparing constituent elution efficiency, salt chemical requirements, and waste production. Elution efficiency was evaluated based on cumulative mass recovery, peak sharpness, and the presence of tailing, all of which impact overall process performance. Salt use directly compares regeneration chemical consumption. Waste volume is directly related to operating costs (Jensen and Darby, 2016).

To minimize waste in full-scale regeneration processes, the leading and tail edge of the regeneration are often recycled to the SBA process headworks or secondary holding tanks for use in a subsequent regeneration cycle. To allow for comparison between regeneration approaches, standard operating criteria were assumed. Under these criteria, brine at the beginning of regeneration with a conductivity less than 20 mS/cm would be recycled to the SBA process headworks and would not require disposal. This fraction would include the 0.2 N Stage in the 2-Stage approaches and leading edge in the 1-Stage and NaCl/NaHCO₃ approaches. An additional criterion on the tail end of the regeneration sequence assumed that once the effluent chromium concentration equaled 5 meq/L (~130 mg/L), the process would switch to rinse water. This concentration is less than 5% of the maximum measured chromium concentration. At this point,

it was assumed that 0.5 BV of the relevant brine was still present in the interstitial pore space (~50% porosity). This volume was included in the salt dose and waste calculations. It was also assumed that an additional 1 BV of rinse water would require disposal and was included in the waste calculations.

Elution efficiency

Chromium elution efficiency

For total chromium elution, the 2-Stage approaches eluted more chromium, but the mass in the waste fraction was similar between all approaches. Within each regeneration cycle, the 2-Stage regeneration approaches eluted 20-30% more chromium than the 1-Stage approaches (i.e., R1 vs R3 and R4 vs R6) (Table 2.3, Figure A 7). Cumulative chromium elution from the NaCl/NaHCO₃ regeneration (R5) was similar to the 1-Stage regenerations. The increased total recovery of chromium during the 2-Stage regenerations was attributed to the elution that occurred during the 0.2 N Stage, not increased removal efficiency during the 2 N Stage. From a system mass balance perspective, the impact of the increased chromium elution using the 2-Stage approach depends on the fate of the brine produced during the 0.2 N Stage. Some full-scale implementations of 2-Stage regeneration recycle the 0.2 N brine to the SBA process headworks over the water treatment cycle. Under this approach, capacity for chromium could decrease as the influent sulfate and chromate concentrations increase. The impact of recycling brine to the SBA headworks on influent concentrations depends on the recycle rate. If the 0.2 N brine produced were recycled back to the headworks and bled in over 20,000 BV, the influent sulfate concentration would increase 26% or 16% for the R3 and R6 regenerations, respectively. Influent chromate concentration would increase 29% or 12% for the R3 or R6 regenerations, respectively. Therefore, the benefit of increased chromium removal during the 2-Stage regeneration approach could be limited by recycling the chromium and sulfate during the subsequent treatment cycle due to the inverse relationship between influent sulfate concentration and throughput to chromium breakthrough (Gorman et al., 2016).

Table 2.3 Comparison of regeneration processes in terms of chromium, uranium and nitrate elution, salt requirements and waste produced.

Regen. Number	Approach	Stage	Duration (BV _{avg})		Contaminant Elution				Salt Dose		Waste Produced	
			Start	Stop	Cr	NO ₃	U	V	eq _{Cl-} /L _{resin}	g _{NaCl} / (1000 L _{H2O}) ⁽¹⁾	BV	L _{waste} / (1000 L _{H2O}) ⁽¹⁾
					(g/L _{resin})		(mg/L _{resin})					
R1	1-Stage	--	0.59	2.2	1.3	6.7	30	⁽²⁾	4.0	4.6	3.1	0.06
R3	2-Stage	0.2 N ⁽³⁾	0	7.1	0.23	1.7	0.06	32	1.4	1.6	8.6	0.17
		2.0 N ⁽⁴⁾	7.1	8.6	1.4	6.1	0.23	47	3.0	3.5	3.1	0.06
		Total	0	8.6	1.6	7.8	0.3	78	4.4	5.2	--	--
R4	1-Stage	--	0.50	2.0	1.0	7.3	50	26	3.7	4.4	3.0	0.06
R5	NaCl/ NaHCO ₃	--	0.60	2.8	1.2	10	92	87	5.1	5.9	3.7	0.07
R6	2-Stage	0.2 N ⁽³⁾	0	4.4	0.08	0.9	0.22	13	0.8	0.9	5.9	0.12
		2.0 N ⁽⁴⁾	4.4	5.7	1.3	4.5	47	29	2.7	3.2	2.7	0.05
		Total	0	5.7	1.3	5.4	48	42	3.5	4.1	--	--

(1) Treated water volume (L_{H2O}) assumes throughput of 50,000 BV (resin exhausted for chromium)

(2) Not calculated

(3) Stage transitions to 2 N Stage with no rinse water

(5) Salt dose includes extra 0.5 BV of interstitial brine at 2 N. Waste calculation includes 0.5 BV of interstitial brine plus 1 BV of rinse water.

Using the conductivity and effluent chromium concentration criteria as process setpoints to define the waste fraction, all regeneration approaches exhibited little difference in chromium elution when exposed to 2 N NaCl (Table 2.3). Fig. 4 illustrates that the peak height and breadth of the chromium elution peak were similar between approaches. If chromium elution under 2 N NaCl ultimately governs the net mass of chromium removed from the system, this metric did not favor selecting one regeneration approach over another.

Hexavalent Chromium Treatment Technologies

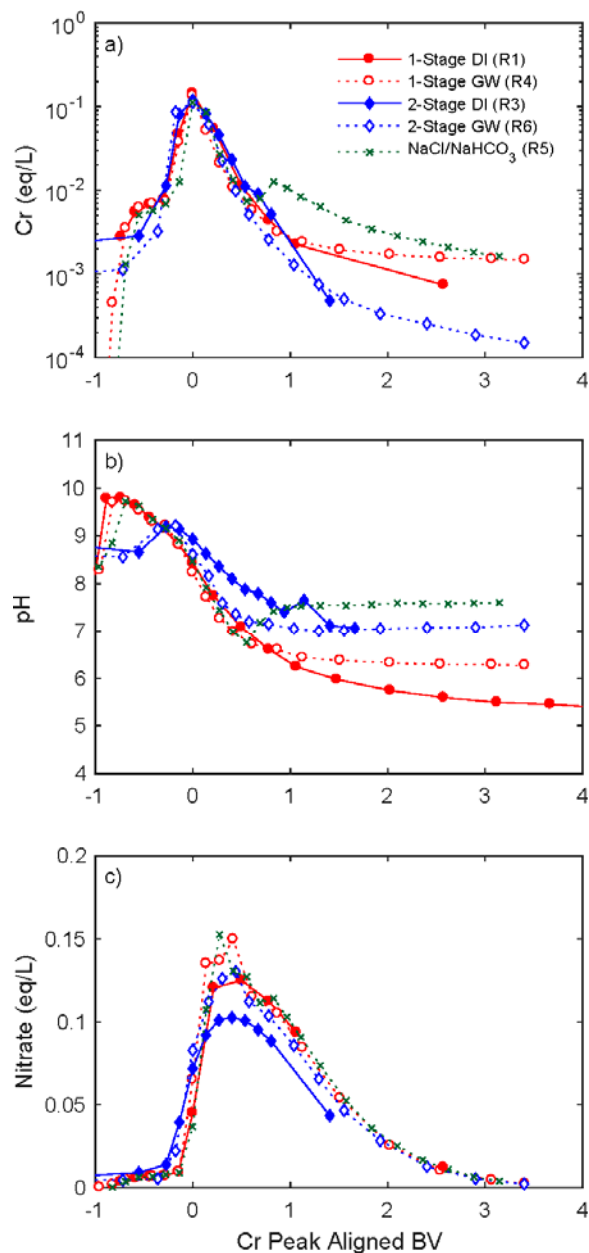


Figure 2.5 Comparison of elution curves for a) chromium, b) pH and c) nitrate for all regeneration approaches. Bed volumes are plotted with chromium elution peaks aligned.

A significant difference between regeneration approaches, however, was the presence of effluent chromium concentration tailing. Since the effluent chromium concentration is a direct indication of residual chromium in the exchanger phase, tailing is indicative of inefficient regeneration at the end of the cycle. Fig. 4a highlights the differences in tailing and shows that the 1-Stage (R1 and R4) and NaHCO_3 (R5) regenerations exhibited tailing where effluent concentrations decreased asymptotically. Differences in chromium elution efficiency were confirmed by batch regeneration tests conducted on resin aliquots removed from the column after the first regeneration cycle. Figure A 8a shows that more chromium remained at the bottom of the resin bed post-regeneration for 1-Stage DI (R1) compared to 2-Stage DI (R3).

Comparing the 1-Stage (R1 and R4) and 2-Stage (R3 and R6) regenerations, differences in pH may explain some of the differences in elution efficiency at the end of the regeneration cycle. After the elution of bicarbonate, pH decreased through the remainder of the regeneration process. One BV_{avg} after peak chromium elution, the pH values in the 2-Stage regenerations were 0.5-1 unit higher than the 1-Stage regenerations (Figure 2.5b). While using softened groundwater (R4) led to systematically higher pH values at the end of regeneration, the background alkalinity was not sufficient to prevent pH decreases relative to the raw water (pH=8) due to alkalinity uptake by the resin.

In both 1-Stage regenerations, the effluent pH dropped below 6.5. This transition from alkaline to acidic pH has multiple impacts on ion exchange mechanisms. Under acidic conditions, the Cr(VI) speciation in the bulk liquid phase shifts from chromate to bichromate ($HCrO_4^-$). In the exchanger phase, however, the formation of dichromate ($Cr_2O_7^{2-}$) through the dimerization of bichromate is favored, because the selectivity of dichromate is greater than that of bichromate (Sengupta, 1988, 1986). Dichromate will occupy half the number of exchange sites at acidic pH and decrease the fraction of active sites occupied in the exchanger phase without changing the total mass of Cr(VI). Not only does the selectivity for Cr(VI) increase at acidic pH, but the nature of the Cr(VI)-chloride isotherm also changes from favorable at alkaline pH to unfavorable at acidic pH (Sengupta, 1986). Regeneration is more difficult at low pH using NaCl alone, because regeneration now requires two steps: deprotonation by a hydroxide ion followed by chloride ion exchange (Sengupta, 1988). For this reason, regeneration of SBA resin operated under acidic conditions often uses caustic soda and NaCl during regeneration (Sengupta, 1995).

The NaCl/ $NaHCO_3$ regeneration (R5) demonstrates that pH is not the only factor impacting chromium elution. Upon $NaHCO_3$ addition, pH increased to 7.5, which was greater than the effluent pH in the 2-Stage regenerations. After an initial increase, effluent chromium concentrations also exhibited tailing. At 3 BV_{avg} after peak chromium elution (Figure 2.5a), the effluent chromium concentration in the NaCl/ $NaHCO_3$ regeneration was 20 times higher than the 2-Stage GW (R6) regeneration at the same point. Therefore, additional factors other than pH impact chromium tailing and warrant further investigation for regeneration optimization.

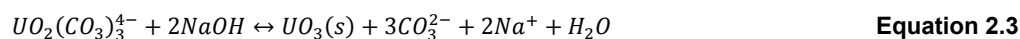
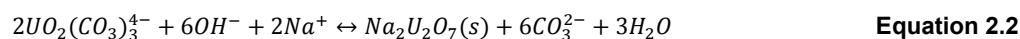
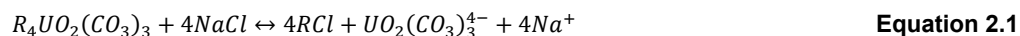
A key difference in elution efficiency between approaches was the location of residual chromium in the exchanger phase. Residual chromium at the bottom of the column can cause leakage during the next loading cycle, which was observed for Column 1 (Figure A 9). For the 2-Stage approach, the 20-30% of additional chromium that eluted in the 0.2 N Stage would be recycled to the headworks, exchange with the resin due to its high selectivity, but likely not have a significant impact on the throughput to chromium saturation compared to the 1-Stage approach (neglecting the effects of increased sulfate concentration). The 0.2 N Stage recycled chromium, however, would be reloaded on the top of the column and be less prone to leakage.

Uranium elution efficiency

Regeneration approach impacted the elution efficiency of uranium. To compare regeneration efficiency, only select regeneration profiles could be compared directly, because the elution efficiency of the first regeneration cycle (R1-R3) directly impacted the initial exchanger phase uranium concentration for the second loading cycle (R4-R6).

Comparing the first cycle, the 1-Stage DI (R1) removed 100 times more uranium than the 2-Stage DI (R3) approach. Previous work has shown that uranium regeneration depends on both the regenerant solution concentration and total salt dose, but these factors cannot explain differences in uranium elution efficiency. At the same total salt dose ($\text{eq}_{\text{Cl}}/\text{eq}_{\text{resin}}$), previous work has shown that more uranium is eluted at higher salt concentrations (Clifford and Zhang, 1995; Zhang and Clifford, 1994). Over the entire 1-Stage DI regeneration (Figure 2.3a-d), the resin was exposed to a total of $3.3 \text{ eq}_{\text{Cl}}/\text{eq}_{\text{resin}}$. The uranium elution peak tailed off by $1.9 \text{ BV}_{\text{avg}}$, at which point the column had been exposed to only an excess of $0.65 \text{ eq}_{\text{Cl}}/\text{eq}_{\text{resin}}$ with a maximum concentration of 1.8 eq/L chloride. Peak uranium removal preceded complete chloride breakthrough in the column. During the 2 N Stage of the 2-Stage DI (R3) regeneration, the column was exposed to an excess of $1.2 \text{ eq}_{\text{Cl}}/\text{eq}_{\text{resin}}$ at concentrations greater than 1.9 eq/L , yet negligible uranium elution was observed. Therefore, a difference in uranium regeneration efficiency could not be accounted for by chloride dose or concentration.

Differences in uranium regeneration efficiency are partially attributed to bicarbonate concentrations. In the 1-Stage regeneration, uranium concentrations peaked at $1.4 \text{ BV}_{\text{avg}}$ with a concomitant bicarbonate concentration of 0.25 eq/L . In the 2-Stage regeneration approach, the mobile phase was depleted in bicarbonate during the 2 N Stage. Peak uranium elution occurred at $7.8 \text{ BV}_{\text{avg}}$ at which point chromate was the most abundant counterion (0.12 eq/L) other than chloride (1.1 eq/L). The bicarbonate concentrations never exceeded (0.06 eq/L) in the 2 N Stage. Previous work investigating the hydrometallurgical processes to concentrate and purify uranium has recognized the importance of carbonate in the regenerant to prevent the hydrolysis and precipitation of uranium (Hollis, 1958; Streat and Naden, 1987). As a general guideline, Streat and Naden (1987) suggests that sodium carbonate concentrations around 0.1 M are needed to prevent hydrolysis and precipitation of uranium complexes. The mechanisms are summarized in Equation 2.1 to Equation 2.3 from Clifford and Zhang (1995). The uranyl carbonate complex can be displaced (Equation 2.1) by chloride during regeneration. At high pH or low carbonate concentrations, the equilibrium shifts to form solid sodium pyrouanate or uranium oxide while liberating carbonate (Equation 2.2 and Equation 2.3). Compared to the 1-Stage approach, the 2-Stage DI (R3) had a higher pH (Figure 2.3e) accompanied by lower peak bicarbonate concentrations (Figure 2.6c-d), which may have promoted precipitate formation.



Differences in sulfate may also play a role in the stability of uranyl complexes. At peak uranium elution during the 1-Stage DI regeneration (R1) shown in Figure 2.6a-b, sulfate was the most abundant counterion in the mobile phase (0.88 eq/L) compared to chloride (0.48 eq/L). In comparison, the 2-Stage DI regenerant solution (R3) was relatively depleted in sulfate (0.06 eq/L) at peak uranium elution shown in Figure 2.6c-d. Uranyl ions can also form sulfate complexes (e.g., $\text{UO}_2(\text{SO}_4)_3^{4-}$), although the stability constants for uranyl sulfate complexes in bulk solutions are many orders of magnitude lower than those of uranyl carbonate complexes (Zhang and Clifford, 1994). Given the high exchanger phase sulfate concentration prior to regeneration (Table A 1), it is possible that some uranyl sulfate complexes may also be present in the exchanger phase. Gu et al. (2005) has shown that sulfate concentrations can play an

important role in uranium recovery during regeneration using synthetic groundwater (Gu et al., 2005). Similar to uranyl carbonate, uranyl sulfate complex instability may also promote the formation of insoluble uranium oxides, preventing uranium recovery during regeneration.

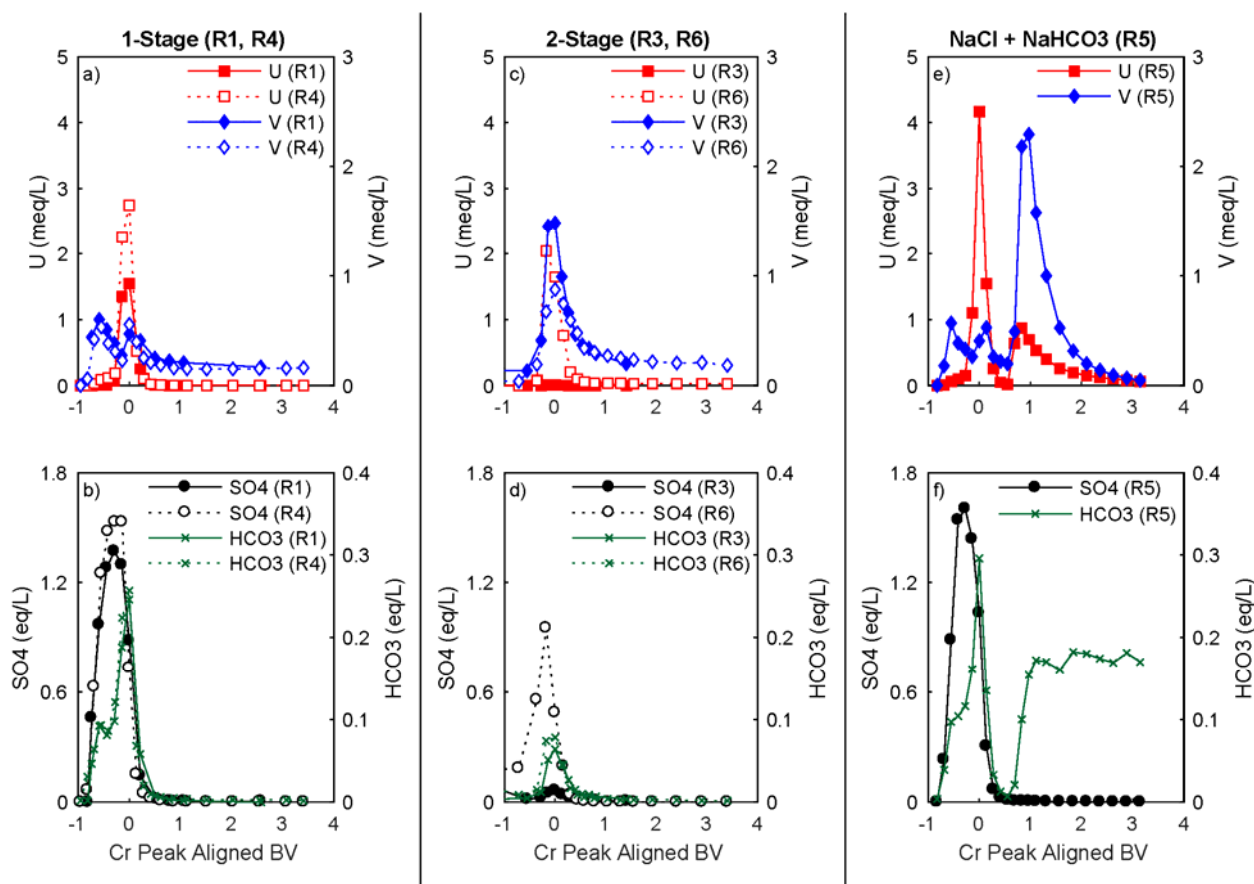


Figure 2.6. Chromium peak aligned chromatograms for uranium and vanadium (top row) and sulfate and bicarbonate (bottom row) for each regeneration approach. The regeneration cycle is differentiated as 1st regeneration (solid) and 2nd regeneration (dashed) in a-d.

For the second round of column regenerations, care must be taken in directly comparing the total mass of uranium eluted as R5 and R6 had a higher starting mass of uranium due to inefficient elution in the first cycle, and the availability of the uranium to be eluted by NaCl is unknown. Coupled with the acid regeneration performed after the second regeneration cycle, uranium elution trends emerge. The 2-Stage GW regeneration (R6) exhibited significant cumulative elution of uranium (1.8 meq), which is nearly 200 times more than the first regeneration cycle (2-Stage DI (R3)). Since the 0.2 N Stage removed most of the bicarbonate (Figure 2.3e-h), stabilization of uranyl complexes depends on either background alkalinity in the groundwater or sulfate. At peak uranium elution for regeneration R6, the bicarbonate concentration was 0.07 eq/L, which is similar in magnitude to the concentrations observed in the 2-Stage DI regeneration (R3) and cannot explain the increased uranium elution in regeneration R6. Therefore, the difference can be attributed to the higher sulfate concentrations co-eluting with uranium during the 2-Stage GW regeneration (R6). Since the length of the 0.2 N Stage was shortened by nominally 3 BV in the 2-Stage GW regeneration (R6), complete elution of sulfate

did not occur leading to a greater sulfate peak (0.95 eq/L) in the 2 N Stage. These results affirm that sulfate concentrations play an important role in uranium elution from ion exchange columns with high initial sulfate concentrations in the exchanger phase.

The NaCl/NaHCO₃ regeneration (R5) reveals that uranium elution is incomplete under the two other regeneration approaches that only use NaCl. In regeneration R5, the first uranium peak concentration occurred concurrently with the chromium peak and was greater than other regenerations, which may be attributed to higher initial uranium concentrations on the resin. With the introduction of NaHCO₃, additional uranium eluted from the resin (Figure 2.6e), demonstrating residual uranium remained after regeneration with NaCl alone. Regeneration with HCl elutes uranium as a uranyl cation and is a common regeneration method in hydro-metallurgy (Streat and Naden, 1987). Of the total mass of uranium eluted during both NaCl and HCl regenerations, 35-40% of the total recoverable uranium eluted by HCl (Table A 2) indicating significant residual uranium was left after NaCl regeneration for chromium removal.

Incomplete uranium elution may impact the resin capacity, disposal, subsequent regenerations and plant licensing requirements. Uranium could accumulate in the resin with each regeneration. Over time, entrained uranium precipitate could foul resin, reducing capacity during water treatment operations and requiring more frequent regeneration. Uranium accumulation could result in a plant requiring U.S. Nuclear Regulatory Commission licensing and resin that must be handled and disposed of as technologically enhanced naturally occurring radioactive materials (TENORM).

Vanadium elution efficiency

Regeneration approach also impacted the elution of vanadium from SBA resin. While not regulated by the Safe Drinking Water Act, accumulation of vanadium through multiple loading cycles may also impact long-term operation of SBA for Cr(VI) removal.

During regeneration with only NaCl, multiple vanadium elution peaks indicate that either 1) vanadium moieties with different relative selectivities eluted from the resin and/or 2) the co-elution of other anions impacted vanadium elution. In the 2-Stage NaCl regenerations, vanadium eluted during both the 0.2 N and 2 N Stages (Figure 2.3h) suggesting different relative selectivities of moieties. Two elution peaks were observed during the 1-Stage and NaCl/NaHCO₃ regenerations spanning either side of the sulfate elution peak. The impact of sulfate is discussed below. In the NaCl/NaHCO₃ regeneration, an additional and more concentrated vanadium peak was observed when a higher NaHCO₃ concentration was present (Figure 2.6e-f). Significant tailing in vanadium elution was also observed indicating inefficient recovery during regeneration (Figure 2.3d, h, Figure A 2 to Figure A 4).

Regeneration approaches with NaCl alone did not completely elute vanadium from the resin. Batch tests conducted after the first regeneration cycle recovered additional vanadium, specifically from the middle and lower column sections (Figure A 8). Acid regeneration following the second cycle eluted 25-30% of the total recovered vanadium (Table A 2).

Insight into this behavior can be garnered from studies investigating the separation of uranium and vanadium from low-grade uranium ores, such as carnotite (K₂(UO₂)₂(VO₄)₂·3H₂O) (Bailes, 1957; Ghorbani and Montenegro, 2016). In carbonate leachates from carnotite,

vanadium exhibits a higher selectivity for SBA resins than uranium (Kaufman and Lower, 1954). At high concentrations, vanadium can undergo polymerization reactions similar to chromium to form anions with a greater charge, such as $\text{HV}_2\text{O}_7^{3-}$, $\text{V}_3\text{O}_9^{3-}$, and $\text{V}_6\text{O}_{17}^{4-}$ (Rice, 1983). While predominantly present as H_2VO_4^- in the raw groundwater, more selective forms through deprotonation (HVO_4^{2-}) or polymerization ($\text{HV}_2\text{O}_7^{3-}$) in the exchanger phase can explain the multiple elution peaks in the 2-Stage regenerations.

Incomplete elution of vanadium can be attributed to sulfate suppression. The 2-Stage DI (R3) regeneration exhibited a vanadium elution peak with the highest concentration compared to the other NaCl-only regeneration approaches (Figure 2.6a, c, e). During this regeneration, co-eluting sulfate concentrations were also the lowest. One method for selectively eluting uranium over vanadium from SBA resins is by ammonium sulfate (Bailes et al., 1958). While poorly characterized, Bailes et al. (1958) suggests that vanadium elutes but converts to a sulfate complex and is re-adsorbed. In the same method, sodium carbonate is used to elute vanadium and any residual uranium for complete regeneration. The appearance of two vanadium peaks during the 1-Stage regeneration (Figure 2.6a) may actually be the suppression of a single peak by sulfate. Only a single vanadium peak was observed during the 2 N Stage of the 2-Stage (R3) approach (Figure 2.6c), where sulfate concentrations were significantly lower. The efficiency of carbonate to elute vanadium is evident in the NaCl/NaHCO₃ regeneration approach (Figure 2.6e-f). Table A 2 shows that the NaCl/NaHCO₃ left less residual vanadium on the resin as indicated by the lower fraction recovered by acid regeneration. The absence of vanadium elution after sulfate elution suggests that sodium chloride alone is not sufficient for complete vanadium regeneration.

While not radioactive, accumulation of vanadium on resin could impact long-term operation of SBA processes for chromium removal. Regeneration approaches tailored to vanadium and uranium elution may be periodically required to maintain long-term performance.

Salt use and waste production

Salt use

Differences in total salt use were largely governed by the chromium elution tailing, because the assumed operational setpoint to start the rinse cycle was an effluent chromium concentration of 5 meq/L. The salt requirements for the 1-Stage GW (R4) and 2-Stage GW (R6) regenerations were similar at 3.7 and 3.5 eq_{Cl}-/L_{resin}, respectively, as summarized in Table 2.2. These regenerations are the most comparable, because each improves upon disadvantages identified in the first regeneration cycle. Use of softened water maintained a higher pH in the effluent for the 1-Stage approach, and a shortened 0.2 N Stage in the 2-Stage approach improved uranium elution. The salt requirement for the NaCl/NaHCO₃ regeneration was greatest due to the second chromium peak and prominent tailing. While the chromium elution peak height and width were similar between all regeneration methods, the regenerant volume needed to reach this 5 meq/L setpoint varied up to 0.2 BV, which accounts for much of the variation in salt requirements. In the NaCl only regenerations, the chromium setpoint was triggered 0.6-0.8 BV after peak chromium elution. The 2-Stage GW regeneration (R6) exhibited the least chromium tailing and required the least salt to conduct regeneration (Table 2.3).

Defining an operational regeneration setpoint with respect to chromium would leave significant nitrate on the resin. With an assumed 0.5 BV of brine remaining in the bed pore space, nitrate elution would continue until about 1.1 BV-1.3 BV after peak chromium elution. At this point, 20-30% of the total nitrate would be left on the resin. Little difference in nitrate elution was observed between methods (Figure 2.5c). If complete nitrate elution is a regeneration objective, salt requirements would increase compared to Table 2.3, but there would be little difference between regeneration approaches.

Waste production

With the exception of the NaCl/NaHCO₃ regeneration (R5), there was little difference in waste production between approaches. The 1-Stage regenerations produced 3.1 BV and 3.0 BV of waste for regenerations R1 and R4, respectively (Table 2.3). If the 0.2 N Stage waste is recycled to the headworks, only the 2 N Stage and rinse water constitutes the waste volume for the 2-Stage approaches. Regenerations R3 and R6 generated 3.1 BV and 2.7 BV of waste, respectively. Due to prolonged chromium elution, the NaCl/NaHCO₃ regeneration generated 3.7 BV of waste. If the regeneration duration is governed by nitrate elution, the waste volume would increase compared to Table 2.3, but there would be little difference between regeneration approaches.

Conclusions

1-Stage and 2-Stage regeneration approaches with 2 N NaCl have trade-offs primarily associated with uranium, vanadium and chromium regeneration efficiency rather than waste production or salt use. Little difference was observed in the chromium elution efficiency using a 2 N NaCl regenerant solution, resulting in similar waste volumes and salt requirements. Tailing effects for chromium elution can be significant for 1-Stage co-current regeneration approaches and can promote leakage during the subsequent water treatment (loading) cycle. Uranium elution efficiency is improved by the co-elution of both bicarbonate and sulfate. Vanadium elution efficiency is suppressed by co-eluting sulfate and promoted by bicarbonate in the regenerant solution. Regeneration approaches specifically targeting removal of uranium and vanadium is important for long-term operation of SBA for Cr(VI) treatment to prevent constituent accumulation across water treatment loading/regeneration cycles.

Chapter 3. Nanofiltration for Waste Brine Management

This chapter is a reprint of the following peer-reviewed journal article:

Korak, J. A., Huggins, R., & Arias-Paic, M. (2018). Nanofiltration to Improve Process Efficiency of Hexavalent Chromium Treatment using Ion Exchange. *Journal American Water Works Association*, 110 (6), E13-E26.

Introduction

Hexavalent chromium (Cr(VI)) in drinking water sources presents a risk to human health and may require specific treatment to remove. Cr(VI) occurrence in groundwater is due to natural weathering of chromium-bearing minerals and anthropogenic sources (Frey et al., 2004; McNeill et al., 2013). Total chromium (hexavalent and trivalent) is currently regulated by the US Environmental Protection Agency at 100 $\mu\text{g/L}$. In 2014, the State of California (CA) passed a Cr(VI) maximum contaminant level (MCL) for drinking water of 10 $\mu\text{g/L}$, which caused hundreds of entry points in CA to require Cr(VI) treatment (Seidel et al., 2013). In 2017, the Superior Court of California issued a judgment invalidating the regulation citing economic feasibility (Superior Court of California - County of Sacramento, 2017).

Strong base anion exchange (SBA) is a best available technology for removing the predominant form of Cr(VI), chromate (CrO_4^{2-}), from source waters (Sengupta and Clifford, 1986a). SBA uses an inert, polymeric resin with positively charged functional groups that undergo ion exchange with anions in water. Raw source water is passed through SBA contactors and anions present in the water exchange with the resin counter-ions, depending on concentration and resin selectivity. Although found at low concentrations, CrO_4^{2-} has a higher selectivity than other anions commonly found in groundwater at much higher concentrations (e.g., sulfate, bicarbonate, nitrate, etc.). SBA also removes other co-occurring metals that form oxyanions, such as vanadium, selenium, arsenic, molybdenum and uranium (Izbicki et al., 2015).

SBA resin eventually becomes exhausted for chromium removal, which is operationally defined depending on configuration (i.e., single pass or lead-lag). SBA resin is regenerated using a concentrated salt brine solution (commonly sodium chloride (NaCl)) that leads to selectivity reversal and elutes anions removed during water treatment. SBA resin is typically regenerated using 3 to 6 bed volumes (BVs) of NaCl at concentrations of 0.2 N – 2 N. NaCl is typically used due to its availability, relatively low cost, and high solubility (Li et al., 2016b). SBA regeneration produces a concentrated waste brine composed primarily of unused regenerant salt with lower concentrations of other anions removed during water treatment that can be hazardous and require costly disposal (Gorman et al., 2016; Li et al., 2016a).

Minimizing waste brine produced from Cr(VI) SBA processes is important, since disposal is the major environmental and economic consideration of SBA. Several approaches have been investigated for reusing or minimizing waste brine, such as direct brine reuse for

multiple regenerations (Li et al., 2016a; McGuire et al., 2006; Seidel et al., 2014) and chemical treatment using ferrous sulfate (Li et al., 2016b) or calcium polysulfide (Pakzadeh and Batista, 2011). Chemical treatment often forms solids that require additional handling, and it may not be effective to remove other anions that co-elute with chromium, such as uranium, arsenic, and vanadium. Researchers found that direct brine reuse decreased regeneration efficiency starting on the fifth reuse cycle, possibly due to accumulation of sulfate, Cr(VI), or other divalent anions in the regeneration brine (Li et al., 2016a; McGuire et al., 2006; Seidel et al., 2014).

Nanofiltration (NF) is an approach that has not been thoroughly investigated to manage SBA waste brine from Cr(VI) drinking water treatment processes. NF membranes have an effective pore size between 1 and 10 nm, enabling them to reject large ions while allowing permeation of small monovalent anions. Solvent (i.e., water) and solute (i.e., chromate, sulfate, chloride) transport across NF membranes is governed by several mechanisms (Bhattacharjee et al., 2001; Bowen and Mukhtar, 1996; Hagemeyer and Gimbel, 1998; Tsuru et al., 1991). Water flux depends on the intrinsic membrane permeability, transmembrane membrane pressure (TMP) and osmotic pressure difference across the membrane. When operated as a batch process, rejection of solutes increases the osmotic pressure of the feed solution (e.g., waste brine), which decreases the water flux with increasing batch recovery. Solute flux across the membrane is governed by the extended Nernst-Planck equation which describes the flux in terms of solute diffusion, convection and electrical mobility (i.e., electrostatic effects, Donnan potential). Donnan exclusion occurs when the surface charge (e.g., negative charge) of the membrane increases the rejection of ions with the same charge (e.g., anions) due to electrostatic repulsion. Surface charge depends not only on the membrane material charge density but also the solution ionic strength due to co-ion adsorption (Bowen and Mukhtar, 1996; Peeters et al., 1999; Perry and Linder, 1989). At the high ionic strengths found in SBA waste brines, however, exclusion by electrostatic effects are expected to be a minor contributor due to a screening of the membrane surface charge (Peeters et al., 1999; Tsuru et al., 1991; Wang et al., 2007). As solvent flux decreases, solute transport across the membrane is dominated by diffusion rather than convection (Bowen and Mukhtar, 1996; Hagemeyer and Gimbel, 1999). In low salinity groundwaters, Cr(VI) is strongly rejected by NF membranes due to its divalent charge (Brandhuber et al., 2004; Hafiane et al., 2000; Yoon et al., 2009).

NF has demonstrated technical promise for both reducing waste and recovering NaCl from SBA waste and other high ionic strength applications. High Cr(VI) rejection across NF membranes has been demonstrated for high salinity solutions found in tannery wastewater (Cassano et al., 2007) and chlor-alkali production (Madaeni and Kazemi, 2008; Wang et al., 2007; Wang and Chung, 2006). While different applications, the composition of tannery wastewater and chlor-alkali brine is similar to SBA waste brine, as it is composed primarily of chloride, sulfate, chromate and sodium. With respect to ion exchange processes, NF has been used to achieve regenerant salt and water recoveries over 70% in the sugar refining and organic dye processing industries (Allègre et al., 2006; Cartier et al., 1997; Meadows et al., 1992; Salehi et al., 2011). If NF could reduce the operating costs of SBA processes for Cr(VI) removal by minimizing disposal costs, meeting proposed MCLs could become more economically feasible.

While previous studies demonstrated the technical feasibility of separating Cr(VI) and sulfate from chloride using NF, this approach has never been evaluated for drinking water treatment systems to determine the potential for waste reduction and regenerant salt recovery.

The objectives of this study were to 1) treat waste brines from Cr(VI) SBA treatment processes with NF, 2) determine the practical limits of waste minimization and salt recovery, and 3) evaluate how resin regeneration and NF can be coupled to improve overall process performance.

Methods/Materials

Waste Brine Generation, Collection and Fractionation

Three SBA Cr(VI) waste brines (Brines A, B, and C) were collected from the regeneration of full-scale and pilot-scale processes. Both full- and pilot-scale systems were located in California but at different water districts. Purolite A600E/9149, a type 1 quaternary amine resin, was used at both locations. Pilot- and full-scale plants were operated in a single-pass configuration and operating parameters for each process are summarized in Table 3.1. Notably, the full-scale (1 mgd) system (Brine A) operated until the effluent Cr(VI) concentration equaled $8 \mu\text{g/L}$, whereas the pilot-scale system (Brines B and C) operated to complete chromium exhaustion with respect to influent Cr(VI) concentration ($40 \mu\text{g/L}$).

Table 3.1 Operating parameters for the full-scale and pilot-scale SBA treatment plants

Parameter	Full-Scale	Pilot-Scale
Vessel Material	Fiberglass Reinforced Plastic	Schedule 80 Clear PVC
Vessel Diameter	4 ft	2 in
Bed Volume	51.9 ft ³	0.07 ft ³
Configuration	Single Pass	Single Pass
Flow Path	Down flow	Down flow
Resin	Purolite A600E/9149	Purolite A600E/9149
Loading Rate	12.9 gpm/ft ²	8 gpm/ft ²
Operational Cutoff	Chromium breakthrough [Cr(VI)] _{eff} = $8 \mu\text{g/L}$	Chromium exhaustion [Cr(VI)] _{inf} = [Cr(VI)] _{eff} = $40 \mu\text{g/L}$

Resin from both sites was regenerated using a 2 N NaCl solution in a co-current flow configuration using a single-stage regeneration method as summarized in Table 3.2. The full-scale process was regenerated onsite, and a composite waste sample was collected to form Brine A. The Brine A regeneration process used approximately ~ 3 BV of 2 N NaCl. The elution profile for Brine A is shown in Table 3.1a. Using sodium as a conservative tracer, the composite brine sample contained some interstitial water, as the sodium concentration was less than 2 N. The pilot-scale column (Brines B and C) was regenerated in controlled laboratory conditions, and the waste was fractionated into high density polyethylene bottles as it eluted from the column. Brine B included the initial increase in Cr(VI) elution and the tail end of the Cr(VI) elution peak (Figure 3.1b). Brine C was the Cr(VI) elution peak obtained from the same regeneration that produced Brine B. Detailed elution profiles for the pilot-scale contactor can be found elsewhere (Korak et al., 2017).

Hexavalent Chromium Treatment Technologies

Table 3.2. Regeneration and nanofiltration operating parameters for the full-scale and pilot-scale SBA processes used to produce brines A-C.

Process	Parameter	Unit	Brine A	Brine B	Brine C
Regeneration	Process Scale	—	Full	Pilot	
	Regenerant Volume	BV	3	4	
	Regenerant Concentration (NaCl)	N	2.0	2.0	
	Regenerant Solvent	—	Softened service water	Deionized water	
	Flow Direction	—	Co-current	Co-current	
	Loading Rate	BV/hr	1	2.6	
	Fraction to Nanofiltration	—	Composite	Chromium Tails ⁽¹⁾	Chromium Peak ⁽¹⁾
	Volume to Nanofiltration	BV	3 ⁽²⁾	2.4	1.1
Nanofiltration	Termination criteria		Flux limited ⁽³⁾	Volume limited ⁽⁴⁾	Volume limited ⁽⁴⁾
	Waste brine temperature	°C	23.9 ± 0.8	25.4 ± 0.3	24.1 ± 0.1
	Transmembrane Pressure	bar	17.4 ± 0.13	17.4 ± 0.19	17.6 ± 0.07
(1)	Brines B and C are fractions from the same regeneration. See Figure 1b for distinction.				
(2)	A 14.2 L composite sample collected from the full-scale 3 BV waste was processed on the lab-scale nanofiltration unit.				
(3)	Nanofiltration was terminated, because flux decreased to less than 3% of the initial membrane flux				
(4)	Nanofiltration was terminated, because batch volume decreased to the minimum volume needed to operate system				

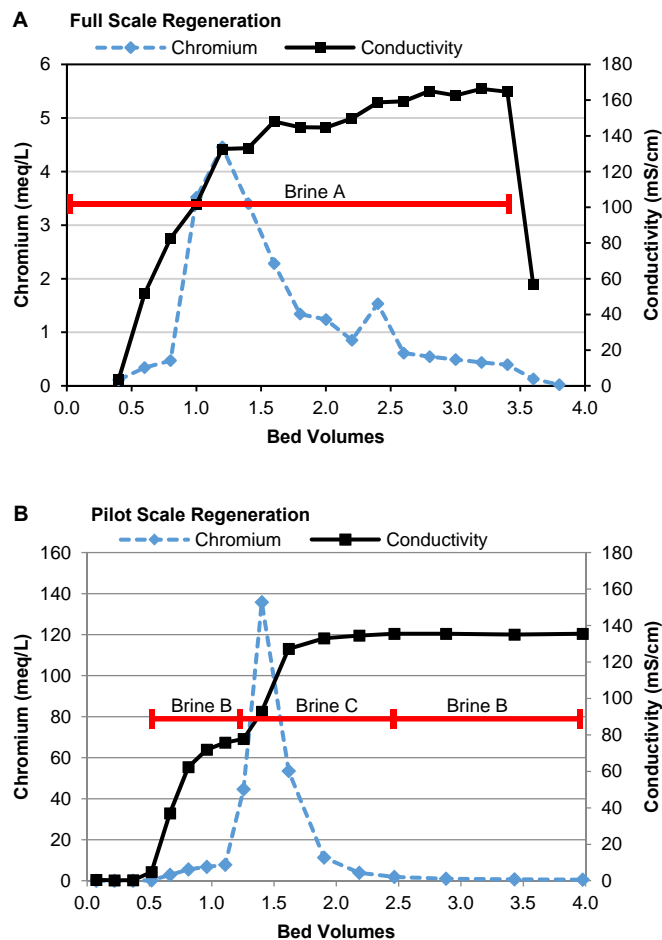


Figure 3.1. Chromium and conductivity regeneration elution profiles and composite brine fractions used for nanofiltration experiments

Nanofiltration of SBA Waste Brine

NF experiments were conducted as a batch concentration process using three crossflow filtration cells in series as shown in Figure 3.2 (SEPA, Sterlitech Corp., Kent, WA). All experiments used a flat sheet polyamide, thin-film composite membrane (NF5, Applied Membranes, Vista, CA). Each filtration cell had a membrane area of 0.014 m² but different feed side channel depths of 1.9 mm (cell 1), 0.80 mm (cell 2), and 0.85 mm (cell 3). Waste brine was recirculated on the feed side of the membranes using a positive displacement pump (0-57 LPM, HydraCell, Wanner Eng. Minneapolis, MN), and permeate was collected on a scale (Entris 8201-1S, Sartorius) to calculate total flux and recovery for the entire system. The NF unit was integrated to a data acquisition system (Labview, National Instruments Corp., Austin, TX) for online measurements of flow, pressure, electrical conductivity, pH and permeate mass. All pH and conductivity probes were calibrated prior to each test.

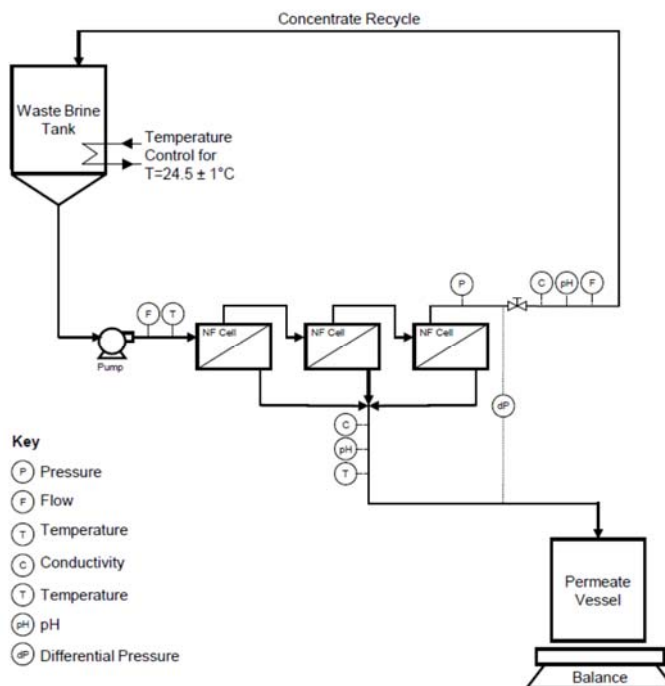


Figure 3.2. Schematic of nanofiltration system

For all batch concentration experiments, a constant feed flowrate of 2.0-2.2 L/min was used, which corresponded to an average crossflow velocity of 0.2 – 0.4 m/s depending on channel depth and a Reynolds number of approximately 680 for an open rectangular conduit, without considering the feed spacer mesh that would increase turbulence. Permeate and concentrate spacers were placed in the SEPA cell flow channels to support the membrane, increase turbulence, and reduce concentration polarization. Waste brine temperature was held constant at $24.5 \pm 1^\circ\text{C}$, and the back pressure valve was modulated to maintain a constant transmembrane pressure (TMP) of 17.4 ± 0.2 bar. The NF treatment was stopped when membrane flux decreased to less than 3% of initial flux or the feed solution volume decreased to the minimum operating volume (~ 750 mL). Batch recovery was determined by dividing the volume of permeate collected by the initial feed volume, with the permeate volume calculated from mass and density measurements.

Membranes were compacted prior to testing by recirculating deionized water ($14 \text{ M}\Omega\text{-cm}$) at 21 bar overnight. After compaction, pure water permeability was determined. Pure water flux for the NF5 membrane was linear ($R^2=0.999$) over a TMP range of 11.0 to 24.5 bar at a constant temperature of $23 \pm 0.1^\circ\text{C}$. The temperature corrected pure water permeability coefficient was $14.7 \pm 0.16 \text{ L/m}^2\text{/hr/bar}$, similar to the reported range for other NF membranes (Luo and Wan, 2011; Nghiem and Hawkes, 2007). After compaction, the membrane was allowed to equilibrate with the brine by recirculating brine through the filtration cell for at least one hour without applied TMP followed by complete permeate recycle to the feed tank at a TMP of 17.2 bar until the permeate flux stabilized. Following each batch treatment process, the system was drained and refilled with deionized water. No chemical or physical cleaning was performed prior to measuring the temperature corrected pure water permeability after each treatment batch. The

pure water permeability post-run was 15.4 ± 1.4 L/m²/hr/bar, showing no statistically significant change in membrane transport properties due to fouling or scaling.

Sampling and Analytical Methods

Concentrate and permeate samples were collected during testing in high density polyethylene bottles and analyzed for basic water quality, trace metals, and major anions. Standard Method 2320 was used for the determination of total, carbonate, and bicarbonate alkalinity, assuming bicarbonate alkalinity was representative of bicarbonate concentrations.

Inductively coupled plasma mass spectrometry (ICP-MS) (7900, Agilent, Santa Clara, CA) was used to measure a suite of elements (Cr, V, As, Mo, Se, U, Na, Cl). Samples were diluted based on the instrument calibration range using 1% nitric acid. The instrument was calibrated and verified with an independent standard for each sample batch as summarized in Korak et al. (2017). Quality control samples were analyzed every 10 samples. Matrix spike recoveries were between 85% and 110% for chromium, vanadium and uranium, and duplicate relative percent differences (RPDs) were less than 5% for sodium, chloride and trace metals measured above the detection limit.

Assumptions were made regarding the ionic form of elemental constituents. Since trivalent chromium Cr(III) does not readily exchange with SBA resins, it was assumed that total chromium (Cr) and Cr(VI) concentrations were equal. Total elemental chlorine was used as a surrogate for chloride as other chlorine sources would be small in comparison to the regenerant salt. For trace metals that form oxyanions, the anionic form was assumed given the pH and assuming oxidizing conditions as described in Korak et al. (2017). The charge balances for waste brines were within 6%.

Nitrate and sulfate were determined using flow injection analysis (QuikChem Method 10-107-04-1-A for nitrate, QuikChem Method 10-116-10-1-A for sulfate). The average RPD between duplicates was ~1% for both nitrate and sulfate. Matrix spike recoveries were between 83% and 105% for nitrate and sulfate quality control samples.

Results and Discussion

Brine characterization

Waste brines A, B and C had high conductivity between 115 and 123 mS/cm and an alkaline pH of 8.3 to 9.0 (Table 3.3). Brine A had the lowest Cr(VI) concentration (1.1 meq/L, 28.6 mg/L as Cr), because the full-scale plant was regenerated when Cr(VI) effluent concentrations reached 8 µg/L and contained a composite sample across the entire regeneration. The pilot-scale contactors for Brines B and C had higher Cr(VI) concentrations (2 meq/L and 35 meq/L, respectively), because they were operated until complete Cr(VI) exhaustion with an effluent concentration of 40 µg/L as Cr. All brines had similar chloride concentrations and were between 1.1 and 1.4 eq/L, which is less than initial concentrations in the regenerant solution (2 eq/L, 71 g/L as Cl) due to exchange onto the resin during regeneration and dilution by interstitial water in the SBA resin. Aside from chloride, sulfate was the other dominant anion in the waste brine with concentrations between 0.19 eq/L and 0.34 eq/L (9 g/L to 16 g/L). Mass balances across the pilot-scale regeneration process found that approximately 48% of the resin active sites

were occupied by sulfate prior to regeneration (Korak et al., 2017). Brines A-C also had other trace metals, such as vanadium, arsenic, selenium, molybdenum, and uranium (Table 3.3). Negligible concentrations of other cations (magnesium, calcium and potassium) were measured.

Table 3.3. Initial and final brine composition

Parameter ⁽²⁾	Units	Brine A Composition			Brine B Composition			Brine C Composition		
		Initial	Final	CF	Initial	Final	CF	Initial	Final	CF
Volume	L	14.2	2.8	--	4.9	1.2	--	2.3	1.7	--
Conductivity	mS/cm	123	138	1.1	117	131	1.1	115	118	1.0
pH	SU	8.3	8.8	--	8.9	9.3	--	8.7	8.7	--
Sodium (Na ⁺)	eq/L	1.8	2.9	1.6	1.6	2.1	1.3	1.7	2.0	1.2
Chloride (Cl)	eq/L	1.4	1.2	0.9	1.4	1.4	1.0	1.1	1.2	1.0
Nitrate (NO ₃ ⁻)	meq/L	37	34	0.9	29	24	0.8	76	71	0.9
Bicarbonate (HCO ₃ ⁻)	meq/L	48	63	1.3	33	47	1.4	66	89	1.3
Carbonate (CO ₃ ²⁻)	meq/L	<MRL	16	--	--	42	--	4	12	3.0
Sulfate (SO ₄ ²⁻)	eq/L	0.34	1.7	4.9	0.19	0.7	3.7	0.28	0.5	1.9
Chromium (CrO ₄ ²⁻)	meq/L	1.1	4.6	4.1	2.0	6.8	3.5	35.2	63.8	1.8
Vanadium (H ₂ VO ₄ ⁻)	meq/L	0.099	0.35	3.5	0.225	0.75	3.3	0.252	0.45	1.8
Molybdenum (MoO ₄ ²⁻)	meq/L	0.030	0.15	4.8	0.144	0.53	3.7	2.837	5.17	1.8
Uranium (UO ₂ (CO ₃) ₃ ⁴⁻)	meq/L	0.052	0.26	5.0	0.005	0.02	3.9	0.362	0.67	1.9
Selenium (SeO ₄ ²⁻)	meq/L	0.016	0.057	3.5	0.013	0.048	3.8	0.034	0.072	2.1
Arsenic (HAsO ₄ ²⁻)	meq/L	0.0031	0.014	4.6	0.0372	0.138	3.7	0.0093	0.013	1.4
Initial Cl:Na Ratio	%	81%			89%			67%		
Chloride fraction, X _{Cl} ⁽¹⁾	—	0.81	0.43	—	0.88	0.67	—	0.80	0.69	—
Maximum Batch Recovery	%	81%			78%			44%		
<p>(1) Chloride fraction calculated according to Equation 1. (2) Assumed ionic form shown in parentheses CF: Concentration factor. Final concentration divided by initial concentration</p>										

Although generated from a SBA process designed for Cr(VI) removal, the composition of the waste brine is essentially a ternary ion mixture containing sodium chloride and sodium sulfate (NaCl/Na₂SO₄) with trace concentrations of other anions. For Brines A and B, the sum of chloride and sulfate concentrations (on an equivalents basis) account for more than 95% of the anions present. For Brine C, chloride and sulfate account for 88% of all anions. Since NF performance is strongly affected by the composition with respect to monovalent and divalent anions, the bulk composition of the waste brine can be characterized by calculating the chloride fraction (X_{Cl}) according the Equation 3.1, where concentrations are expressed in units of eq/L. X_{Cl} is operationally-defined, because it is a simplifying assumption to only include the dominant anions (i.e., chloride and sulfate).

$$X_{Cl} = \frac{[Cl]}{[Cl] + [SO_4]} \quad \text{Equation 3.1}$$

Nanofiltration of SBA Regeneration Waste

Brines A-C were concentrated using NF with the goal of reducing the waste volume and selectively permeating the regenerant salt (i.e., NaCl) for use in a subsequent regeneration cycle. Batch concentration continued until the process became either flux-limited (Brine A) or volume-limited (Brines B and C) as summarized in Table 3.2. Brines A and B were able to achieve 81% and 79% water recovery, respectively. Brine C containing the chromium elution peak had a low initial volume and was only able to achieve 44% water recovery before the NF system had insufficient volume to operate.

Figure 3.3a summarizes the temperature-corrected membrane flux as a function of water recovery. The flux decreased and conductivity (Figure 3.3b) increased with increasing water recovery for all brines. Flux decreased during NF treatment from 46 L/m²/hr to 1.2 L/m²/hr for Brine A with 81% recovery, from 65 L/m²/hr to 20 L/m²/hr for Brine B with 78% recovery, and from 54 L/m²/hr to 34 L/m²/hr with 44% recovery for Brine C. Based on clean water permeability tests conducted after each batch, no statistically significant decrease in membrane permeability was observed, suggesting a low potential for particulate fouling, organic fouling, or chemical scaling for sodium-based regeneration salts. Additional tests across multiple regeneration cycles would be needed to assess the long term fouling potential. Fouling from organic matter is also source water dependent. Waste brine conductivity (Figure 3.3b) increased from about 120 mS/cm to 140 mS/cm. Permeate conductivity was lower than the waste brine and increased with batch recovery, demonstrating some selective salt rejection across the membrane.

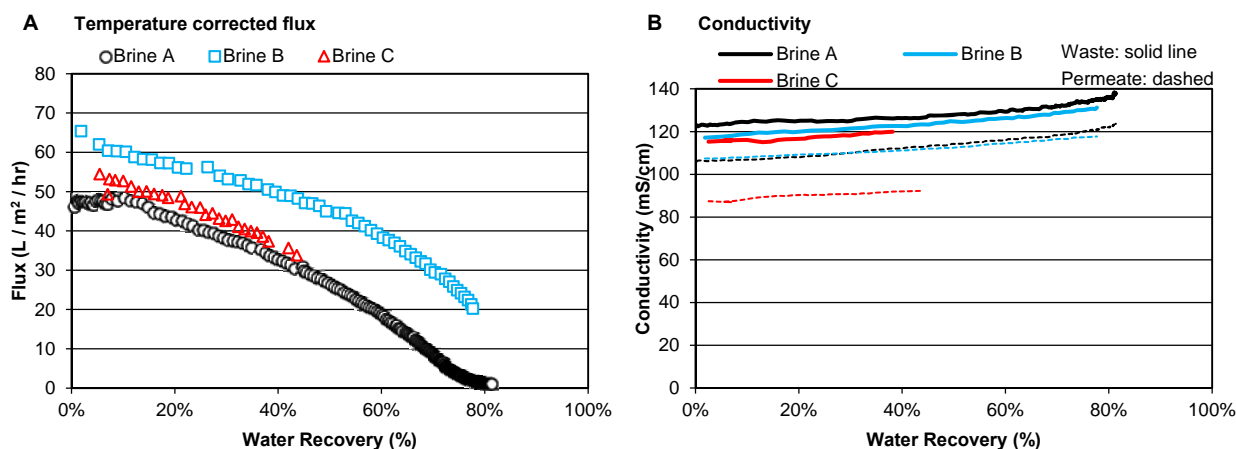


Figure 3.3. Temperature corrected flux and brine conductivity as a function of water recovery

Divalent and monovalent anions exhibited characteristically different observed rejections (R_{obs}), as shown for Brines A and B in Figure 3.4a and Figure 3.4b, respectively. Divalent anions (i.e., sulfate, chromate and other trace anions) exhibited good rejections greater than 0.9 at the start of each batch concentration process. Trace anions include the total concentration on an equivalent basis of vanadium, selenium, arsenic, uranium and molybdenum oxyanions using anionic form assumptions from Korak et al. (2017). For Brine A, rejections were constant up to about 65% water recovery and decreased with increasing recovery. While Brine B did not exhibit this rejection decrease, this run was terminated due to volume limitations and would likely have exhibited a similar behavior at higher recoveries, as subsequently discussed. The increased

concentration of divalent anions and decreased solvent flux both contribute to reduced rejections at high recoveries as diffusion becomes a dominant transport mechanism (Bowen and Mukhtar, 1996; Hagemeyer and Gimbel, 1998)

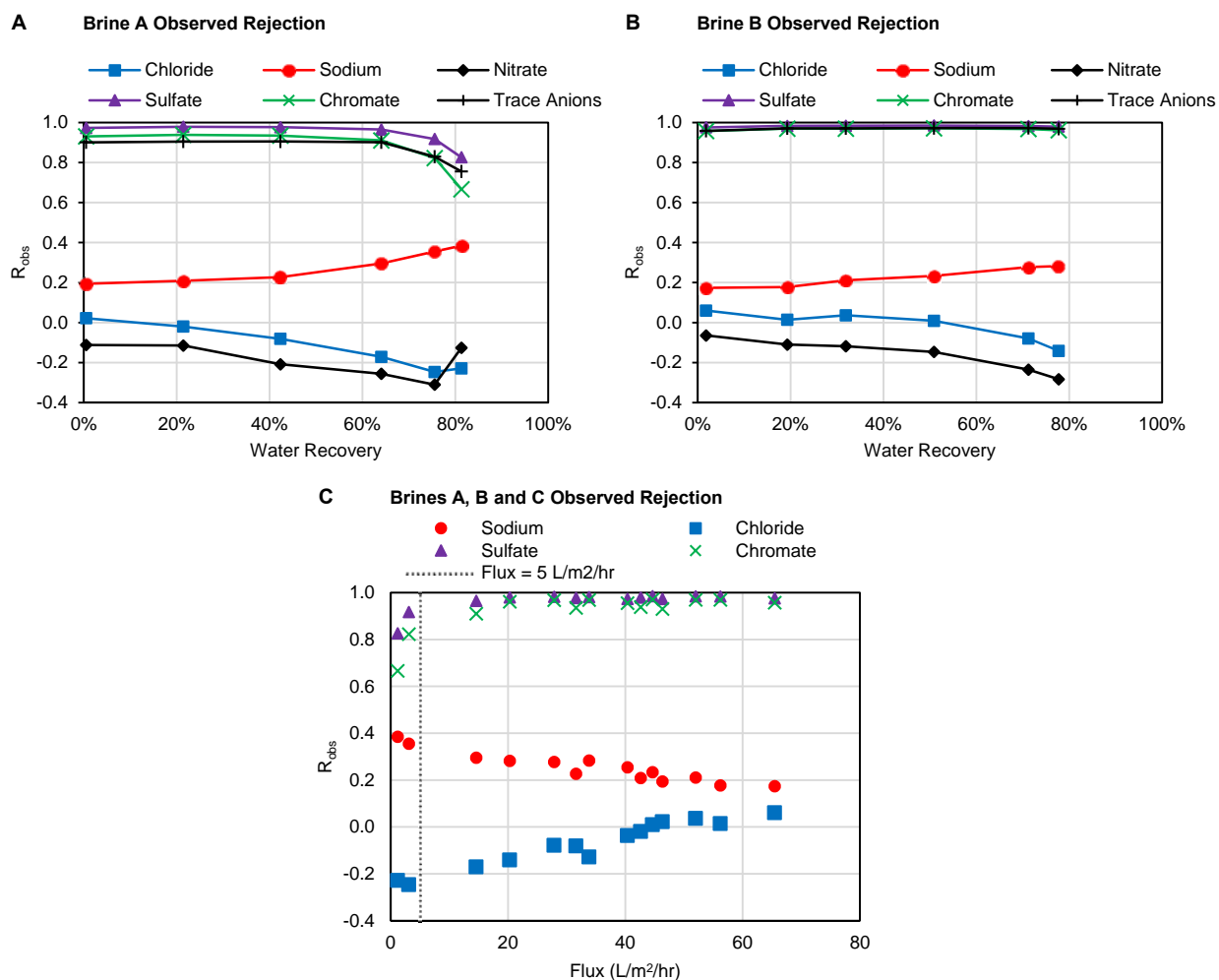


Figure 3.4. Nanofiltration membrane rejection as a function of water recovery or flux. Trace anions includes V, Se, As, U and Mo

Monovalent anions (i.e., chloride and nitrate) exhibited negative rejections that became increasingly negative with increased recovery. A rejection near 0 indicates that electrostatic effects are negligible and cannot repel monovalent anions, as was observed by others at concentrations near 1 N NaCl (Tsuru et al., 1991; Wang et al., 1997). At high ionic strengths, membrane electrostatic repulsion of co-ions (i.e., anions) decreases, which decreases membrane rejection (Peeters et al., 1999). For this system, electrostatic repulsion is not effective for small anions, and convective and diffusive hindrance effects govern solute transport. Negative rejections are commonly observed for small, monovalent anions due to a preferential passage of anions compared to the solvent and are more prominent as membrane flux decreases and compositions become enriched in di- and poly-valent anions (Bowen and Mukhtar, 1996; Gilron et al., 2001; Hagemeyer and Gimbel, 1999; Levenstein et al., 1996; Rautenbach and Gröschl, 1990; Tsuru et al., 1991; Yaroshchuk, 2001). Negative rejection is possible due to the Donnan exclusion between the bulk solution and the membrane that increases the concentration of

monovalent solutes in the membrane compared to the feed solution. The decreasing chloride R_{obs} trend is not confounded by concentration polarization, as concentration polarization effects decrease as membrane flux decreases (Gilron et al., 2001). Mass transfer rates would also decrease as the solute concentration, density and viscosity increase in waste brine with increased batch recovery. A worst-case scenario for concentration polarization was assessed using a thin film model for a rectangular conduit (no spacers) using diffusion coefficients, brine density and brine viscosity values estimated using modeling software (OLI Stream Analyzer, OLI Systems). The results confirmed that the concentration polarization modulus (CPM) would be most severe at low batch recoveries with high fluxes (CPM=1.7-3.3 depending on channel depth) compared to low fluxes at high batch recoveries (CPM=1.04-1.09) and is not confounded with chloride R_{obs} . These results show that Donnan exclusion and diffusion is an important solute transport mechanism for this system, especially when trying to achieve high recoveries at low permeate fluxes.

Sodium, the common cation, had an initial R_{obs} of 0.2 that increased with increasing water recovery. Previous work has shown that cation rejection is controlled by the rejection of dominant anions (Bhattacharjee et al., 2001). Up to 64% recovery for Brine A, more than 93% of the sodium in the permeate had a chloride counter-ion to maintain electroneutrality. At higher recoveries (75.6% and 81.3%), only 81-84% of sodium cations in the permeate could be paired with chloride to maintain charge balance, showing that divalent anions increasingly control sodium transport at higher recoveries. With increasing water recovery, the waste brine is enriched in divalent anions (i.e., sulfate), thus increasing the rejection of sodium.

Nitrate rejection was consistently lower and more negative than chloride, demonstrating preferential passage over chloride. Preferential passage of nitrate compared to chloride has been attributed to a weaker hydration energy with solvating water molecules (Paugam et al., 2004a, 2004b; Santafé-Moros et al., 2007; Tansel et al., 2006). Even though nitrate is preferentially transported across the membrane, the concentration is small compared to chloride. The concentration of nitrate (0.04 eq/L, 2.5 g/L) in the permeate is less than 3% of the chloride concentration (1.4 eq/L, 50 g/L) on an equivalents basis. The addition of NaCl to form a 2 N NaCl solution for the subsequent regeneration cycle would decrease the nitrate impurity to less than 2%. The impact of using a recycled regenerant solution with nitrate impurities on regeneration efficiency warrants further investigation.

Figure 3.4c shows that R_{obs} is strongly tied to permeate flux and does not exhibit systematic differences between the brines. R_{obs} values from all three brines plotted as a function of flux shows that chloride rejection decreases and becomes more negative as flux decreases and sulfate becomes more abundant in the concentrated waste brine, a trend that is well established (Bhattacharjee et al., 2001; Hagemeyer and Gimbel, 1999, 1998). Figure 3.4c shows that rejection of sulfate and chromate decreases at low permeate fluxes as the divalent solute flux becomes diffusion controlled. These results show that operating an NF system at fluxes less than 5 L/m²/hr for waste reduction and chloride recovery would have diminishing returns with respect to membrane area, treatment time and impurity (i.e., sulfate, chromate, trace anion) passage.

NF can be effectively coupled with ion exchange for Cr(VI) removal to reduce waste volumes and recover unused regeneration salt. Future work with multiple regenerations is needed to quantify the full benefit of using NF over direct brine reuse. Previous studies demonstrated that direct brine reuse led to decreased regeneration efficiency after about 5 regeneration cycles

(Li et al., 2016a). It has not been demonstrated if the decreased regeneration efficiency is due to the accumulation of sulfate or nitrate in the recycled brine. NF treatment is highly effective at preventing sulfate accumulation for brine reuse. With each regeneration cycle, however, nitrate can accumulate in the NF permeate and increase with each reuse. Additional work is needed to determine at what concentration the presence of nitrate impurities in the regenerant solution adversely affects regeneration efficiency.

Empirical Relationships

Combining the data from all brines, two empirical relationships were developed that relate brine composition to flux and chloride rejection. Figure 3.5a shows a non-linear relationship between membrane flux and sulfate concentration. Membrane flux decreases as the waste brine sulfate enriches. As the sulfate concentrates in the waste brine, the osmotic pressure difference between the waste brine and permeate increases, and at constant TMP, solvent flux decreases, aligning with fundamental theory governing solvent flux across a membrane (Bhattacharjee et al., 2001; Bowen and Mukhtar, 1996). Using an electrolyte modeling software (OLI Stream Analyzer, OLI Systems) and assuming complete sulfate rejection, the bulk solution osmotic pressure due to sodium sulfate should equal the TMP (17.5 bar) at a sulfate concentration of ~ 0.65 eq/L (31 g/L). However, membrane flux was sustained at higher sulfate concentrations even in the presence of other highly rejected, divalent anions that would contribute additional osmotic pressure difference across the membrane. Comparing observed to model predicted results demonstrates that the equilibrium boundary condition at the membrane interface, where osmotic pressure is calculated for solvent flux, is playing an important role to deplete the membrane pore space of sulfate compared to the bulk solution (Perry and Linder, 1989). Based on the empirical relationship in Figure 3.5, flux decreased below 5 L/m²/hr at a bulk solution sulfate concentration of 1.4 eq/L (67 g/L). While the empirical relationships are specific to this system with a chloride concentration of about 1.4 eq/L (50 g/L), it allows for the NF treatment process to be generalized and incorporated into a model to assess overall process feasibility, as discussed in the following section.

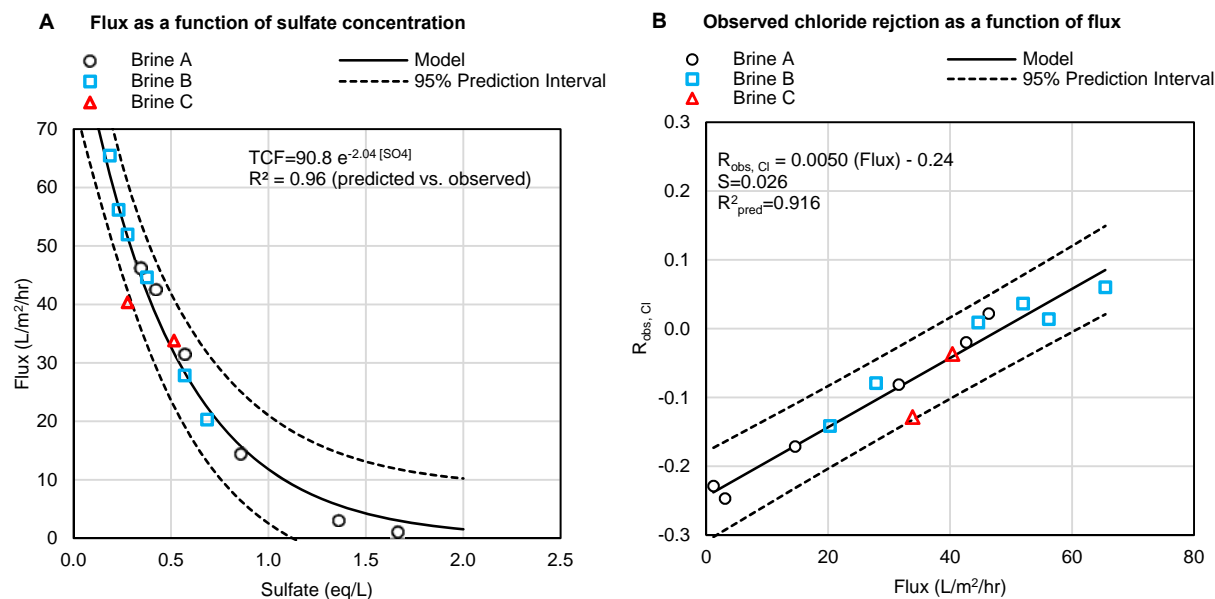


Figure 3.5. Empirical relationships for flux and chloride rejection

A strong, linear relationship also predicts chloride rejection given solvent flux as shown in Figure 3.5b. A positive, but not necessarily linear, relationship between solvent flux and chloride rejection has been recognized by many studies (Bowen and Mukhtar, 1996; Gilron et al., 2001; Hagemeyer and Gimbel, 1999; Levenstein et al., 1996). The mass transport equations (i.e., extended Nernst-Planck equation with appropriate boundary conditions) that govern chloride flux are not fundamentally linear. At low chloride concentrations, the relationship between flux and chloride rejection is non-linear with a concave-down curvature (Hagemeyer and Gimbel, 1999). At high ionic strengths, where electrostatic effects become increasingly negligible compared to steric effects, several studies have shown practically linear relationships. Levenstein et al. (1996) and Gilron et al. (2001) demonstrated that the relationship between flux and rejection becomes practically linear at concentrations of 2.5% NaCl and 15,000 ppm, respectively. The 2 N NaCl regenerant solution concentration is 4-5 times more concentrated, supporting the linear approximation presented in Figure 3.5b. Importantly, embedded in the empirical constants is the confounding factor that sulfate concentration increased as flux decreased. Increasing the ratio of sulfate to chloride (or a decrease in X_{Cl}) also decreases the chloride rejection at constant flux (Bowen and Mukhtar, 1996; Hagemeyer and Gimbel, 1998).

It is important to reiterate that the empirical relationships and reported constants are only appropriate within the context developed. All waste brines were generated using a 2 N NaCl regeneration process and had similar initial sodium concentrations, dominant anions and X_{Cl} values. The system bounds that apply to these empirical relationships are for high ionic strength solutions (e.g., sodium concentrations greater than 1 eq/L) and chloride fractions, X_{Cl} , greater than 0.4. It would not be appropriate to apply these relationships to different ionic strengths, compositions other than NaCl/Na₂SO₄ dominated solutions, NF membranes or transmembrane pressures.

Modeling Batch Concentration of Regeneration Brine

A batch NF model was developed by discretizing the filtration process into small recovery increments. At each recovery step, the composition, rejection, and flux were calculated using mass balances and the empirical relationships in Figure 3.5. The model batch process was terminated when permeate flux equaled 5 L/m²/hr, at which point the rejection of undesirable divalent anions decreased (Figure 3.4c). Since chloride and sulfate were the most abundant anions in the waste brine, a batch filtration model was developed assuming that membrane flux and practical terminal recovery were driven by the sulfate concentration, neglecting other trace anions. At each recovery increment, flux was estimated using

Equation 3.2, and chloride rejection was estimated using Equation 3.3. Since the NF model was designed to terminate at a flux of 5 L/m²/hr, it was assumed that sulfate rejection was constant according to Equation 3.4.

$$Flux_i \left[\frac{L}{m^2 \cdot hr} \right] = 90.8 * e^{-2.04 [SO_4]} \quad \text{Equation 3.2}$$

$$Rej_{Cl,i} = 0.0050 * Flux_i \left[\frac{L}{m^2 \cdot hr} \right] - 0.24 \quad \text{Equation 3.3}$$

$$Rej_{SO_4,i} = 0.975 \quad \text{Equation 3.4}$$

The batch treatment process was discretized into small recovery steps (Rec_{*i*}), where *i* represents the step number. In each step, feed volume (V_{*i+1*}) was calculated based on the recovery increment and initial volume (V₀) following Equation 3.5 and Equation 3.6.

$$\Delta V = \frac{Rec_{i+1} - Rec_i}{V_0} \quad \text{Equation 3.5}$$

$$V_{i+1} = V_i - \Delta V \quad \text{Equation 3.6}$$

The batch processing time for each recovery increment (Δt) was calculated (Equation 3.7) based on the decrease in waste brine volume (ΔV), flux, and membrane area. The cumulative run time (t_{*i+1*}) was determined for each recovery step (Equation 3.8).

$$\Delta t = \frac{\Delta V}{Flux * Area} \quad \text{Equation 3.7}$$

$$t_{i+1} = t_i + \Delta t \quad \text{Equation 3.8}$$

The concentration of both chloride and sulfate in the permeate ([C]_p in eq/L) was determined using the appropriate rejection (Rej_{c,*i*}) equation (Equation 3.3 or Equation 3.4) and the feed concentration from the previous recovery step (Equation 3.9). By mass balance, the new feed concentration ([C]_f in eq/L) was calculated for both chloride and sulfate following Equation 3.10. The time-averaged, design flux across the run was calculated using the numerical integration in Equation 3.11 to account for the non-linear relationship between flux and time.

$$[C]_{p,i+1} = (1 - Rej_{c,i}) * [C]_{f,i} \quad \text{Equation 3.9}$$

$$[C]_{f,i+1} = \frac{[C]_{f,i} * V_i - [C]_{p,i+1} * \Delta V}{V_{i+1}} \quad \text{Equation 3.10}$$

$$\text{Average Flux} = \frac{\int_0^t Flux(t) dt}{t} \quad \text{Equation 3.11}$$

The iterative model terminated when flux equaled 5 L/m²/hr, termed the critical recovery. The critical recovery represents the maximum practical recovery at which a decrease in divalent rejection would be expected (Figure 3.4c). Using Brine B as an example, this model provided a good fit to the experimental data (Figure 3.6). The model predicts that the batch concentration could have achieved a critical recovery of 85% had the NF system not been volume limited.

Hexavalent Chromium Treatment Technologies

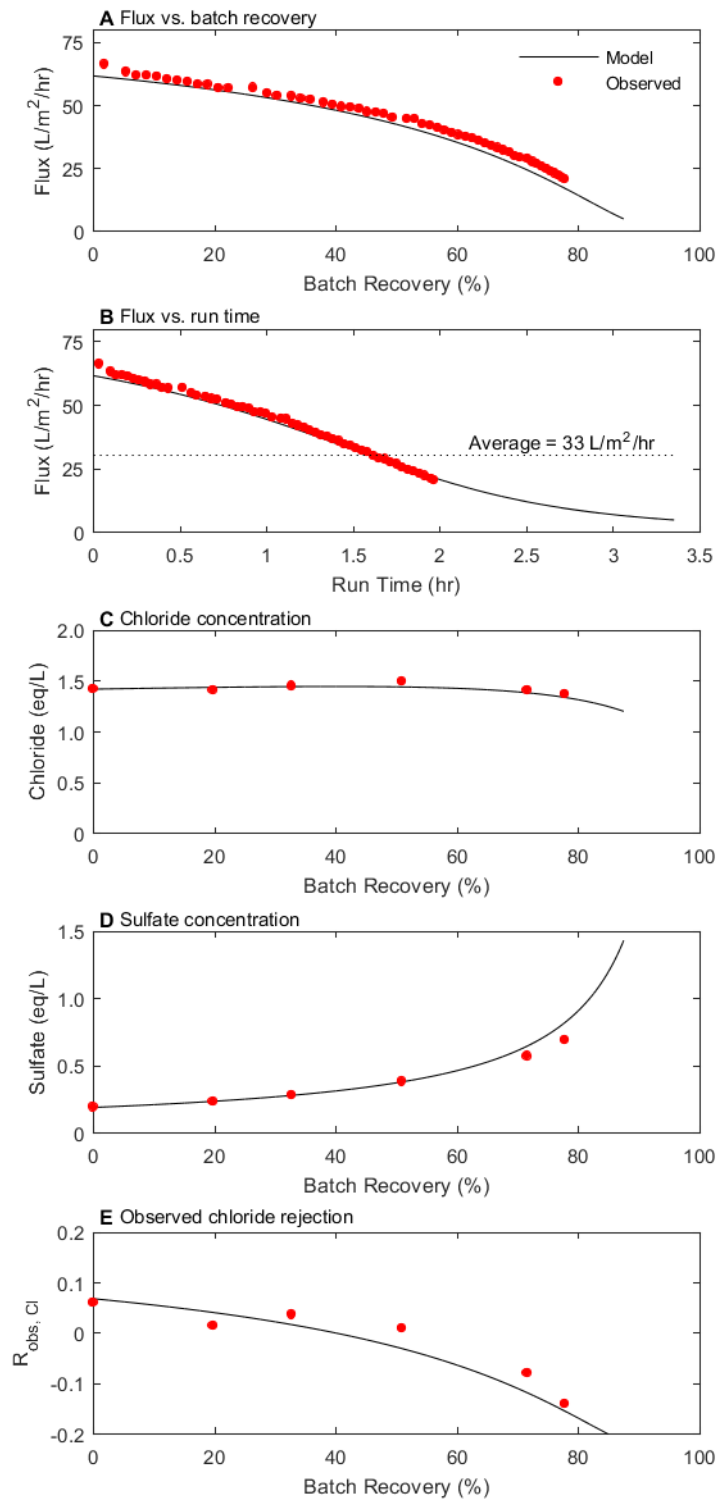


Figure 3.6. Verification of batch nanofiltration model for Brine B
Feasibility of nanofiltration: Resin regeneration case study

The batch NF model was applied to an ion exchange regeneration profile to determine the general feasibility of this process. The model input used regeneration data from a pilot-scale, 2 N NaCl regeneration carried out to 6.3 bed volumes (BV) to fully elute nitrate (Figure 3.7a) as described in Korak et al. (2017). It was assumed that the leading edge of the waste brine with a conductivity less than 20 mS/cm would be recycled and not be included in the volume sent for NF treatment, which corresponded to the first 0.5 BV. The regenerant solution volume used depends on specific treatment objectives. For example, near complete chromium elution could be achieved if the regeneration in Figure 3.7a was terminated (i.e., switched to rinse water) at 2 BV. If complete nitrate elution was important, more than 4 BV would be needed. Pairing the NF model with regeneration data allows for the tradeoffs between chemical use, waste production and resin regeneration efficiency to be explicitly compared for different regeneration approaches.

Figure 3.7b-e evaluate the feasibility of applying NF to reduce waste and recover NaCl from waste brine as a function of regeneration solution BV by selecting different regeneration termination points and modeling the brine concentration process for the resulting composite waste brine. For example, a “Regeneration Termination Bed Volume” of 3 evaluates the scenario where waste brine collected from 0.5 BV to 3 BV, with a composition determined by integrating the elution profile up to 3 BV (Figure 3.7a), is treated by NF to different terminal recoveries. Regeneration scenarios that terminate at less than 1.8 BV were not considered due to incomplete chromium regeneration, and the ionic strength and composition of the composite waste brine would fall outside the constraints under which the empirical relationships were developed.

Waste reduction and NF critical recovery depend on the initial sulfate concentration, which determines the scenarios under which NF for waste management would be feasible. Figure 3.7b shows that the initial sulfate concentration (terminal recovery = 0%) decreases with increasing termination BV, because sulfate elution is complete by 2 BV (Figure 3.7a). For example, a regeneration that terminates at 2 BV would result in a composite brine of all solutes eluted between 0.5 BV and 2 BV. The initial sulfate concentration would be 0.6 eq/L (29 g/L), and a NF terminal recovery 58% could be achieved before sulfate accumulation in the waste brine would limit flux. If regeneration proceeded to 5 BV for complete nitrate elution, the initial sulfate concentration would be 0.22 eq/L (11 g/L), and the waste volume could be reduced by 85% using NF.

NF could decrease the waste volume requiring off-site disposal to less than 1 BV regardless of regeneration termination point. With NF, the final waste volume would not significantly depend on the regeneration termination point as shown in Figure 3.7c. Sulfate is the dominant multivalent anion that accounts for nearly all the osmotic pressure difference across the membrane. Since sulfate completely elutes before chromium, the total mass of sulfate in the regeneration brine would not depend on regeneration termination point beyond 2 BV. While the water recovery (%) would be higher for extended regenerations that completely elute nitrate, the final waste volume would be theoretically the same if NF becomes flux-limited at a constant sulfate concentration (e.g., 1.4 eq/L). For a wide range of regeneration approaches, coupling regeneration with NF could be highly effective for reducing waste brine volume and disposal costs.

Hexavalent Chromium Treatment Technologies

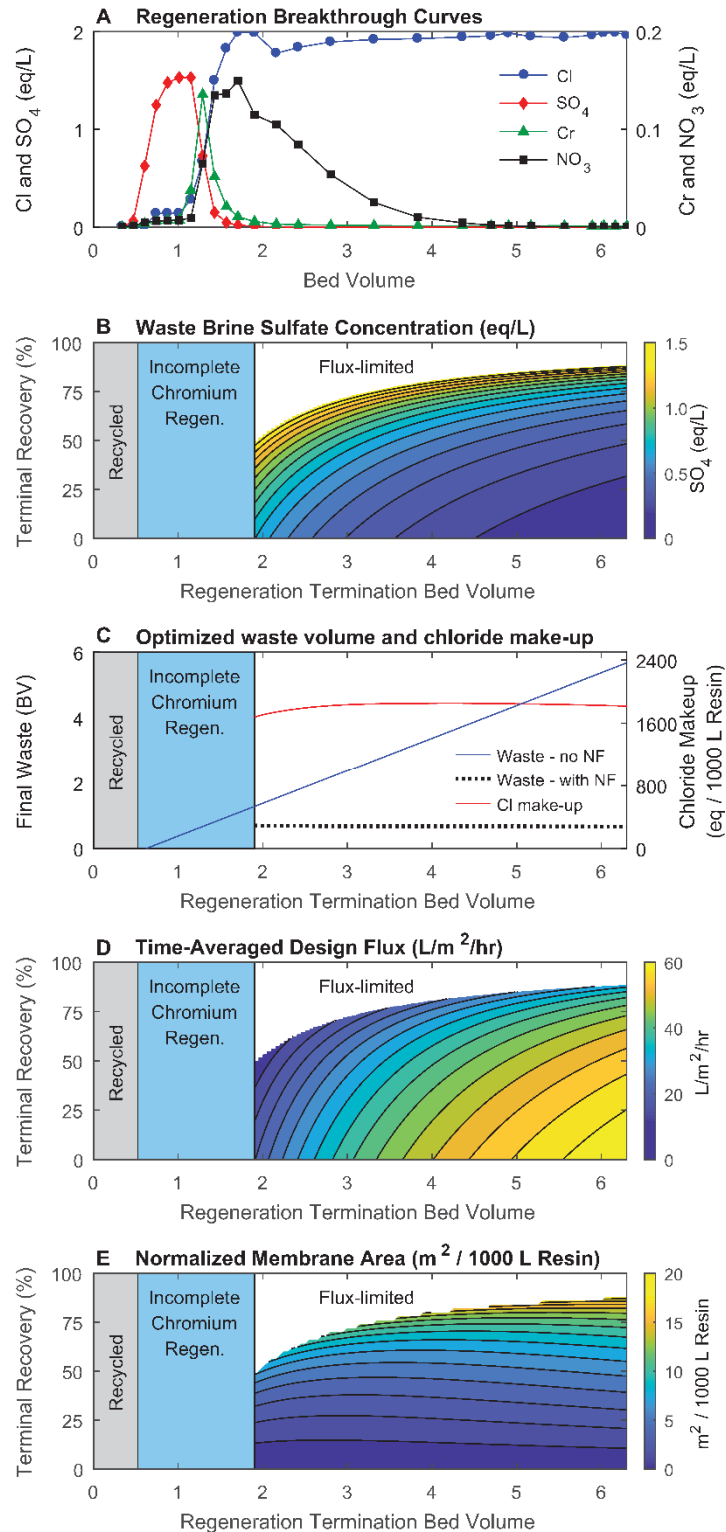


Figure 3.7 Case study coupling nanofiltration with resin regeneration

Figure 3.7c also shows that NF can greatly reduce chemical costs by recovering sodium chloride that would otherwise be lost to off-site disposal. Chloride make-up required for the next regeneration was determined by comparing the quantity (equivalents) of chloride in a composite

permeate sample to the quantity of sodium in the initial waste brine. By using sodium as a conservative tracer, the amount of regenerant salt needed to repeat the same regeneration can be determined, accounting for dispersion through the resin bed at the start of the regeneration. Figure 3.7c shows that as the regeneration termination BV increases, there is little variation in the amount of make-up salt needed for the next regeneration. Although extended regenerations would require more salt, higher batch recoveries using NF could be achieved. The quantity of make-up salt shows little variation with termination bed volume, because most of the chloride would exchange with the resin by 2 BV, and the final waste volume and composition with respect to chloride would be similar regardless of termination bed volume.

Without NF, most of the chloride used for regeneration would end up in the waste stream for disposal and not exchange with the resin. For example, the resin used in this study has a capacity of about 1.6 eq/L. If regeneration requires 3 BV of 2 N NaCl, a maximum of 27% of the chloride in the regenerant solution could exchange with resin, and 73% would pass through the contactor to the waste stream. If about 55% of the salt needed for the next regeneration could be recovered in NF permeate, the fraction of regenerant salt lost to the waste stream would decrease from 73% to 18%. Recovering regenerant salt from the waste brine using NF would significantly reduce chemical operating costs for the process.

System size was also screened for different regeneration and terminal recovery scenarios using the NF model. Figure 3.7d shows that the time-averaged, design flux (Eqn 11) depends on both initial composition and target terminal recovery. Initial membrane fluxes (terminal recovery = 0%) increases up to 60 L/m²/hr with extended regenerations when the sulfate concentration decreases to 0.2 eq/L (10 g/L). Time-averaged flux decreases as the terminal recovery increases. For regeneration scenarios between 2 and 6 BV, the time-average flux to achieve the critical (maximized) recovery ranged from 13 L/m²/hr to 31 L/m²/hr.

To assess the required system size, the membrane area needed to concentrate the waste brine within 8 hours was determined. This time was selected, because it could facilitate a mobile unit treating the brine within 1 operator shift. Membrane area was determined by iteratively solving for the membrane area such that the cumulative batch treatment time (Eqn 8) equaled 8 hours. The reported membrane area was normalized to a resin bed volume of 1000 L. Figure 3.7e shows that membrane area increases with terminal recovery but not with regeneration termination BV. For example, a regeneration carried out for 4 BV would require 5 m² of membrane area to achieve 50% water recovery and 14 m² to achieve a critical recovery of 80%. Regeneration termination BV has little effect on membrane area, because as the waste brine volume increases, the time-average flux increases due to the lower initial sulfate concentration. For perspective, a typical 2.5" NF element has a membrane area of 7-8 m². Therefore, two to four 4"x40" membrane elements for every 1000 L of resin would be sufficient to treat most combinations of regenerant solution volumes and terminal water recoveries with 8 hours of operating time. This membrane area is appealing to mobile treatment units that could serve a network of groundwater wells applying the SBA process.

Conclusions

NF could play an integral role in managing waste brine from SBA processes treating for Cr(VI) by reducing waste volumes to less than 1 BV and reducing regenerant salt make-up for

next regeneration cycle. This study presents a system-specific, empirical approach for assessing waste reduction and salt recovery for a range of resin regeneration scenarios. At ionic strengths typically used for SBA regeneration (e.g., 2 N NaCl), monovalent anions exhibit negative rejections and preferentially permeate through the membrane, which is favorable for recovering excess regenerant salt from spent brine. Polyvalent anions (i.e., sulfate, chromate, and uranium complexes) are highly rejected, depending on waste brine composition and membrane flux. While nitrate is poorly rejected by the membrane, the concentration of nitrate in the recovered regenerant solution is low (<3%) compared to chloride, the practical implications of which require further investigation. As the sulfate concentration increases in the waste brine, both membrane flux and divalent anion rejection decrease. Since sulfate concentrations control the batch recovery at which point the process becomes flux-limited, regeneration approaches that are extended to recover nitrate can be concentrated using NF to the same final waste volume as regeneration approaches that are only tailored for chromium recovery. Preliminary system sizing demonstrated that the membrane area required would be reasonable for a mobile treatment unit to service a decentralized network of SBA treatment processes.

Chapter 4. Chromium removal by Stannous Chloride

This chapter is a reprint of the following peer-reviewed journal article:

Kennedy, A. M., Korak, J. A., Flint, L. C., Hoffman, C. M., & Arias-Paic, M. (2018). Peer Reviewed Pilot-Scale Removal of Total and Hexavalent Chromium from Groundwater Using Stannous Chloride. *Journal - American Water Works Association*, 110(4), E29–E42.

Introduction

Hexavalent chromium (Cr(VI)) is a widely studied drinking water constituent, present naturally in many groundwaters at concentrations ranging from <0.001 up to 0.2 mg/L (Kotas and Stasicka, 2000; McNeill et al., 2012; Seidel and Corwin, 2013). Hexavalent chromium does not have a specific maximum contaminant level (MCL) regulated by the US Environmental Protection Agency (USEPA), but it is regulated as part of the total chromium (Cr(T)) MCL of 0.100 mg/L. As an area of high occurrence and national focus for Cr(VI) in drinking water (Seidel and Corwin, 2013), California was the only state to specifically regulate Cr(VI) at an MCL of 0.010 mg/L. As a result, most Cr(VI) research targets 0.010 mg/L or lower for treated water. Despite the California MCL recently being rescinded (SWRCB, 2017), there is a continued national interest among utilities to address Cr(VI) in drinking water, especially with ongoing toxicological reviews by USEPA and a requirement to develop a new California MCL (SWRCB, 2017; USEPA, 2014).

Total chromium in drinking water sources is primarily found in two oxidation states: the more toxic Cr(VI) and the less toxic trivalent chromium (Cr(III)). At pH 8, Cr(VI) is primarily found as chromate (CrO_4^{2-} , pK_{a2} 6.49) in groundwater (McNeill et al., 2012; Rai et al., 1989; Seidel and Corwin, 2013). Between pH 6.5 and 11.5, Cr(III) is typically present as a neutral chromium hydroxide complex ($\text{Cr}(\text{OH})_3^0$), and will precipitate as $\text{Cr}(\text{OH})_3(\text{s})$ at concentrations above approximately 0.020 mg/L ($10^{-6.84}$ mol Cr/L) (Lee and Hering, 2003; McNeill et al., 2012; Rai et al., 1987). Although $\text{Cr}(\text{OH})_3(\text{s})$ is relatively insoluble, 0.020 mg/L is still quite relevant to Cr(T) and Cr(VI) concentrations found in drinking water sources.

Selection of chromium removal treatment processes depends on both its concentration and oxidation state. Best available technologies for removing low levels (<0.100 mg/L) of Cr(VI) include strong-base anion (SBA) exchange, weak-base anion (WBA) exchange, reverse osmosis (RO), and reduction–coagulation–filtration (RCF) using the ferrous form of iron (Fe(II)) (Blute et al., 2015a, 2015b; Brandhuber et al., 2004; McGuire et al., 2006; Seidel et al., 2013; Wu et al., 2015). Although SBA exchange, WBA exchange, and RO are effective at lowering Cr(VI) and/or Cr(T) concentrations to <0.010 mg/L, disposal of high salinity waste streams (SBA exchange and RO) or resins (WBA exchange) can be costly and/or impractical, as residuals may classify as hazardous or radioactive waste. There can also be other limitations such as competing anion concentrations for SBA exchange or careful pH adjustment for WBA exchange.

Ferrous iron RCF at doses <5 mg/L as Fe(II) can effectively reduce Cr(VI) to Cr(III) and yield filtered Cr(T) concentrations <0.010 mg/L (Blute et al., 2015a, 2015b; Brandhuber et al., 2004; Lee and Hering, 2003; McGuire et al., 2006; Qin et al., 2005). Ferrous iron doses for RCF are typically determined from Fe(II): Cr(VI) molar dose ratios (MDRs), where, for example, a 5 mg/L Fe(II) dose represents an MDR of 47 for an initial Cr(VI) concentration (C_0) of 0.100 mg/L. An analogous parameter for determining doses for Fe(II) RCF is the mass dose ratio, which for the previous example would be 50, also obtained by multiplying the MDR by the ratio of Fe:Cr molar masses, or 1.07.

Several studies have shown filtration of Cr(OH)₃(s) following Fe(II) RCF to be difficult on a strictly particle-size basis using membrane filters with nominal pore sizes of <0.45 μm , likely because of its colloidal nature and solubility (Brandhuber et al., 2004; Lee and Hering, 2003; Rai et al., 1987). Other Fe(II) RCF studies have shown near-complete Cr(T) removal using commercial microfiltration (0.1 μm) and ultrafiltration (0.02 μm) membranes (Blute et al., 2015a). Using anthracite–sand media filters at hydraulic loading rates (HLRs) ranging from 7 to 15 m/h (3–6 gpm/ft²), Qin et al. (2005) observed $>90\%$ Cr(T) removal using 1–5 mg/L as Fe(II). Blute et al. (2015a) and Wu et al. (2015) also observed $>90\%$ Cr(T) removal across anthracite–sand media filters using 3 mg/L as Fe(II). However, following reduction and before filtration, Fe(II) RCF requires aeration or the addition of an oxidant, such as chlorine, to fully convert Fe(II) to ferric iron (Fe(III)) for two reasons. First, this conversion facilitates Cr(OH)₃(s) removal through filtration and adsorption to and/or coprecipitation with ferric hydroxide (Fe(OH)₃(s)) flocs (Blute et al., 2015a, 2015b; McGuire et al., 2006; Qin et al., 2005; Wu et al., 2015). Second, without aeration or the addition of another oxidant, Fe concentrations would likely exceed the USEPA secondary MCL of 0.3 mg/L, as dissolved Fe would freely pass through conventional media filtration, microfiltration, or ultrafiltration. Oxidant addition before Cr(T) removal could also result in reoxidation of Cr(III) back to Cr(VI) (Blute et al., 2015b; Brandhuber et al., 2004; Lai and McNeill, 2006; Wu et al., 2015).

As an alternative to Fe(II), the stannous form of tin (Sn(II)), dosed as stannous chloride (SnCl₂), can be used as a Cr(VI) reductant (Brandhuber et al., 2004; Lai and McNeill, 2006). Stannous chloride is not currently listed as a drinking water treatment chemical by NSF International (NSF/ANSI, 2017) (although it is listed as such by UL (UL, 2017)), as its uses are primarily associated with food preservation, dye manufacturing, metallization, plating, tanning, and pharmaceutical industries (USNLM, 2017). Other than the work by Lai and McNeill (2006) and Brandhuber et al. (2004), which were part of the same study, SnCl₂ for water treatment has been limited to its use as (1) a precursor for novel Cr(VI) reductants/adsorbents (Kaprrara et al., 2017; Pinakidou et al., 2016), (2) a reductant for the treatment of dissolved mercury (Jackson et al., 2013; Mathews et al., 2015), and (3) a corrosion inhibitor in distribution systems (Hozalski et al., 2010, 2005). Compared with Fe(II) RCF, which forms Fe(OH)₃(s) and other hydrolysis products (e.g., Fe(OH)₂⁺), oxidation of Sn(II) to Sn(IV) has been shown to form relatively insoluble stannic oxide or cassiterite (SnO₂(s)) as opposed to other Sn(IV) hydrolysis products (e.g., Sn(OH)₃⁺) that would be relevant to coagulation (Brandhuber et al., 2004; Haynes et al., 2016; Jackson et al., 2013; Kaprrara et al., 2017; Mathews et al., 2015). Therefore, Cr(OH)₃(s) removal mechanisms may be similar in terms of adsorption to and/or coprecipitation with SnO₂(s), but different in terms of particle coagulation, if Fe(III) hydrolysis products do indeed play a role in Cr(OH)₃(s) particle destabilization.

Testing of SnCl_2 for the reduction of Cr(VI) was performed by Lai and McNeill (2006) and Brandhuber et al. (2004) in a natural groundwater supplemented with Cr(VI) to reach an initial Cr(VI) concentration of 0.100 mg/L. At pH values of 5, 7, and 9, SnCl_2 was able to reduce Cr(VI) by approximately 50–60% in unfiltered samples within 30 min at a SnCl_2 dose of 1.3 mg/L as SnCl_2 , a Sn(II):Cr(VI) MDR of 3.6 (multiply MDR by 3.64 to obtain the SnCl_2 :Cr(VI) mass dose ratio). Samples that were filtered using 0.45 μm filters at pH 7 and 9 showed less Cr(VI) removal than unfiltered samples, for reasons unknown. Because of the remaining unknowns and potential of SnCl_2 , additional work is needed to expand upon previous studies, particularly related to the filterability of Cr(T). On the basis of evidence of its small particle size (Brandhuber et al., 2004; Lee and Hering, 2003), depth filtration may enhance removal through the mechanisms of interception, sedimentation, and, most importantly, Brownian motion (Benjamin and Lawler, 2013). As previously mentioned, $\text{Cr}(\text{OH})_3(\text{s})$ removal may also be facilitated by adsorption to and/or coprecipitation with $\text{SnO}_2(\text{s})$, similar to Fe(II) RCF (Blute et al., 2015a; Kaprara et al., 2017; Pinakidou et al., 2016). Therefore, the primary goal of this study was to further investigate SnCl_2 treatment for the removal of Cr(T) over a range of doses, contact times, and filtration approaches. Three natural groundwaters were tested, covering a wide and relevant range of naturally occurring Cr(VI) concentrations. Experiments were designed for Cr(T) removal from a process feasibility standpoint as opposed to elucidating specific Cr(T) removal mechanisms. However, on the basis of observations from testing, several different removal mechanisms are proposed.

Materials and Method

Waters

Three groundwater wells operated by two drinking water utilities in Oklahoma and California were chosen for pilot studies. Average raw water quality values are shown in Table 4.1, where the water tested in Oklahoma is designated as OK, and the two waters tested in California are designated as CA-1 and CA-2. Hexavalent chromium concentrations ranged from <0.020 to >0.090 mg/L. Predictably, nearly all of the Cr(T) in the waters was present as Cr(VI) on the basis of water quality analyses.

Table 4.1. Average raw water quality

Water	Location	Cr(T) (mg/L)	Cr(VI) (mg/L)	pH (SU)	Alkalinity (mg/L as CaCO ₃)	Turbidity (NTU)	Conductivity (μS/cm)	Sulfate (mg/L as SO ₄ ²⁻)	Dissolved Organic Carbon (mg/L)
OK	Oklahoma	0.092±0.004 (17)	0.092±0.003 (14)	7.9±0.2 (10)	225±15 (10)	0.2±0.1 (10)	420±10 (5)	13±1.0 (2)	0.7±0.0 (3)
CA-1	California	0.039±0.004 (16)	0.033±0.004 (16)	8.0±0.2 (3)	95±5 (3)	0.3±0.1 (10)	235±10 (2)	8.2±0.5 (3)	<0.3 (3)
CA-2	California	0.022±0.004 (9)	0.019±0.003 (9)	8.0±0.2 (3)	100±15 (2)	0.3±0.1 (10)	480±15 (2)	120±0.0 (2)	NM

Temperature (all waters): 15 to 20°C
 Values are average ± standard deviation (count)
 CA-1 and CA-2 turbidity values before GAC cartridge filter
 NM – not measured

Pilot Setup and Operation

A schematic of the pilot setup at each well site is shown in Figure 4.1. Pilot materials were mainly polyethylene/polypropylene tubing and fittings, high-density polyethylene (HDPE) containers, and polyvinyl chloride (PVC) piping and fittings. Depending on the testing phase, water was continuously fed to each pilot at flow rates ranging from 1.1 to 3.8 L/min (0.3–1.0 gpm) at 140–170 kPa (20–25 psi), controlled using a rotameter with a needle valve and pressure-reducing valve. Two granular activated carbon (GAC) cartridge filters (AP817, Aqua-Pure, CUNO Inc.) were installed in series at CA-1 and CA-2 wells to remove free chlorine before SnCl₂ injection. GAC filters were also exhausted for the small Cr(VI) adsorption capacity before testing (i.e., influent Cr(VI) concentration was equal to the effluent Cr(VI) concentration). Samples taken before SnCl₂ injection (and after GAC for CA-1 and CA-2) were designated as “raw.”

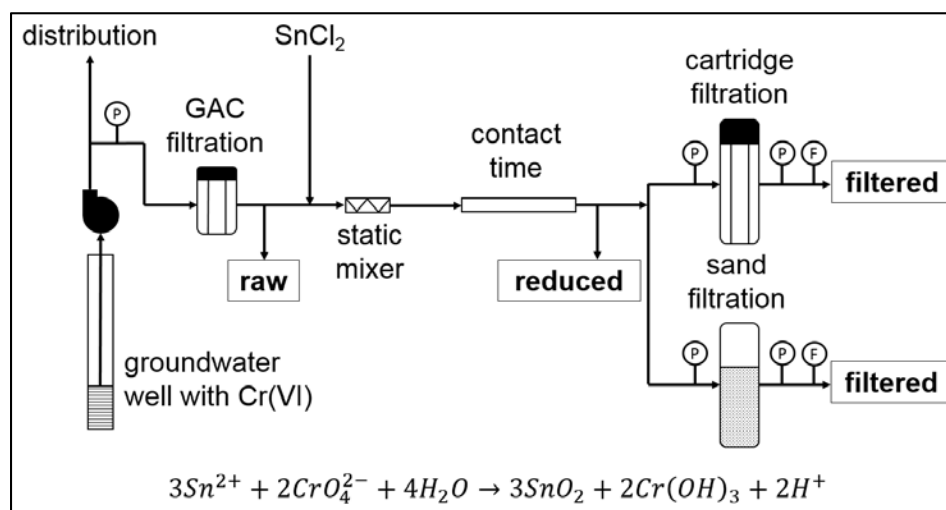


Figure 4.1. Pilot testing schematic Sample points designated as bold and boxed. GAC was used only with CA-1 and CA-2 for the removal of chlorine. P: pressure gauge. F: rotameter (flow)

SnCl₂ was fed to the system through a peristaltic pump from a concentrated stock solution made from reagent-grade (Sigma Aldrich) SnCl₂ and deionized water. Stock solution concentration (~1,000–2,000 mg/L as SnCl₂, pH ~2) and pump speed were adjusted to deliver the desired dose. All SnCl₂ doses here are reported in milligrams per liter as SnCl₂. Although the

SnCl₂ stock concentration was chosen to ensure complete dissolution, stability issues were encountered with the stock age, prompting fresh SnCl₂ stock solutions to be remade regularly. Stability issues were realized with decreased effectiveness of the stock solution (i.e., decreased Cr(VI) reduction at the same pump dosing rate) and yellow color development coupled with a rise in stock solution turbidity (e.g., Sn(IV) precipitation after reacting with dissolved oxygen). A static mixer (3/8-40C-4-6-2, Koflo Corporation) after the SnCl₂ injection point was used to ensure sufficient mixing, and subsequent tubing and/or piping length provided the desired contact times. Samples taken after the desired contact time were designated as “reduced.”

Reduced water was fed to either cartridge filters in polypropylene filter housings or sand filters in PVC columns. Gradient density polypropylene (Pentek DGD series filter) and pleated cellulose polyester (Pentek ECP series filter) cartridge filters, designated as depth cartridge filters (DCFs) and pleated cartridge filters (PCFs), respectively, were tested at HLRs ranging from 1.0 to 24 m/h (0.4–10 gpm/ft²). At the time of testing, manufacturer-recommended HLRs were 24 m/h (10 gpm/ft²) and 2.0 m/h (0.8 gpm/ft²) for DCFs and PCFs, respectively. DCFs with nominal pore sizes of 1, 5, and 25 μm and PCFs with nominal pore sizes of 1, 5, and 20 μm were tested. Filter sand (Lapis Lustre Filter Sand F-105, CEMEX) with an effective size of 0.45–0.55 mm, a uniformity coefficient of 1.5, and a depth of 0.6 m (2.0 ft) was tested at HLRs ranging from 5 to 10 m/h (2.0–4.0 gpm/ft²). Samples taken after filtration were designated as “filtered.”

Water quality analysis

All Cr(T), Cr(VI), and total tin (Sn(T)) samples were collected in HDPE bottles and kept on ice or refrigerated until analysis by certified laboratories. Total metal samples were preserved with nitric acid. Total chromium was measured using inductively coupled plasma atomic emission spectroscopy (ICP–AES) according to USEPA Method 200.7¹ or inductively coupled plasma mass spectrometry (ICP–MS) according to USEPA Method 200.8.² Cr(VI) was measured colorimetrically following its reaction with diphenylcarbazide according to USEPA Method 218.6¹ or Standard Method 3500-Cr B.² For onsite confirmation of Cr(VI) reduction and/or reoxidation in the field, a colorimeter (DR890, Hach) or spectrophotometer (DR 2500, 4000, or 6000, Hach) was used with a programmed method (Hach Method 8023). Total tin was measured using ICP–AES according to USEPA Method 200.7^{2,3}. Depending on the laboratory, minimum reporting levels (MRLs) for Cr(T), Cr(VI), and Sn(T) ranged from 0.0005² to 0.010¹, 0.001¹ to 0.003², and 0.005² to 0.010³ mg/L, respectively. For samples that were below the MRL, the sample concentration was given the value of the MRL. Average relative standard deviations (RSDs) from experimental duplicate samples collected in separate sample bottles for Cr(T), Cr(VI), and Sn(T) were 4, 37, and 21%, respectively. Hexavalent chromium RSDs were skewed by high values from experimental duplicate samples with low concentrations (<0.008 mg/L). At higher Cr(VI) concentrations (0.030–0.100 mg/L), the average RSDs of experimental duplicates were less than 1%. Although not experimental duplicates, consistent Cr(VI) measurements can also be seen by the raw water values in Table 4.1. The pH was measured according to Standard

¹ Clinical Laboratory of San Bernardino, Inc., Grand Terrace, Calif.

² Ana-Lab Corp., Kilgore, Tex.

³ Weck Laboratories, Inc., City of Industry, Calif.

Method 4500-H+. Alkalinity was measured according to Standard Method 2320. Turbidity was measured according to USEPA Method 180.1 using a portable turbidimeter (2100P, Hach).

Microscopy

Scanning electron microscopy (JSM-6400, JEOL USA, Rocky Mountain Laboratories, Golden, CO) (SEM) at 15 keV coupled with energy-dispersive X-ray spectroscopy (EDS) was used to produce images and elemental spectra of deposits on filters used in this study. Gold was sputter-deposited on dried filter samples (area $\sim 1 \text{ cm}^2$) to a thickness of 3–6 nm. EDS was operated at a take-off angle of 35° and could detect all elements except hydrogen, helium, lithium, and beryllium with a typical detection limit of one part per thousand (0.1%). An image and spectral acquisition system (IXRF Systems) was used to acquire the SEM images and EDS spectra. Specifically, EDS was used to determine the relative compositions of chromium and tin captured on tested filters. Although atomic or mass percentages are part of the EDS output, interpretation of EDS data was largely qualitative in that environmental samples were not compared back with standards with known compositions. EDS elemental compositions are determined based on sensitivity factors built into software algorithms. EDS spectra are also limited to small areas of an entire SEM image and assume that the area selected for EDS is homogenous. The areas selected for EDS analysis were chosen as representing the entire filter, based on SEM observations of the entire sample and several EDS scans of different areas.

Chlorination

Unfiltered OK, CA-1, and CA-2 water was shipped to Denver, Colorado, for chlorination experiments. Each water was chlorinated following a modified uniform formation condition procedure from Summers et al. (1996) to investigate the potential reoxidation of Cr(III) to Cr(VI) (Summers et al., 1996). None of the waters were filtered before chlorination, which would represent a worst-case scenario as there would be more Cr(III) available for reoxidation. These experiments were conducted in chlorine demand free glassware. A SnCl_2 stock solution was added at doses ranging from 0.1 to 1.3 mg/L to 1 L of each water sample in a volumetric flask, which was then mixed for 1 min using a stir plate and stir bar. Reduced Cr(VI) concentrations between 0.010 and 0.020 mg/L were targeted to remain above the spectrophotometer detection limit of 0.010 mg/L. The average RSD for Cr(VI) from experimental duplicate samples was 7%. Following reduction, laboratory-grade (Thermo Fisher Scientific) 6% sodium hypochlorite (NaOCl) was dosed at 1.1 mg/L as Cl_2 to target a chlorine residual of $1.0 \pm 0.2 \text{ mg/L}$ as Cl_2 after one day. After mixing for an additional minute, water was poured into 250 mL amber glass bottles, headspace-free, and stored in the dark at $22 \pm 1^\circ\text{C}$. Free chlorine was measured using a spectrophotometer with a programmed method (Hach Method 8021), which was also the method used to confirm the absence of chlorine following GAC cartridge filtration at CA-1 and CA-2 well sites. Buffering and pH adjustment were not necessary, as pH was stable for all waters at 8.2 ± 0.2 . In the first test, samples were analyzed for Cr(VI) at one and four days after chlorine addition. In a second test, samples were analyzed for Cr(VI) at 10 min, one day, and three days after chlorine addition. Control bottles containing reduced water with no chlorine addition were included as part of the second test.

Results and Discussion

Stannous chloride dose response

Ideal reduction of Cr(VI) to Cr(III) by Sn(II) was assumed to follow the chemical equation shown in Figure 4.1. Accordingly, the stoichiometric MDR would be 1.5, and although other Cr(III) and Sn(IV) hydrolysis products likely form, the primary products (and potential precipitates) were assumed to be Cr(OH)₃(s) and SnO₂(s) (Brandhuber et al., 2004; Haynes et al., 2016; Jackson et al., 2013; Kaprara et al., 2017; Mathews et al., 2015; Pinakidou et al., 2016). Thermodynamic modeling software (OLI Systems, Inc.) also supported SnO₂(s) as the most favorable solid to form. Although an MDR of 1.5 would appear to be sufficient for complete Cr(VI) reduction, it was also assumed there would be competing reactions including reductant demands from oxidized species such as dissolved oxygen (Hozalski et al., 2010; Lee and Hering, 2003; Qin et al., 2005).

Therefore, multiple MDRs, ranging from 1.5 to 10, were tested for each water and sampled after contact times of 1, 2, and 4 min. The goal was to capture a range of removal levels down to a target final Cr(VI) concentration of <0.010 mg/L. Contact times of 1, 2, and 4 min were chosen following preliminary testing and highlight the fast reduction kinetics of SnCl₂. By comparison, typical contact times for Fe(II) RCF are 15–60 min, although 5 min is sufficient for Cr(VI) reduction if the Fe(II) dose is increased and chlorine is used to oxidize the remaining Fe(II) to Fe(III) (Blute et al., 2015a, 2015b; Qin et al., 2005; Wu et al., 2015). All samples taken during dose–response testing were collected through filter housings directly connected to sampling ports. Reduced water was sampled by filtering through 0.45 µm mixed cellulose ester filters in an attempt to distinguish the different contact times by changes in Cr(T) concentrations. This approach assumed that Cr(OH)₃(s) formation or filterability would change with the contact time. For example, if a contact time of 4 min yielded lower Cr(T) and Cr(VI) concentrations than a 1 min contact time, it could be concluded that the increased contact time allowed for more Cr(OH)₃(s) formation (that could be removed by 0.45 µm filtration). Otherwise, there would be no way to evaluate the effect of contact time, as the samples could not be analyzed within reagent reaction times for onsite analysis and hold times before certified laboratory analysis. On-site colorimetric or spectrophotometric methods were used to confirm Cr(VI) reduction, but otherwise all data presented are results from certified laboratories with lower MRLs. An oxidant such as chlorine could have been used to quench the reaction by oxidizing the remaining Sn(II) to Sn(IV) but would also interfere with speciation by reoxidizing Cr(III) to Cr(VI) (Brandhuber et al., 2004; Lai and McNeill, 2006; McNeill et al., 2012). It should also be noted that over the range of SnCl₂ doses tested, there was little to no change in pH or alkalinity for all three waters following SnCl₂ addition.

From a kinetic analysis standpoint, the data did not reveal any discernable difference between contact times. This lack of difference is likely a result of both fast reduction kinetics and logistical difficulties in sample collection and analysis. Two-way analysis of variance (ANOVA) was performed for each water using statistical software (Minitab, Inc) for both contact time and MDR. MDR was significant for all waters at the 95% confidence level. CA-1 and CA-2 ANOVA p-values for contact time were >0.2, indicating the insignificance (at the 95% confidence level) of contact time or at least the inability to capture an effect. The ANOVA p-value for OK was

<0.05 , indicating the significance of contact time, but the range of Cr(VI) concentration averages only spanned 0.005 mg/L, with overlapping 95% confidence intervals. As such, Cr(VI) concentrations at each contact time were averaged for each water and are shown as a function of SnCl₂ dose in Figure 2, part A, in which the error bars demonstrate the small spread of Cr(VI) concentrations across the three contact times. As shown in Figure 4.2a, SnCl₂ was effective at reducing Cr(VI) concentrations at all contact times tested. Interpolated SnCl₂ doses of 1.4, 0.6, and 0.2 mg/L, shown as the dashed lines in Figure 4.2a, would be sufficient to reduce Cr(VI) concentrations in OK, CA-1, and CA-2, respectively, to below 0.010 mg/L.

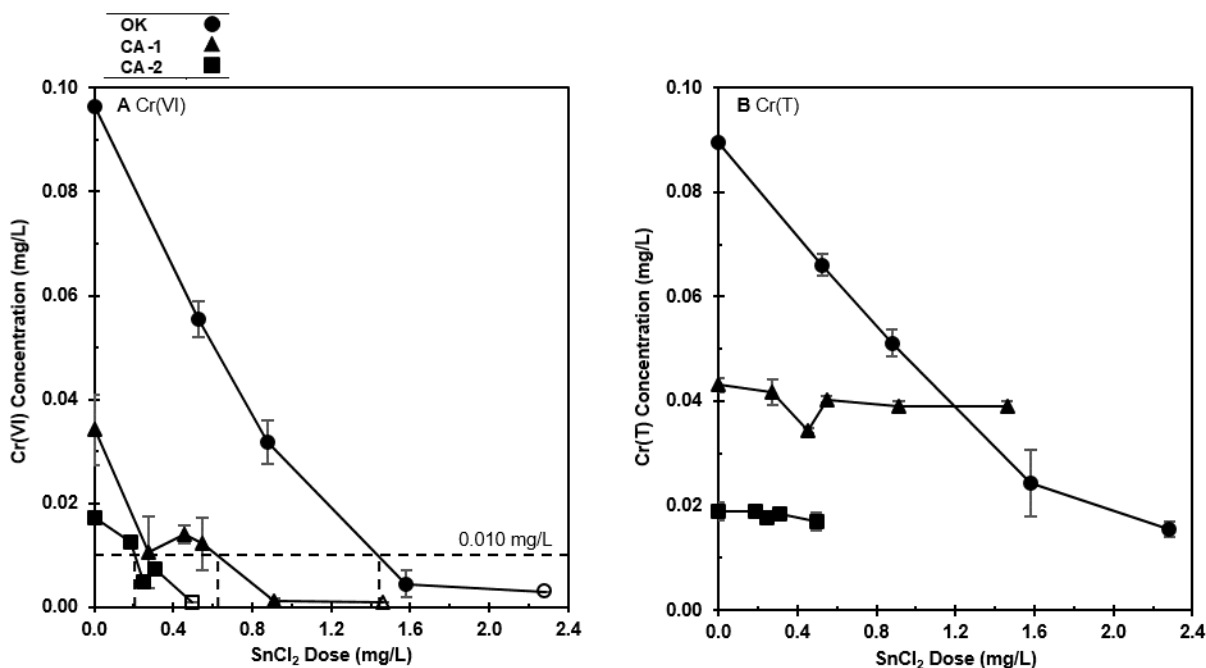


Figure 4.2. Dissolved Cr(VI) and Cr(T) concentrations in reduced samples after contact with SnCl₂ for all three waters. Each data point represents the average of the three contact times (1, 2, and 4 minutes) with errors bars as the standard deviation. Open symbols represent concentration less than MRL.

Similar to Figure 4.2a, Cr(VI) concentration as a function of normalized SnCl₂ dose, or MDR, is shown in Figure 4.3. Normalizing the SnCl₂ dose by the initial Cr(VI) concentration caused the three curves to collapse in the MDR range of 3–5, shown more clearly in the inset of Figure 4.3. For all three waters, an MDR of approximately 4 was required to reduce Cr(VI) to below 0.010 mg/L. Compared with Fe(II) RCF, McGuire et al. (2006) and Qin et al. (2005) observed a reduction in Cr(VI) from 0.100 to <0.010 mg/L at MDRs ranging from 9 to 47. More recently, Wu et al. (2015) observed the same Cr(VI) reduction using Fe(II) RCF at an MDR of 19, demonstrating a potential advantage of Sn(II) on a molar ratio basis. Given an initial Cr(VI) concentration, the curves in Figure 4.3 (and Figure 4.2a) can be useful for predicting SnCl₂ requirements to reach a target treated water Cr(VI) concentration. Preliminary SnCl₂ dose predictions would be limited to an initial Cr(VI) concentration range between 0.020 and 0.100 mg/L in groundwaters near pH 8. Regardless, bench-scale testing is recommended to determine site-specific SnCl₂ doses.

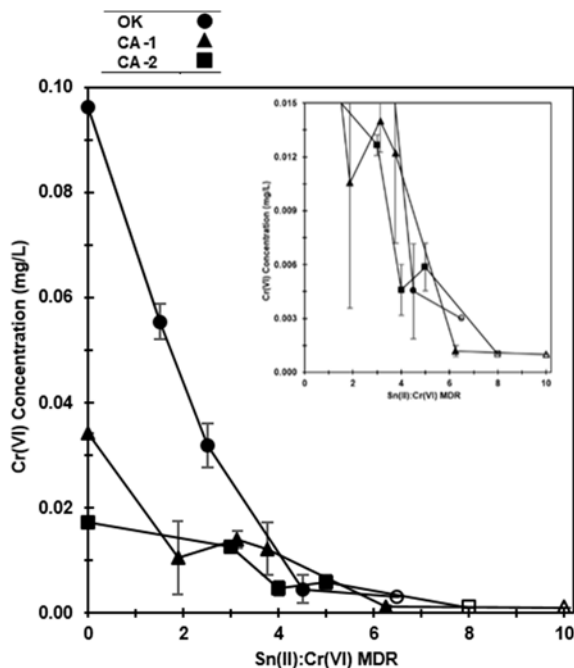


Figure 4.3. Dissolved Cr(VI) concentrations after contact with SnCl_2 for all three waters as function of MDR Each data point represents the average of the three contact times (1, 2, and 4 minutes) with errors bars as the standard deviation. Inset shows Cr(VI) concentrations less than 0.015 mg/L. Open symbols represent concentration less than MRL.

Total chromium removal or lack thereof by a $0.45\ \mu\text{m}$ filter as a function of SnCl_2 dose is shown in Figure 4.2b, for all three waters, averaged across contact times. The initial or raw Cr(T) concentration in OK shown in Figure 4.2b, is approximately $0.006\ \text{mg/L}$ lower than the Cr(VI) concentration shown in Figure 4.2a. This instance of a higher Cr(VI) concentration compared with Cr(T) was the only instance during testing and was attributed to experimental and analytical variability. No Cr(T) removal was observed in CA-1 and CA-2, indicating that any $\text{Cr}(\text{OH})_3(\text{s})$ particle formation was nominally smaller than $0.45\ \mu\text{m}$, likely related to its colloidal nature and solubility, as previously discussed. Conversely, Cr(T) removal was observed for OK and increased with SnCl_2 dose, for which a proposed explanation is twofold. First, it is hypothesized that increased $\text{SnO}_2(\text{s})$ formation and retention on $0.45\ \mu\text{m}$ filters in OK facilitated the removal of $\text{Cr}(\text{OH})_3(\text{s})$ through cake filtration (straining), adsorption, and/or coprecipitation. OK had the highest initial Cr(VI) concentration, which in all cases was assumed to be the limiting reactant. Therefore, increasing the Cr(VI) concentration at a given SnCl_2 dose would allow increased oxidation of Sn(II) to Sn(IV) (i.e., $\text{SnO}_2(\text{s})$ formation). This increase in Sn(II) to Sn(IV) oxidation is supported by the higher observed Sn(T) concentrations following $0.45\ \mu\text{m}$ filtration in CA-1 and CA-2 compared with OK. At a SnCl_2 dose of approximately $1.5\text{--}1.6\ \text{mg/L}$, OK and CA-1 had filtered Sn(T) concentrations of 0.1 ± 0.02 and $0.5\pm 0.03\ \text{mg/L}$, respectively. At a SnCl_2 dose of $0.3\ \text{mg/L}$, CA-2 had a filtered Sn(T) concentration of $0.08\pm 0.02\ \text{mg/L}$, which is the same as OK at a SnCl_2 dose of $0.9\ \text{mg/L}$. For lower Cr(VI) concentrations like those in CA-1 and CA-2, this indicates that the addition of an oxidant may aid filtration through forcing the formation of $\text{SnO}_2(\text{s})$. Second, it is hypothesized that higher particle concentrations in OK compared with CA-1 and CA-2 resulted in larger particle sizes and thus filterability. This concept is consistent with flocculation theory, which assumes that the rate of particle formation is proportional to the

number of smaller particles that collide to form larger particles (Benjamin and Lawler, 2013). Although reduced water turbidity values were similar for all waters (<2 NTU), it was assumed OK had higher particle concentrations from those existing in the raw water (Figure S1, Supporting Information), as it was not prefiltered using GAC cartridge filters, and from increased formation of $\text{Cr}(\text{OH})_3(\text{s})$ and $\text{SnO}_2(\text{s})$. Turbidity is also not the most accurate measure of particle concentrations. In general, $\text{Cr}(\text{OH})_3(\text{s})$ removal in OK, and not CA-1 or CA-2, was likely a result of higher concentrations of both $\text{Cr}(\text{OH})_3(\text{s})$ and $\text{SnO}_2(\text{s})$.

As briefly mentioned previously, in all cases during dose–response and subsequent testing, the addition of SnCl_2 caused the raw water turbidity to increase as a result of the formation of $\text{Cr}(\text{OH})_3(\text{s})$ and $\text{SnO}_2(\text{s})$ by a factor of 2–10 (e.g., 0.2–2.0 NTU). Most of the turbidity formation was attributed to tin because of its higher concentration, and EDS spectra showed higher signals, or counts, for tin compared with chromium. SEM images of used filters and the corresponding EDS spectra revealed that filtration removed amorphous solids without a well-defined crystalline structure. SEM images of the dried 0.45 μm filters used to remove Cr(T) from OK at a SnCl_2 dose of 1.6 mg/L are shown in Figure 4, parts A through C. The EDS spectrum of a representative area of an as-received filter revealed that >99% of the main elements in Figure 4.4a, were oxygen and carbon on an atomic basis, consistent with mixed cellulose ester filter materials. Solids captured on a used filter, shown in Figure 4.4b-c, reveal a visible cake for which the EDS spectrum (Figure B 2) showed significant signals for oxygen (68%) and tin (16%), with a small amount of chromium (2%), on an atomic basis. Therefore, the images in Figure 4.4b-c, as well as the associated EDS spectrum, are consistent with the mechanisms of cake filtration of $\text{Cr}(\text{OH})_3(\text{s})$ and its adsorption to and/or coprecipitation with $\text{SnO}_2(\text{s})$, resulting in the removal of Cr(T) in OK shown in Figure 4.2b. A cake was not observed in SEM images following filtration of CA-1 and CA-2, even at similar SnCl_2 doses. Therefore, through interpretation of Figure 4.2b, and Figure 4.4a-c through C, $\text{Cr}(\text{OH})_3(\text{s})$ removal appears to depend on its interactions with $\text{SnO}_2(\text{s})$ and raw water particle concentrations.

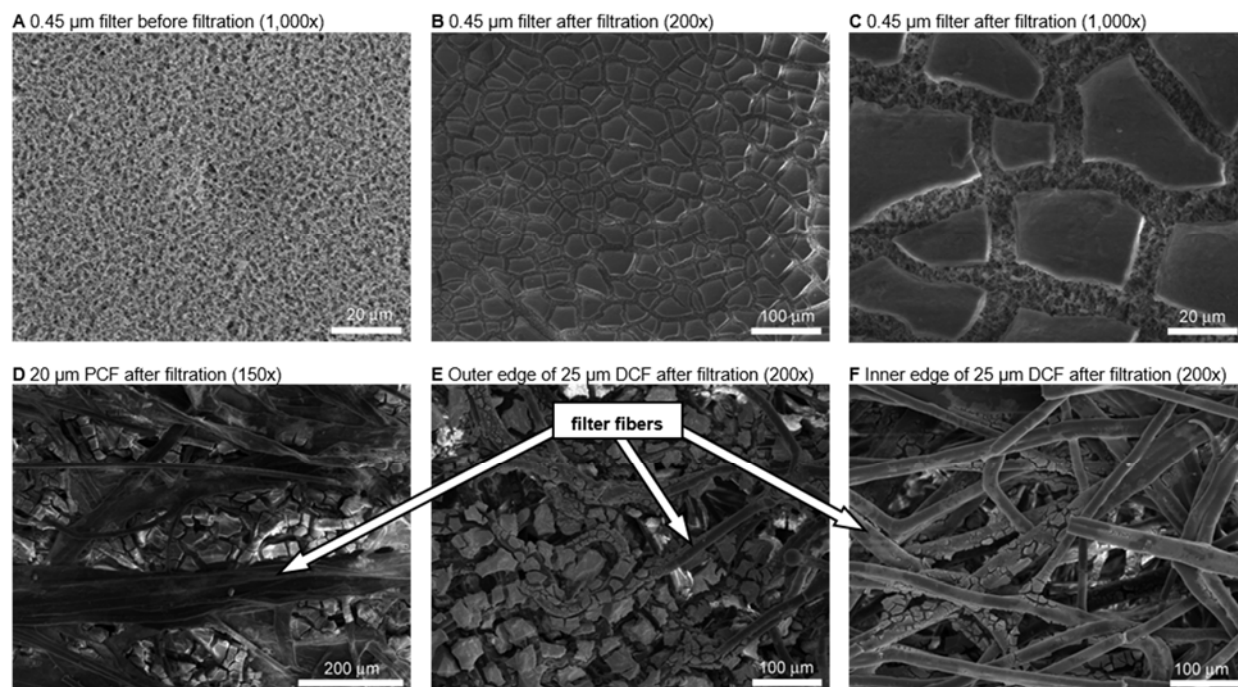


Figure 4.4. SEM images of filters tested with OK at SnCl_2 doses ranging from 1.5 to 1.8 mg/L

Cartridge filtration

With the dose requirements established, commercially available cartridge filters were tested with the goal of removing Cr(T) to <0.010 mg/L. Thus, SnCl_2 was dosed at concentrations targeting Cr(VI) reduction to <0.010 mg/L according to trends in Figure 4.2a, and Figure 4.3. Upon Cr(T) breakthrough, turbidity breakthrough, or terminal head loss, cartridge filters could be disposed of in a municipal or hazardous waste landfill. Waste classification would depend on whether Cr(T) concentrations are <5.0 mg/L in the extract from a toxicity characteristic leaching procedure (TCLP, SW-846 Test Method 1311). More stringent testing requirements and/or state regulations could exist as well, such as the California waste extraction test. Another reason cartridge filters were tested is their potential for use as decentralized treatment at individual wells as opposed to a large centralized facility.

PCFs were initially tested with the hypothesis that although Cr(T) was not removed by 0.45 μm filters from CA-1 and CA-2, the relatively large depth and surface area of PCFs would provide more opportunities for $\text{Cr}(\text{OH})_3(\text{s})$ attachment and/or adsorption to $\text{SnO}_2(\text{s})$. PCFs were operated at an HLR of 2.0 m/h (0.8 gpm/ft²) for all waters. Within hours of starting filtration, it was clear from the lack of turbidity removal that PCFs were unable to remove significant amounts of Cr(T) and Sn(T) despite a visible green precipitate on the filter with OK (Figure B 3), indicative of the presence of $\text{Cr}(\text{OH})_3(\text{s})$ (Haynes et al. 2016). Sampling of the PCF influent and effluent water confirmed little to no removal of Cr(T) or Sn(T). An SEM image of a 20 μm PCF after 10 h of filtration of OK is shown in Figure 4.4d. The SEM image shows that the majority of particles were captured in the pores between the PCF fibers as opposed to on the fibers. Unlike 0.45 μm filtration, a surface cake did not form, likely due to larger pore sizes.

On the basis of the results of PCF testing, DCFs were tested to investigate whether even greater depth and surface area would provide more opportunities for $\text{Cr}(\text{OH})_3(\text{s})$ attachment and/or adsorption to $\text{SnO}_2(\text{s})$. It should be acknowledged here that the term “depth filtration” is used loosely for DCFs, as depth filtration mechanisms for particle capture are generally associated with granular media filtration (Benjamin and Lawler, 2013). Fibers in cartridge filters are synthetic and closer in diameter (20–100 μm) to filterable particles (0.1–100 μm) compared with granular media for which grain or collector diameters (400–2,000 μm) are orders of magnitude larger than filterable particles. There are likely some similarities between DCFs and granular media filters, but the main design mechanism of DCFs is straining—hence the nominal pore size ratings.

Initial DCF experiments were performed with OK and CA-1 at a relatively low HLR of 1.0 m/h (0.4 gpm/ft²) with three DCFs (25, 5, and 1 μm) operated in series and showed good Cr(T) removal. Stannous chloride contact time was 5 and 1 min for OK and CA-1, respectively. DCFs operated 552 h at OK and 16 h at CA-1 pilot locations, with relatively slow head loss development of 103 kPa (15 psi) and <9.7 kPa (1.4 psi), respectively. Results are shown in Figure 4.5 and were averaged over the entire run as Cr(VI) and Cr(T) filtered concentrations were relatively consistent. Total tin was not measured during this phase of testing.

As expected from the dose–response testing, Cr(VI) was reduced to below 0.010 mg/L for both OK (Figure 5, part A) and CA-1 (Figure 4.5b). Total chromium was removed in OK to below 0.010 mg/L during the first 100 h for the 25 μm DCF and the entire run for the 5 and 1 μm DCFs. Total chromium was removed in CA-1 to below 0.010 mg/L by the 25 μm DCF throughout the entire run. These results indicate that DCFs were able to capture $\text{Cr}(\text{OH})_3(\text{s})$, likely due in part to simultaneous capture of $\text{SnO}_2(\text{s})$, and the added filtration depth. $\text{Cr}(\text{OH})_3(\text{s})$ capture was also observable by the green color of the DCFs following testing (Figure B 4). All Cr(T) removal in OK (first 100 h) and CA-1 occurred across the first 25 μm DCF, indicating that the increase in filtration depth and surface area of the DCFs compared with PCFs (in addition to the lower HLR) was more important than the nominal pore size of the DCFs. Interestingly, as shown in Figure 4.5b, Cr(T) in the effluent of the 25 μm DCF in CA-1 was able to pass through the 5 and 1 μm DCFs, which may be due to a lack of accumulation of $\text{SnO}_2(\text{s})$ on those filters.

Total chromium breakthrough in OK, a depth filtration and adsorption phenomenon, was observed in the effluent of the 25 μm DCF, which is the reason for the high Cr(T) concentration and large error bars in Figure 5, part A. Total chromium breakthrough in OK is shown separately in Figure 4.5c. Integration of the breakthrough curve in Figure 4.5c, reveals that approximately 2 g of chromium was captured on the 25 μm DCF. Although a TCLP test was not performed on any DCFs, this solid-phase concentration highlights the potential for DCFs to qualify as hazardous waste. Turbidity breakthrough, also shown in Figure 4.5c, trended with Cr(T), suggesting that turbidity may be a useful surrogate for monitoring Cr(T) breakthrough. DCFs were not operated long enough to observe Cr(T) or turbidity breakthrough in OK in the effluents of the 5 or 1 μm DCFs. Total chromium capture in OK by both the 25 and 5 μm DCFs further emphasized the importance of filter depth and likely $\text{SnO}_2(\text{s})$ accumulation over nominal pore size.

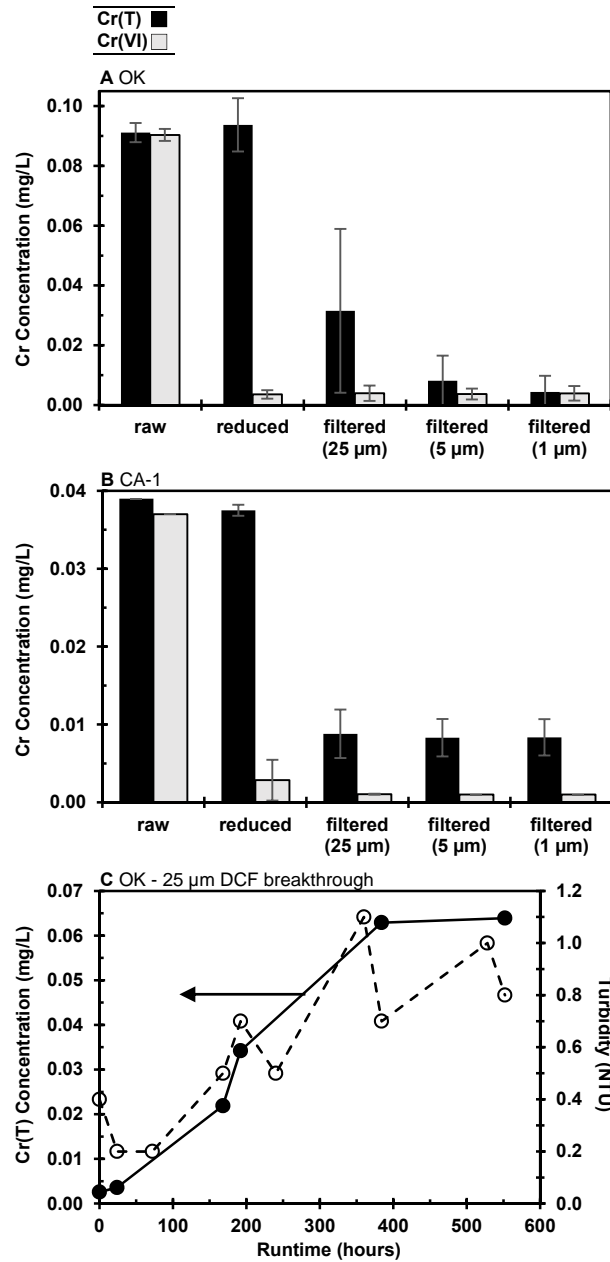


Figure 4.5. Raw, reduced, and filtered Cr(T) and Cr(VI) concentrations during low HLR DCF testing Each bar represents the average over entire run with error bars as the standard deviation (n=2 to 7). HLR: 1.0 m/h (0.4 gpm/ft²). OK conditions: 2.5 mg/L SnCl₂, 5 minute contact time, 552 hour runtime. CA-1 conditions: 0.7 mg/L SnCl₂, 1 minute contact time, 16 hour runtime

Following initial DCF experiments, testing was performed on individual DCFs (not in series) at a higher HLR of 24 m/h (10 gpm/ft²), as this HLR would be more realistic of full-scale operation. DCFs were not run in series at the higher HLR because the results from low HLR testing demonstrated nominal pore size had less of an impact than the added filtration depth and surface area of DCFs compared with PCFs. For all three waters, however, Cr(T) removal significantly decreased compared with the lower HLR testing, as it is hypothesized that higher HLRs decreased the time available for attachment to DCF fibers. Results are shown in Figure 4.6

and were averaged over the entire run as Cr(VI) and Cr(T) filtered concentrations were relatively consistent. Total chromium removals between 60 and 70% were observed in OK, while Cr(T) removals in CA-1 and CA-2 were less than 50%. Higher Cr(T) removal in OK was likely due to the previously discussed mechanisms pertaining to SnO₂(s) interactions and increased raw water particle concentrations. Head loss development in all waters was typical for pressure filters, up to 200 kPa (29 psi) over 24 h. However, considering that the DCFs tested are typically not reusable, the rate of head loss accumulation was deemed unacceptable.

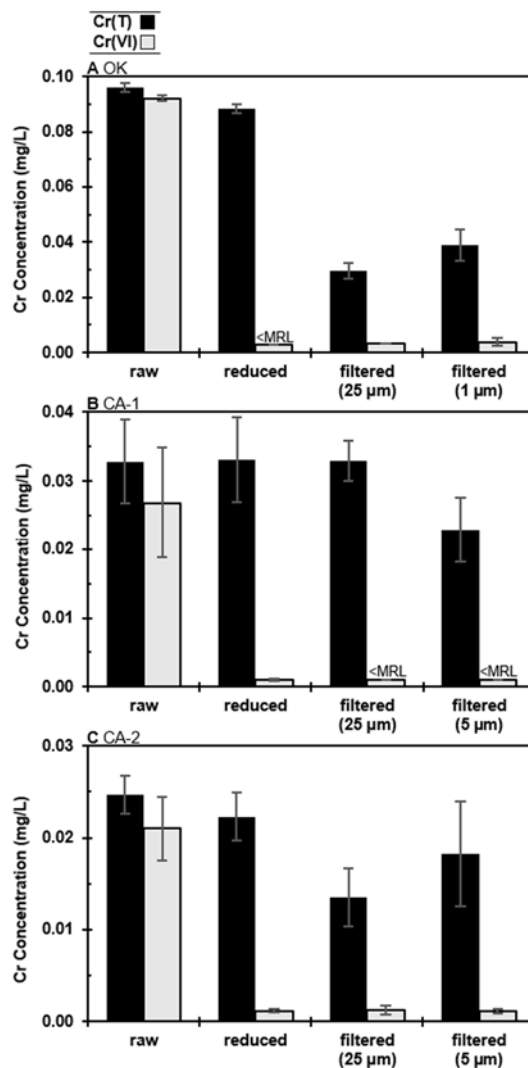


Figure 4.6. Raw, reduced, and filtered Cr(T) and Cr(VI) concentrations during high HLR DCF testing Each bar represents the average over entire run with error bars as the standard deviation (n=2 to 7). HLR: 24 m/h (10 gpm/ft²). SnCl₂ contact time: 1 minute (OK) and 3 minutes (CA-1 and CA-2). OK conditions: 1.5 mg/L SnCl₂, 20 to 24 hour runtime. CA-1 conditions: 0.7 mg/L SnCl₂, 3 to 41 hour runtime. CA-2 conditions: 0.4 mg/L SnCl₂, 2 to 40 hour runtime.

There was no significant difference in Cr(T) removal between the different pore size DCFs when operated at the same HLR, further confirming that increased Cr(T) removal was attributable to the increased depth and surface area compared with 0.45 µm filters and PCFs. Particle removal in OK with depth is illustrated by the SEM images shown in Figure 4.4, where

the outer edge of the 25 μm DCF is shown in Figure 4, part E, and the inner edge of the same DCF is shown in Figure 4.4f. Near-complete coverage of the outer fibers was observed, while a smaller but still visible degree of coverage was observed on the inner fibers after a run time of 24 h. Regardless, because filtered Cr(T) concentrations were >0.010 mg/L and head loss development was unacceptable, DCFs were deemed impractical for removal of Cr(T) under the range of conditions tested.

Sand Filtration

Despite the conclusion that DCFs were not a practical solution for the removal of Cr(T), DCF experiments indicated that depth filtration using granular media may be successful by greatly increasing the attachment opportunities through increased filter depth and collector surface area. Thus, a typical drinking water sand filter was operated with OK and CA-1 at SnCl₂ doses targeting Cr(VI) reduction to <0.010 mg/L according to trends in Figure 2, part A, and Figure 4.3. OK was run at an HLR of 5.0 m/h (2.0 gpm/ft²), while CA-1 was run at HLRs of 5.0 m/h, termed run 1, and 10 m/h (4.0 gpm/ft²), termed run 2 following a backwash. Samples for certified laboratory analysis were collected only for Cr(T) and Sn(T), as Cr(VI) reduction was verified on-site using a colorimeter or spectrophotometer. Results are shown in Figure 4.7a, for Cr(T) and Figure 4.7b, for Sn(T), and were averaged over the entire run as Cr(T) and Sn(T) filtered concentrations were relatively consistent.

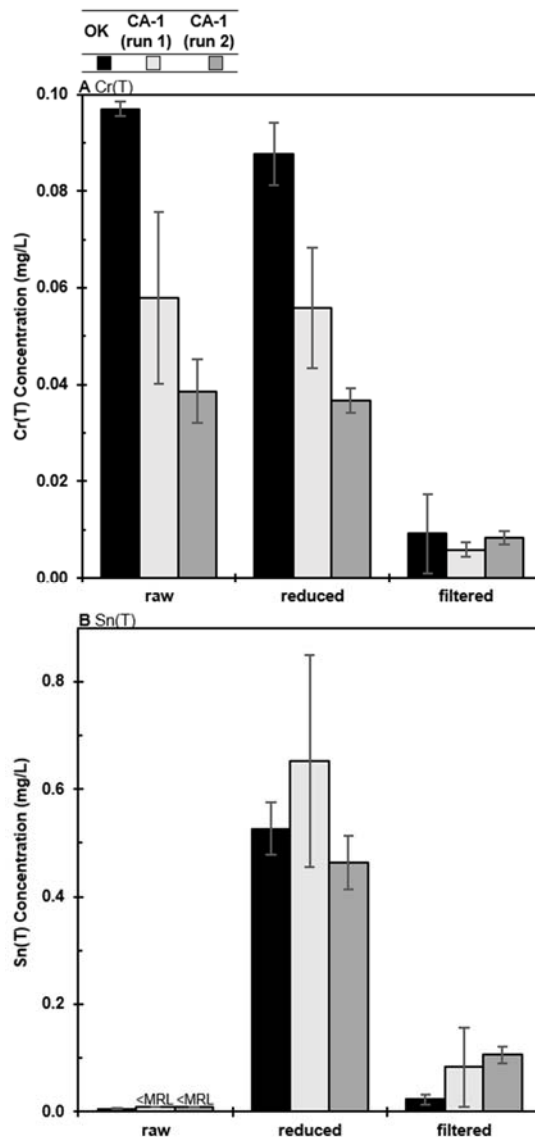


Figure 4.7. Raw, reduced, and filtered Cr(T) and Sn(T) concentrations during sand filtration testing. Each bar represents the average over the entire run with error bars as the standard deviation (n=4 to 7). OK conditions: 1.5 mg/L SnCl₂ at 1 minute of contact time, 55 hour runtime, HLR of 5.0 m/h (2.0 gpm/ft²) CA-1 (run 1) conditions: 1.2 mg/L SnCl₂ at 3 minutes of contact time, 37 hour runtime, HLR of 5.0 m/h (2.0 gpm/ft²). CA-1 (run 2) conditions: 1.2 mg/L SnCl₂ at 3 minutes of contact time, 24 hour runtime, HLR of 10 m/h (4.0 gpm/ft²).

Total chromium was removed to <0.010 mg/L over run times of 55, 37, and 24 h for OK, CA-1 (run 1), and CA-1 (run 2), respectively. These results indicate that increased depth and surface area from an increased number of collectors were able to successfully capture Cr(OH)₃(s) and SnO₂(s). Unlike DCFs at higher HLRs, head loss was minimal for all sand filter runs at <28 kPa (4 psi), and therefore run time was the trigger for terminating filter runs. Total chromium concentrations in raw CA-1 during run 1 fluctuated between 0.033 and 0.074 mg/L, as shown by the large error bars in Figure 4.7a. This was due to Cr(VI) desorption from the GAC cartridge filter, but influent Cr(VI) concentrations stabilized to the concentrations in Table 4.1 by the start

of run 2. Doubling the HLR with CA-1 (run 2) did not negatively affect Cr(T) removal or head loss development, indicating that higher HLRs should be tested further.

Total tin results in Figure 4.7b, show concentrations <0.010 mg/L in the raw waters, followed by an increase after SnCl₂ addition. However, concentrations in reduced water were consistently lower than expected for all testing by approximately 15–45%. Tin deposition as a gray solid, which is indicative of SnO₂(s) (Haynes et al., 2016), was visually apparent on pilot equipment, especially within the static mixer. This is a concern not only for the treatment process but also for a distribution system, especially if SnO₂(s) can adsorb Cr(III) (Kaprra et al., 2017; Pinakidou et al., 2016). Therefore, Sn(T) removal by filtration may be necessary for preventing accumulation in the distribution system. The results in Figure 4.7b, appear promising, as Sn(T) was removed by sand filtration to <0.015 mg/L. In regulatory terms, tin is not listed in the USEPA primary or secondary drinking water regulations, but the Minnesota Department of Health has set a human health–based guideline for tin at 4 mg/L as Sn in drinking water (MDH, 2017). Related to the previous discussion concerning Cr(T) removal or lack thereof in Figure 4.2b, the results in Figure 4.7b, also show higher Sn(T) concentrations in CA-1 compared with OK following filtration.

Although effective for the removal of Cr(T) and Sn(T), the approach to testing sand filters was solely as a proof of concept and did not simulate full-scale filter operation. Therefore, further testing is needed to evaluate long-term operation, backwashing, and backwash residual management.

Trivalent Chromium Reoxidation

Following reduction of Cr(VI) to Cr(III) using SnCl₂ (or any reductant), there is a concern about reoxidizing Cr(III) back to Cr(VI) in the distribution system following chlorine disinfection—hence the primary importance of Cr(T) removal before distribution. Reoxidation experiments performed by Lai and McNeill (2006) and Brandhuber et al. (2004) with 0.5–10 mg/L as Cl₂ (free chlorine and chloramines) over two to seven days resulted in 25–82% reoxidation of Cr(III) to Cr(VI) ($C_0 = 0.100$ mg/L) in a natural groundwater at pH 7. Clifford and Chau (1988) observed $<5\%$ reoxidation of Cr(III) ($C_0 = 0.200$ mg/L, added as chromium chloride (CrCl₃)) to Cr(VI) in deionized water, deionized water with 0.01 M sodium chloride (NaCl), or tap water at pH 7 and 8 (Clifford and Chau, 1988).

Results of chlorination experiments shown in Table 4.2 are averages of two tests with simulated distribution system hold times of three and four days, indicating the potential for partial reoxidation within this contact time. The second test revealed that a significant portion of the reoxidation occurred within 10 min of chlorine addition. Therefore, changes in Cr(VI) concentrations $\Delta\text{Cr(VI)} = \text{Cr(VI)}_t - \text{Cr(VI)}_0$ were averaged across time for each water. Following chlorine addition, the amount of Cr(III) to Cr(VI) reoxidation ranged from 0.005 to 0.021 mg/L, and increased with increasing raw water Cr(VI) concentrations. Little to no Cr(VI) reoxidation was measured in the control bottles. Therefore, in agreement with Lai and McNeill (2006) and Brandhuber et al. (2004), it is apparent that under similar conditions, Cr(T) should be removed following SnCl₂ reduction and before chlorine addition and distribution.

Table 4.2. Cr(VI) concentrations after SnCl₂ reduction followed by contact with free chlorine for 3 to 4 days

Water	Initial Cr(VI) Concentration (mg/L)	SnCl ₂ Dose (mg/L)	Sn(II):Cr(VI) MDR	Reduced Cr(VI) Concentration (mg/L)	ΔCr(VI) Concentration (mg/L)	
					1.1 mg/L as Cl ₂	No Cl ₂ added
OK	0.102±0.004	1.3	3.5	0.013±0.002	+0.021±0.011	-0.002±0.002
CA-1	0.035±0.001	0.2	1.6	0.018±0.002	+0.008±0.000	+0.000±0.001
CA-2	0.026±0.001	0.1	1.1	0.015±0.002	+0.005±0.001	+0.003±0.001

Values are average ± standard deviation (n=3 to 4) combined from two tests
 SnCl₂ contact time was 1 minute
 Chlorine demand measured in all bottles was 0.1 to 0.2 mg/L as Cl₂ at all hold times

Conclusions

General conclusions of this study are qualitatively summarized in Table 4.3. SnCl₂ doses ranging from 0.2 to 1.5 mg/L (MDRs of 3.2–4.3) were effective for reducing Cr(VI) concentrations ranging from 0.019 to 0.092 mg/L, respectively, to <0.010 mg/L within 5 min of contact time in three natural groundwaters. Using 0.45 μm filters, Cr(T) or Cr(OH)₃(s) was only filterable in OK, likely as a result of the formation of a SnO₂(s) cake. By plotting Cr(VI) concentrations as a function of normalized SnCl₂ dose, or MDR, sufficient Cr(VI) reduction can be expected with MDR values of approximately 4. Following SnCl₂ dose testing, a series of filtration studies were performed using PCFs, DCFs, and sand filters. PCFs were unable to sufficiently remove Cr(T) at rated HLRs. At low HLRs, DCFs were able to remove Cr(T) to <0.010 mg/L, but adequate Cr(T) removal was not achieved at more realistic, higher HLRs. Conventional sand filtration was able to remove Cr(T) to <0.010 mg/L over day-long filter runs with low head loss. On the basis of the filtration studies, it can be concluded that depth filtration mechanisms are required for Cr(T) removal. Without filtration, there is the potential for partial Cr(III) reoxidation to Cr(VI) in the presence of free chlorine. As these tests were highly controlled, they also highlight that Cr(III) reoxidation under variable distribution system conditions is unknown and may be problematic on the basis of these findings.

Table 4.3. Qualitative summary of testing

Treatment Step	Cr(VI)	Cr(T)	Turbidity	Head Loss
SnCl ₂ addition	Cr(VI) to Cr(III) reduction within minutes	Shift from Cr(VI) to Cr(III)	High compared to raw water	N/A
Pleated cartridge filtration	No removal	No removal	No removal	Minimal at practical HLRs
Depth cartridge filtration	No removal	Poor removal at practical HLRs	Near raw water	High at practical HLRs
Sand filtration	No removal	Good removal at practical HLRs	Near raw water	Minimal at practical HLRs
Chlorination (no filtration)	Partial Cr(III) to Cr(VI) reoxidation	Partial shift from Cr(III) to Cr(VI)	Not measured	N/A

Although the results of this study build upon previous work and show promise for using SnCl₂ as a Cr(VI) treatment process, there are still many potential issues with the long-term use of SnCl₂, which will require further research, including (1) SnCl₂ solution stability, (2) SnO₂(s)

deposition on water treatment and distribution system components (e.g., filter media, piping), (3) Cr(III) and potentially Cr(VI) adsorption to SnO₂(s), and (4) disposal of filter media and/or backwash residuals. Long-term pilot studies should be performed to address the remaining questions to more fully assess the feasibility of using SnCl₂ for Cr(VI) treatment in drinking water.

Conclusions and Recommendations

Two treatment technologies were tested to determine hexavalent chromium removal efficiency and associated waste production. Each process was tested at the pilot scale of operation over several months of operation and multiple runs. Bench scale testing was used to augment the pilot testing when necessary.

Strong base anion exchange was one of the treatment technologies tested. Strong base anion exchange uses exchangeable functional groups that have a higher affinity for constituents, such as hexavalent chromium, than the chloride ion used for regeneration. Tests were conducted at loading rates ranging from 8 to 15 gpm/ft² at resin bed depths of 36 inches as recommended by the resin suppliers. Pilot columns of 1.5 and 2 inches in diameter were operated until complete exhaustion with respect to hexavalent chromium. Operational throughput was at least 30,000 bed volumes until hexavalent chromium was detected in the effluent, for the waters tested in these studies. When strong base ion exchange columns are regenerated, a concentrated chloride regeneration solution was passed through the columns at a regeneration rate of approximately 0.37 gpm/ft³. A 2-stage regeneration process was determined to be optimal for regeneration with respect to hexavalent chromium to minimize leakage when the process was put back online treating water. Approximately 2 to 5 bed volumes of 2.0 N NaCl regenerant solution was required to elute the majority of the hexavalent chromium, where greater regenerant volumes were required to fully elute nitrate. The waste brine eluting from the regeneration of the strong base ion exchange column is the greatest cost and environmental consideration for operating the process. Treating the waste brine with nanofiltration could play an integral role in managing waste brine from SBA processes treating for hexavalent chromium by reducing waste volumes to less than 1 BV and reducing regenerant salt make-up for next regeneration cycle. Further studies would be required to assess the impacts of concentrating nitrate in the regenerant brine after nanofiltration treatment. Preliminary system sizing demonstrated that the membrane area required would be reasonable for a mobile treatment unit to service a decentralized network of SBA treatment processes.

Stannous chloride reduction of hexavalent chromium was the second treatment technology tested in this study. Stannous chloride doses ranging in molar dose ratio from 3.2 to 4.3 were effective for reducing hexavalent chromium concentrations to below 0.010 mg/L, and form a filterable chromium precipitate, within 5 minutes of contact time for three natural groundwaters. A series of filtration studies were performed using pleated and depth cartridge filters and sand media filters. Of the filtration technologies tested, only conventional sand filtration was able to remove filterable chromium to less than 0.010 mg/L over day-long filter runs, at loading rates reasonable for plant design (2-4 gpm/ft²) coupled with low head loss. On the basis of the filtration studies, it can be concluded that depth filtration mechanisms were required for filterable chromium removal. It is recommended that further testing be conducted to optimize filtration, focusing on filter response following a backwash, filtration rate, filter run time, filter media material and filter media size.

The basis of the work contained within this study is to test process and chemical concepts and ultimately validate their application to full-scale treatment designs through rigorous and extended operational pilot and bench scale tests. Using results determined from the loading rate, regeneration, backwash rate, waste generation and chemical dosing requirements for each respective process, water treatment equipment sizing and footprint can be accurately designed.

Optimal technology selection can be made based on spatial distribution of raw water sources, infrastructure tie-in availability at sites (sewer, power), waste generation and disposal and process operational requirements.

Chapter 5. References

- Allègre, C., Moulin, P., Maisseu, M., Charbit, F., 2006. Treatment and reuse of reactive dyeing effluents. *J. Memb. Sci.* 269, 15–34. <https://doi.org/10.1016/j.memsci.2005.06.014>
- Bailes, R.H., 1957. Topical Report DOW-162, Raw Materials Division of the U.S. Atomic Energy Commission.
- Bailes, R.H., Ellis, D.A., Long, R.S., 1958. Anionic Exchange Process for the Recovery of Uranium and Vanadium from Carbonate Solutions. 2,864,667.
- Ball, J.W., Izbicki, J.A., 2004. Occurrence of hexavalent chromium in ground water in the western Mojave Desert, California. *Appl. Geochemistry* 19, 1123–1135. <https://doi.org/10.1016/j.apgeochem.2004.01.011>
- Benjamin, M.M., Lawler, D.F., 2013. *Water quality engineering : physical/chemical treatment processes*. John Wiley & Sons, Hoboken, NJ.
- Bhattacharjee, S., Chen, J.C., Elimelech, M., 2001. Coupled model of concentration polarization and pore transport in crossflow nanofiltration. *AIChE J.* 47, 2733–2745. <https://doi.org/10.1002/aic.690471213>
- Bissen, M., Frimmel, F.H., Ag, C., 2003. Arsenic – a Review . Part I : Occurrence , Toxicity , Speciation , Mobility. *Acta Hydrochim. Hydrobiol.* 31, 9–18.
- Blute, N., Wu, X., Cron, C., Fond, L., Froelich, D., Abueg, R., 2015a. Microfiltration in the RCF Process for Hexavalent Chromium Removal From Drinking Water, Water Research Foundation Report No. 4365. Denver, CO.
- Blute, N., Wu, X., Imamura, G., Song, Y., Porter, K., Cron, C., Fong, L., Froelich, D., Abueg, R., Henrie, T., Ramesh, S., Vallejo, F., 2015b. Assessment of Ion Exchange , Adsorptive Media, and RCF for Cr (VI) Removal, Water Research Foundation, Project No. 4423. Denver, CO.
- Boari, G., Liberti, L., Merli, C., Passino, R., 1974. Exchanger Equilibria on Anion Resin. *Desalination* 15, 145–166. <https://doi.org/10.1017/CBO9781107415324.004>
- Bowen, W.R., Mukhtar, H., 1996. Characterization and prediction of separation performance of nanofiltration membranes. *J. Memb. Sci.* 112, 263–274. [https://doi.org/10.1016/0376-7388\(95\)00302-9](https://doi.org/10.1016/0376-7388(95)00302-9)
- Brandhuber, P., Frey, M., McGuire, M., Chao, P.F., Seidel, C., Amy, G., Yoon, J., McNeil, L., Banerjee, K., 2004. Low-Level Hexavalent Chromium Treatment Options: Bench-Scale Evaluation, Water Research Foundation, Project No. 2814. Denver, CO.
- Cartier, S., Theoleyre, M., Decloux, M., 1997. Treatment of sugar decolorizing resin regeneration waste using nanofiltration. *Desalination* 113, 7–17.

[https://doi.org/10.1016/S0011-9164\(97\)00110-0](https://doi.org/10.1016/S0011-9164(97)00110-0)

- Cassano, A., Della Pietra, L., Drioli, E., 2007. Integrated membrane process for the recovery of chromium salts from tannery effluents. *Ind. Eng. Chem. Res.* 46, 6825–6830. <https://doi.org/10.1021/ie070144n>
- Clifford, D.A., Chau, J.M., 1988. The Fate of Chromium (III) in Chlorinated Water: Project Summary, 94th Editi. ed. US Environmental Protection Agency, Water Engineering Research Laboratory.
- Clifford, D.A., Zhang, Z., 1995. Removing Uranium and Radium from Groundwater by Ion Exchange Resins, in: Sengupta, A.K. (Ed.), *Ion Exchange Technology*. Technomic Publishing AG, Basel, Switzerland, p. 377.
- Clifford, D., Weber, W., 1983. The Determinants of Divalent/Monovalent Selectivity in Anion Exchangers. *React. Polym.* 1, 77–89.
- Frey, M.M., Seidel, C., Edwards, M., Parks, J.L., McNeill, L., 2004. Occurrence Survey of Boron and Hexavalent Chromium, Water Research Foundation Project #2759. Water Research Foundation Project #2759, Denver, CO.
- Ghorbani, Y., Montenegro, M.R., 2016. Leaching behaviour and the solution consumption of uranium-vanadium ore in alkali carbonate-bicarbonate column leaching. *Hydrometallurgy*. <https://doi.org/10.1016/j.hydromet.2016.02.004>
- Gilron, J., Gara, N., Kedem, O., 2001. Experimental analysis of negative salt rejection in nanofiltration membranes. *J. Memb. Sci.* 185, 223–236. [https://doi.org/10.1016/S0376-7388\(00\)00639-6](https://doi.org/10.1016/S0376-7388(00)00639-6)
- Gorman, C., Seidel, C., Henrie, T., Huang, L., Thompson, R., 2016. Pilot Testing Strong Base Anion Exchange for CrVI Removal. *J. Am. Water Works Assoc.* 108, 240–246.
- Gu, B., Ku, Y.K., Brown, G.M., 2005. Sorption and desorption of perchlorate and U(VI) by strong-base anion-exchange resins. *Environ. Sci. Technol.* 39, 901–907. <https://doi.org/10.1021/es049121f>
- Guter, G.A., 1995. Nitrate Removal from Contaminated Groundwater By Anion Exchange, in: Sengupta, A.K. (Ed.), *Ion Exchange Technology*. Technomic Publishing AG, Lancaster, Pennsylvania, p. 377.
- Hafiane, A., Lemordant, D., Dhahbi, M., 2000. Removal of hexavalent chromium by nanofiltration. *Desalination* 130, 305–312. [https://doi.org/10.1016/S0011-9164\(00\)00094-1](https://doi.org/10.1016/S0011-9164(00)00094-1)
- Hagemeyer, G., Gimbel, R., 1999. Modelling the rejection of nanofiltration membranes using zeta potential measurements. *Sep. Purif. Technol.* 15, 19–30. [https://doi.org/10.1016/S1383-5866\(98\)00050-1](https://doi.org/10.1016/S1383-5866(98)00050-1)

- Hagmeyer, G., Gimbel, R., 1998. Modelling the salt rejection of nanofiltration membranes for ternary ion mixtures and for single salts at different pH values. *Desalination* 117, 247–256. [https://doi.org/10.1016/S0011-9164\(98\)00109-X](https://doi.org/10.1016/S0011-9164(98)00109-X)
- Haynes, W.M., Lide, D.R., Bruno, T.J., 2016. *CRC Handbook of Chemistry and Physics*, 94th Edition. CRC Press. <https://doi.org/10.1201/B15040>
- Hollis, E.T., 1958. Laboratory Studies in Carbonate Ion Exchange for Uranium Recovery (No. WIN-88), U.S. Atomic Energy Commission.
- Hornig, L.-L., Clifford, D., 1997. The behavior of polyprotic anions in ion-exchange resins. *React. Funct. Polym.* 35, 41–54. [https://doi.org/10.1016/S1381-5148\(97\)00048-5](https://doi.org/10.1016/S1381-5148(97)00048-5)
- Hozalski, R.M., Elizabeth, E.A., Chen, C.F., 2005. Comparison of stannous chloride and phosphate for lead corrosion control. *J. Am. Water Works Assoc.* 97, 89–103.
- Hozalski, R.M., Tan, Y., Dai, X., 2010. An Investigation of Stannous Chloride as an Inhibitor of Lead Corrosion, Water Research Foundation Report No. 3174. Denver, CO.
- Izbicki, J. a., Wright, M.T., Seymour, W. a., McCleskey, R.B., Fram, M.S., Belitz, K., Esser, B.K., 2015. Cr(VI) occurrence and geochemistry in water from public-supply wells in California. *Appl. Geochemistry* 63, 203–217. <https://doi.org/10.1016/j.apgeochem.2015.08.007>
- Jackson, D.G., Looney, B.B., Craig, R.R., Thompson, M.C., Kmetz, T.F., 2013. Development of Chemical Reduction and Air Stripping Processes to Remove Mercury from Wastewater. *J. Environ. Eng.* 139, 1336–1342. [https://doi.org/10.1061/\(ASCE\)EE.1943-7870.0000761](https://doi.org/10.1061/(ASCE)EE.1943-7870.0000761)
- Jensen, V.B., Darby, J.L., 2016. Brine Disposal Options for Small Systems in California's Central Valley. *J. Am. Water Works Assoc.* 108:5, 276–289.
- Kaprara, E., Tziarou, N., Kalaitzidou, K., Simeonidis, K., Balcells, L., Pannunzio, E. V., Zouboulis, A., Mitrakas, M., 2017. The use of Sn(II) oxy-hydroxides for the effective removal of Cr(VI) from water: Optimization of synthesis parameters. *Sci. Total Environ.* 605–606, 190–198. <https://doi.org/10.1016/j.scitotenv.2017.06.199>
- Kaufman, D., Lower, G., 1954. A Summary Report on the Ion Exchange Process for the Recovery of Uranium (No. ACCO-68), U.S. Atomic Energy Commission.
- Korak, J.A., Huggins, R., Arias-Paic, M., 2017. Regeneration of pilot-scale ion exchange columns for hexavalent chromium removal. *Water Res.* 118, 141–151. <https://doi.org/10.1016/j.watres.2017.03.018>
- Kotaś, J., Stasicka, Z., 2000. Chromium occurrence in the environment and methods of its speciation. *Environ. Pollut.* 107, 263–283. [https://doi.org/10.1016/S0269-7491\(99\)00168-2](https://doi.org/10.1016/S0269-7491(99)00168-2)
- Lai, H., McNeill, L.S., 2006. Chromium Redox Chemistry in Drinking Water Systems. *J. Environ. Eng.* 132, 842–851. [https://doi.org/10.1061/\(ASCE\)0733-9372\(2006\)132:8\(842\)](https://doi.org/10.1061/(ASCE)0733-9372(2006)132:8(842))

- Langmuir, D., 1978. Uranium solution-mineral equilibria at low temperatures with applications to sedimentary ore deposits. *Geochim. Cosmochim. Acta* 42, 547–569.
[https://doi.org/10.1016/0016-7037\(78\)90001-7](https://doi.org/10.1016/0016-7037(78)90001-7)
- Lee, G., Hering, J.G., 2003. Removal of chromium(VI) from drinking water by redox-assisted coagulation with iron(II). *J. Water Supply Res. Technol. - Aqua* 52, 319–332.
- Levenstein, R., Hasson, D., Semiat, R., 1996. Utilization of the Donnan effect for improving electrolyte separation with nanofiltration membranes. *J. Memb. Sci.* 116, 77–92.
[https://doi.org/10.1016/0376-7388\(96\)00029-4](https://doi.org/10.1016/0376-7388(96)00029-4)
- Li, X., Green, P.G., Seidel, C., Gorman, C., Darby, J.L., 2016a. Meeting California's Hexavalent Chromium MCL of 10 ug / L using Strong Base Anion Exchange Resin. *J. Am. Water Works Assoc.* E474–E481.
- Li, X., Green, P.G., Seidel, C., Gorman, C., Darby, J.L., 2016b. Chromium Removal From Strong Base Anion Exchange Waste Brines. *J. Am. Water Works Assoc.* 108, 247–255.
- Luo, J., Wan, Y., 2011. Effect of highly concentrated salt on retention of organic solutes by nanofiltration polymeric membranes. *J. Memb. Sci.* 372, 145–153.
<https://doi.org/10.1016/j.memsci.2011.01.066>
- Madaeni, S.S., Kazemi, V., 2008. Treatment of saturated brine in chlor-alkali process using membranes. *Sep. Purif. Technol.* 61, 68–74. <https://doi.org/10.1016/j.seppur.2007.09.028>
- Mathews, T.J., Looney, B.B., Bryan, A.L., Smith, J.G., Miller, C.L., Southworth, G.R., Peterson, M.J., 2015. The effects of a stannous chloride-based water treatment system in a mercury contaminated stream. *Chemosphere* 138, 190–196.
<https://doi.org/10.1016/J.CHEMOSPHERE.2015.05.083>
- McGuire, M.J., Blute, N.K., Seidel, C., Qin, G., Fong, L., 2006. Pilot Scale Studies of Hexavalent Chromium Removal from Drinking Water. *J. Am. Water Works Assoc.* 98, 134–143.
- McNeill, L., McLean, J., Edwards, M., Parks, J., 2013. Trace Level Hexavalent Chromium Occurrence and Analysis, Water Research Foundation, Project No. 4404. Water Research Foundation, Project #4404, Denver, CO.
- McNeill, L.S., McLean, J.E., Parks, J.L., Edwards, M., 2012. Hexavalent chromium review, part 2: Chemistry, occurrence, and treatment. *J. Am. Water Works Assoc.* 104, 39–40.
- MDH, 2017. Human Health-Based Water Guidance Table [WWW Document]. URL <http://www.health.state.mn.us> (accessed 8.7.17).
- Meadows, D.M., Wadley, S., Buckley, C.A., 1992. Evaluation of Nanofiltration for the Recovery of Brine from Sugar Liquor Decolourising Resin Regeneration Waste. *Water Sci. Technol.* 25, 339–350.

- Nghiem, L.D., Hawkes, S., 2007. Effects of membrane fouling on the nanofiltration of pharmaceutically active compounds (PhACs): Mechanisms and role of membrane pore size. *Sep. Purification Technol.* 57, 176–184.
- NSF/ANSI, 2017. NSF/ANSI 60: Drinking Water Treatment Chemicals – Health Effects [WWW Document]. URL www.nsf.org (accessed 8.7.17).
- Pakzadeh, B., Batista, J.R., 2011. Chromium removal from ion-exchange waste brines with calcium polysulfide. *Water Res.* 45, 3055–3064. <https://doi.org/10.1016/j.watres.2011.03.006>
- Paugam, L., Diawara, C.K., Schlumpf, J.P., Jaouen, P., Quéméneur, F., 2004a. Transfer of monovalent anions and nitrates especially through nanofiltration membranes in brackish water conditions. *Sep. Purif. Technol. Purif. Technol.* 40, 237–242. <https://doi.org/10.1016/j.seppur.2004.02.012>
- Paugam, L., Taha, S., Dorange, G., Jaouen, P., Quéméneur, F., 2004b. Mechanism of nitrate ions transfer in nanofiltration depending on pressure, pH, concentration and medium composition. *J. Memb. Sci.* 231, 37–46. <https://doi.org/10.1016/j.memsci.2003.11.003>
- Peeters, J.M.M., Mulder, M.H. V, Strathmann, H., 1999. Streaming potential measurements as a characterization method for nanofiltration membranes. *Colloids Surface. A Physicochem. Eng. Asp.* 150, 247–259.
- Perry, M., Linder, C., 1989. Intermediate reverse osmosis ultrafiltration (RO UF) membranes for concentration and desalting of low molecular weight organic solutes. *Desalination* 71, 233–245. [https://doi.org/10.1016/0011-9164\(89\)85026-X](https://doi.org/10.1016/0011-9164(89)85026-X)
- Pinakidou, F., Kaprara, E., Katsikini, M., Paloura, E.C., Simeonidis, K., Mitrakas, M., 2016. Sn(II) oxy-hydroxides as potential adsorbents for Cr(VI)-uptake from drinking water: An X-ray absorption study. *Sci. Total Environ.* 551–552, 246–253. <https://doi.org/10.1016/J.SCITOTENV.2016.01.208>
- Qin, G., McGuire, M., Blute, N., Seidel, C., Fong, L., 2005. Hexavalent Chromium Removal by Reduction with Ferrous Sulfate, Coagulation, and Filtration: A Pilot-Scale Study. *Environ. Sci. Technol.* 39, 6321–6327. <https://doi.org/10.1021/ES050486P>
- Rai, D., Eary, L.E., Zachara, J.M., 1989. Environmental chemistry of chromium. *Sci. Total Environ.* 86, 15–23. [https://doi.org/10.1016/0048-9697\(89\)90189-7](https://doi.org/10.1016/0048-9697(89)90189-7)
- Rai, D., Sass, B.M., Moore, D.A., 1987. Chromium(III) hydrolysis constants and solubility of chromium(III) hydroxide. *Inorg. Chem.* 26, 345–349. <https://doi.org/10.1021/ic00250a002>
- Rautenbach, R., Gröschl, A., 1990. Separation potential of nanofiltration membranes. *Desalination* 77, 73–84. [https://doi.org/10.1016/0011-9164\(90\)85021-2](https://doi.org/10.1016/0011-9164(90)85021-2)
- Rice, N.M., 1983. Commercial Processes for Chromium and Vanadium, in: Lo, T.C., Baird, M.H.I., Hanson, C. (Eds.), *Handbook of Solvent Extraction*. John Wiley & Sons, Inc., pp.

697–707.

- Salehi, F., Razavi, S.M.A., Elahi, M., 2011. Purifying anion exchange resin regeneration effluent using polyamide nanofiltration membrane. *Desalination* 278, 31–35. <https://doi.org/10.1016/j.desal.2011.04.067>
- Santafé-Moros, A., Gozávez-Zafrilla, J.M., Lora-García, J., 2007. Nitrate removal from ternary ionic solutions by a tight nanofiltration membrane. *Desalination* 204, 63–71. <https://doi.org/10.1016/j.desal.2006.04.024>
- Seidel, C., Corwin, C., 2013. Total chromium and hexavalent chromium occurrence analysis. *J. Am. Water Works Assoc.* 105, 37–38. <https://doi.org/10.5942/jawwa.2013.105.0050>
- Seidel, C., Gorman, C., Ghosh, A., Dufour, T., Mead, C., Henderson, J., Li, X., Darby, J., Green, P., McNeill, L., Clifford, D., 2014. Hexavalent Chromium Treatment with Strong Base Anion Exchange, Water Research Foundation, Project No. 4488. Denver, CO.
- Seidel, C., Najm, I.N., Blute, N.K., Corwin, C.J., Wu, X., 2013. National and California treatment costs to comply with potential hexavalent chromium MCLs. *J. Am. Water Works Assoc.* 105, 39–40. <https://doi.org/10.5942/jawwa.2013.105.0080>
- Sengupta, A.K., 1995. Chromate Ion Exchange, in: *Ion Exchange Technology*. pp. 115–147.
- Sengupta, A.K., 1988. A unified approach to interpret unusual observations in heterogeneous ion exchange. *J. Colloid Interface Sci.* 123, 201–215. [https://doi.org/10.1016/0021-9797\(88\)90236-6](https://doi.org/10.1016/0021-9797(88)90236-6)
- Sengupta, A.K., 1986. Anomalous Ion-Exchange Characteristics of Some Polynuclear Metal Ions. *J. Chromatogr.* 368, 319–328.
- Sengupta, A.K., Clifford, D., 1986a. Important process variables in chromate ion exchange. *Environ. Sci. Technol.* 20, 149–55. <https://doi.org/10.1021/es00144a006>
- Sengupta, A.K., Clifford, D., 1986b. Chromate Ion Exchange Mechanism for Cooling Water. *Ind. Eng. Chem. Fundam.* 25, 249–258.
- Sengupta, A.K., Roy, T., Jessen, D., 1988. Modified Anion-Exchange Resins for Improved Chromate Selectivity and Increased Efficiency of Regeneration. *React. Polym.* 9, 293–299.
- Streat, M., Naden, D., 1987. Ion Exchange in Uranium Extraction, in: Streat, M., Naden, D. (Eds.), *Ion Exchange and Sorption Processes in Hydrometallurgy*. John Wiley & Sons, Inc., pp. 1–56.
- Subramonian, S., Clifford, D., 1988. Monovalent/Divalent Selectivity and the Charge Separation Concept. *React. Polym.* 9, 195–209.
- Summers, R.S., Hooper, S.M., Shukairy, H.M., Solarik, G., Owen, D., 1996. Assessing DBP

- yield: uniform formation conditions. *J. - Am. Water Work. Assoc.* 88, 80.
- Superior Court of California - County of Sacramento, 2017. California Manufacturers and Technology Association and Solano County Taxpayers Association v. State Water Resources Control Board.
- SWRCB, 2017. Announcements: Maximum Contaminant Level for Hexavalent Chromium – Court’s Judgment Invalidating MCL [WWW Document]. Calif. Environ. Prot. Agency, State Water Resour. Control Board. URL www.waterboards.ca.gov (accessed 7.8.17).
- Tansel, B., Sager, J., Rector, T., Garland, J., Strayer, R.F., Levine, L., Roberts, M., Hummerick, M., Bauer, J., 2006. Significance of hydrated radius and hydration shells on ionic permeability during nanofiltration in dead end and cross flow modes. *Sep. Purif. Technol.* 51, 40–47. <https://doi.org/10.1016/j.seppur.2005.12.020>
- Thurman, E.M., 1985. *Organic Geochemistry of Natural Waters*. Martinus Nijhoff/Dr. W. Junk Publishers, Dordrecht.
- Tsuru, T., Urairi, M., Nakao, S., Kimura, S., 1991. Negative rejection of anions in the loose reverse osmosis separation of mono- and divalent ion mixtures. *Desalination* 81, 219–227. [https://doi.org/10.1016/0011-9164\(91\)85055-Y](https://doi.org/10.1016/0011-9164(91)85055-Y)
- UL, 2017. Online Certifications Directory [WWW Document]. URL www.ul.com (accessed 7.8.17).
- USEPA, 2014. Integrated Risk Information System Toxicological Review of Hexavalent Chromium Part 2: Human, Toxicokinetic, and Mechanistic Studies (Preliminary Assessment Materials). Washington, D.C.
- USNLM, 2017. Toxicology Data Network: Stannous Chloride [WWW Document]. URL www.toxnet.nlm.nih.gov (accessed 7.8.17).
- Waite, M., 2015. Regeneration of an Ion Exchange Column. US Patent Application US 2015/0375222 A1.
- Wang, K.Y., Chung, T.-S.S., 2006. Fabrication of polybenzimidazole (PBI) nanofiltration hollow fiber membranes for removal of chromate. *J. Memb. Sci.* 281, 307–315. <https://doi.org/10.1016/j.memsci.2006.03.045>
- Wang, K.Y., Chung, T.S., Rajagopalan, R., 2007. Novel polybenzimidazole (PBI) nanofiltration membranes for the separation of sulfate and chromate from high alkalinity brine to facilitate the chlor-alkali process. *Ind. Eng. Chem. Res.* 46, 1572–1577. <https://doi.org/10.1021/ie061435j>
- Wang, X.-L., Tsuru, T., Nakao, S., Kimura, S., 1997. The electrostatic and steric-hindrance model for the transport of charged solutes through nanofiltration membranes. *J. Memb. Sci.* 135, 19–32. [https://doi.org/10.1016/S0376-7388\(97\)00125-7](https://doi.org/10.1016/S0376-7388(97)00125-7)

- White, A.F., Dubrovsky, N.M., 1994. Chemical Oxidation-Reduction Controls on Selenium Mobility in Groundwater Systems, in: *Selenium in the Environment*. CRC Press, p. 480.
- Wright, M.T., Stollenwerk, K.G., Belitz, K., 2014. Assessing the solubility controls on vanadium in groundwater, northeastern San Joaquin Valley, CA. *Appl. Geochemistry* 48, 41–52. <https://doi.org/10.1016/j.apgeochem.2014.06.025>
- Wu, X., Blute, N., Pierce, M., Santos, M., Chau, K., Rodriguez, D., Cron, C., Hutton, D., Fong, L., Froelich, D., Chan, L., De Ghetto, M., 2015. *Enhanced Reduction / Coagulation / Filtration Testing for Removing Hexavalent Chromium*, Hazen and Sawyer. Glendale, CA.
- Yaroshchuk, A.E., 2001. Non-steric mechanism of nanofiltration: Superposition of donnan and dielectric exclusion. *Sep. Purif. Technol.* 22–23, 143–158. [https://doi.org/10.1016/S1383-5866\(00\)00159-3](https://doi.org/10.1016/S1383-5866(00)00159-3)
- Yoon, J., Amy, G., Chung, J., Sohn, J., Yoon, Y., 2009. Removal of toxic ions (chromate, arsenate, and perchlorate) using reverse osmosis, nanofiltration, and ultrafiltration membranes. *Chemosphere* 77, 228–235. <https://doi.org/10.1016/j.chemosphere.2009.07.028>
- Zhang, Z., Clifford, D., 1994. Exhausting and regenerating resin for uranium removal. *J. Am. Water Works Assoc.* 86, 228–241.

Appendix A — Regeneration Supplemental Information

Regeneration Mass Balances

Column Depth Profiles for Key Constituents

Aliquots (~10 mL) of resin sampled from the top, middle and bottom third of the column were regenerated in separate batches to determine the spatial distribution of constituents throughout the column. Samples were analyzed to determine the relative distribution of key constituents (Table A 1) relative to the total number of active sites on the resin to facilitate a mass balance across the system for comparison in subsequent sections. All concentrations were compared on an equivalents basis taking into account the valence and oxidation state of each anion as described in the main text.

Compared to the total active sites on the resin, sulfate was the most abundant anion accounting for 48% of total equivalent sites on average followed by bicarbonate (16%) and nitrate (7.3%) as summarized in Table A 1. Chromium accounted for 3.1% of the total equivalents eluted from the resin. Vanadium only accounted for 0.12% of equivalents recovered. Elution of vanadium may not have been complete. Selenium and arsenic were present at trace levels in the regeneration brine compared to other constituents. With the exception of uranium, all constituents were evenly distributed along the length of the column. Uranium was enriched at the top of the column (0.5%) but only present at trace amounts at lower depths. Uranium was not detected above the detection limit (1 pCi/L, ~1.4 µg/L) in the raw water, but trace levels were present and exchanging with the resin. The enrichment found only at the top of the column attests to the slow progression of the uranium mass transfer zone within the column limited by the low raw water uranium concentration coupled with the high affinity for resin active sites. Even though influent iron was below detection limits, iron fouling was visible in the upper 4-6 inches of the columns indicated by red discoloration and lower total exchange capacity (69%± 6.8%) compared to the bottom of the column (78% ± 1.8%). Some iron (60-120 mg) was recovered when columns were regenerated with HCl. The combination of these results demonstrate that when the strong base anion exchange column is exhausted with respect to chromium, the majority of the exchanged constituents are sulfate, bicarbonate and nitrate with other constituents present at an order of magnitude lower concentrations.

Table A 1. Distribution of Anionic Equivalents relative to total resin capacity for regenerations R1 and R3 (Average ± Standard Deviation, n=2)

Anion	Top	Middle	Bottom	Average
Sulfate (SO ₄ ²⁻)	42.7% ± 6.7%	49.2% ± 2.4%	51.7% ± 0.3%	47.9% ± 5.2%
Nitrate (NO ₃ ⁻)	6.5% ± 0.7%	7.6% ± 0.130%	7.7% ± 0.4%	7.3% ± 0.68%
Bicarbonate (HCO ₃ ⁻)	16.3% ± 0%	15.6% ± 0.9%	15% ± 1.8%	15.6% ± 1.0%
Chromate (CrO ₄ ²⁻)	2.7% ± 0.4%	3.4% ± 0.048%	3.3% ± 0.009%	3.1% ± 0.4%
Vanadate (H ₂ VO ₄ ⁻)	0.1% ± <0.001%	0.1% ± <0.001%	0.1% ± 0.001%	0.12% ± 0.010%
Uranium Complex (UO ₂ (CO ₃) ₃ ⁴⁻)	0.5% ± 0.3%	0.003% ± <0.001%	0.008% ± 0.010%	0.09% ± 0.048%
Selenate (SeO ₄ ²⁻)	0.006% ± <0.001%	0.006% ± 0.002%	0.006% ± <0.001%	0.006% ± 0.001%
Arsenate (HAsO ₄ ²⁻)	0.006% ± 0.001%	0.007% ± <0.001%	0.007% ± <0.001%	0.007% ± 0.0004%
Molybdate (MoO ₄ ²⁻)	0.183% ± 0.028%	0.228% ± 0.007%	0.227% ± 0.004%	0.005% ± 0.0030%
Total	69% ± 6.8%	76% ± 2.5%	78% ± 1.8%	

1-Stage DI Regeneration (R1)

The number of active sites occupied with anions other than chloride before regeneration was determined by comparing the breakthrough of sodium (conservative tracer) and chloride, which exchanged with the resin. Chloride breakthrough is complete at 2.5 BV_{avg}, approximately 1 BV after sodium breakthrough. Integrating the area under the sodium curve up to 2.5 BV_{avg}, 7.0 equivalents of sodium eluted from the column. Comparing the same area for chloride, 4.5 equivalents of chloride eluted. The difference between equivalents of chloride and sodium eluted was 2.5 equivalents, which corresponds to the exchange of chloride onto the resin (Figure 2.2b). Using the resin bed volume (2 L) and resin capacity (1.6 eq/L) along with the integrated area between chloride and sodium, 79% of the resin sites were exchanged during the 1-Stage DI regeneration process. This mass balance was verified by calculating cumulative equivalents of all anionic constituents other than Cl in the elution profile (i.e., sulfate, bicarbonate, nitrate, chromate, etc.). The relative percent difference (difference divided by average) between both approaches was 3%. These results demonstrate that the constituents selected for measurement in Table S-2 are representative of the principal constituents present on fully loaded resin (with respect to Cr(VI)) prior to a regeneration. Other typical water anionic constituents, such as phosphate or NOM, are present at negligible concentrations compared to the overall system mass balance. This data demonstrates that at chromium exhaustion, about 21% of the active sites on the resin are still in the chloride form.

2-Stage DI (R3)

Performing a mass balance on the cumulative elution of sodium and chloride at 7.26 BV_{avg}, 2.1 eq of chloride exchanged with the resin, representing 65% of the total resin capacity. During the subsequent 2 N Stage, an additional 0.5 eq of chloride exchanged with the resin, corresponding to an additional 16% of the total resin capacity. At the end of the 2-Stage regeneration process, 81% of the total resin capacity was exchanged with chloride, which correlates well with the exchanged capacity of the 1-Stage regeneration process. A mass balance on eluting anions other than chloride (e.g., sulfate, bicarbonate, nitrate, chromate, etc.) agreed with the loss of chloride (RPD = 1%). These results confirm that the suite of anions measured in the effluent account for the exchanged chloride, and any other anions (NOM, phosphate, etc.) were present in trace amounts.

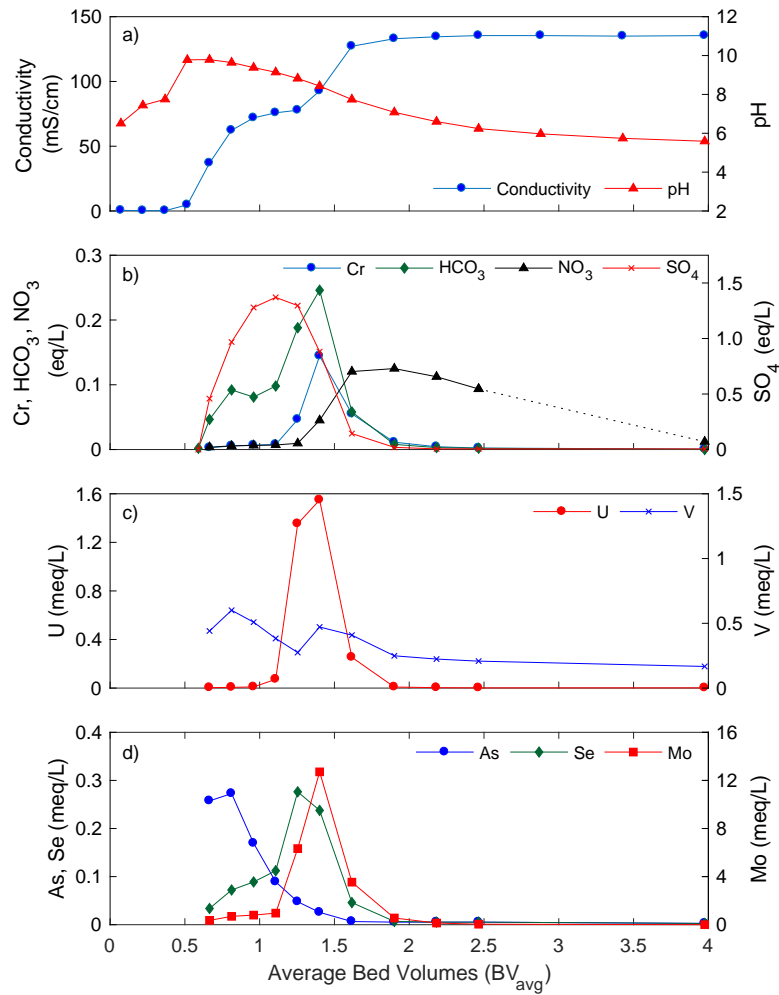


Figure A 1. Elution chromatogram for 1-stage UI regeneration (κ_1) showing a) conductivity and pH, b) chromium, bicarbonate, nitrate and sulfate, c) uranium and vanadium, and d) arsenic, selenium and molybdenum concentration. Only concentrations above the method reporting limit are shown. Dashed line indicates non-consecutive brine fractions analyzed.

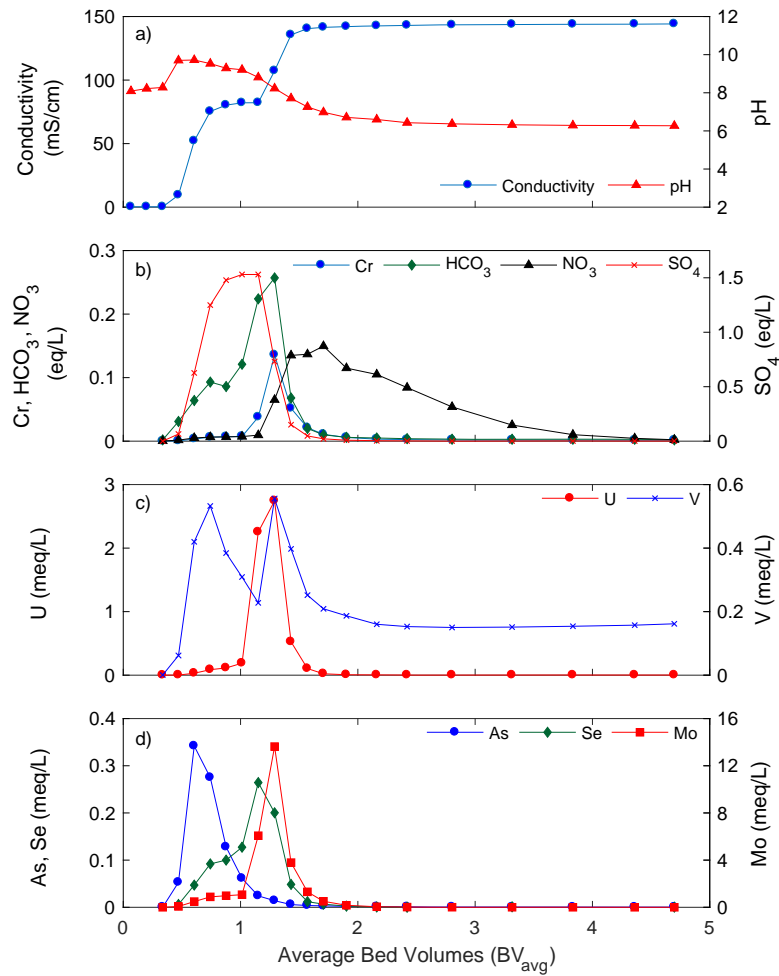


Figure A 2. Elution chromatograph for 1-Stage GW regeneration (R4) showing a) conductivity and pH, b) chromium, bicarbonate, nitrate and sulfate, c) uranium and vanadium, and d) arsenic, selenium and molybdenum concentration. Only concentrations above the method reporting limit are shown.

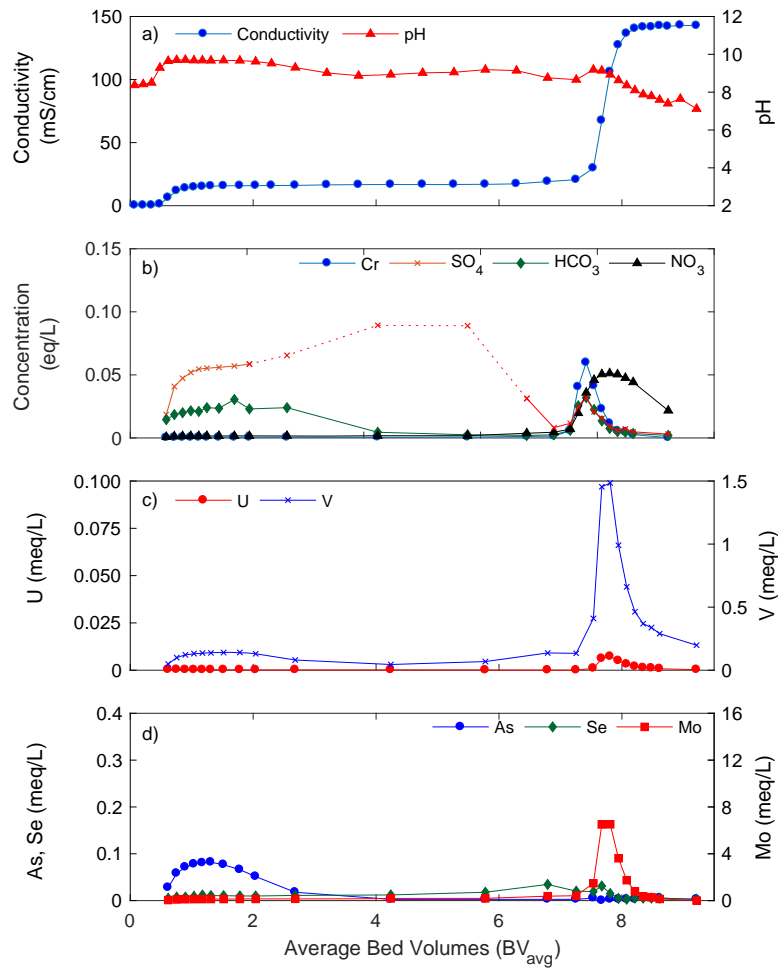


Figure A 3. Elution profiles for a) conductivity and pH, b) chromium, bicarbonate, nitrate and sulfate, c) uranium and vanadium, and d) arsenic, selenium and molybdenum concentration. Uranium concentrations below the MRL are plotted at MRL.

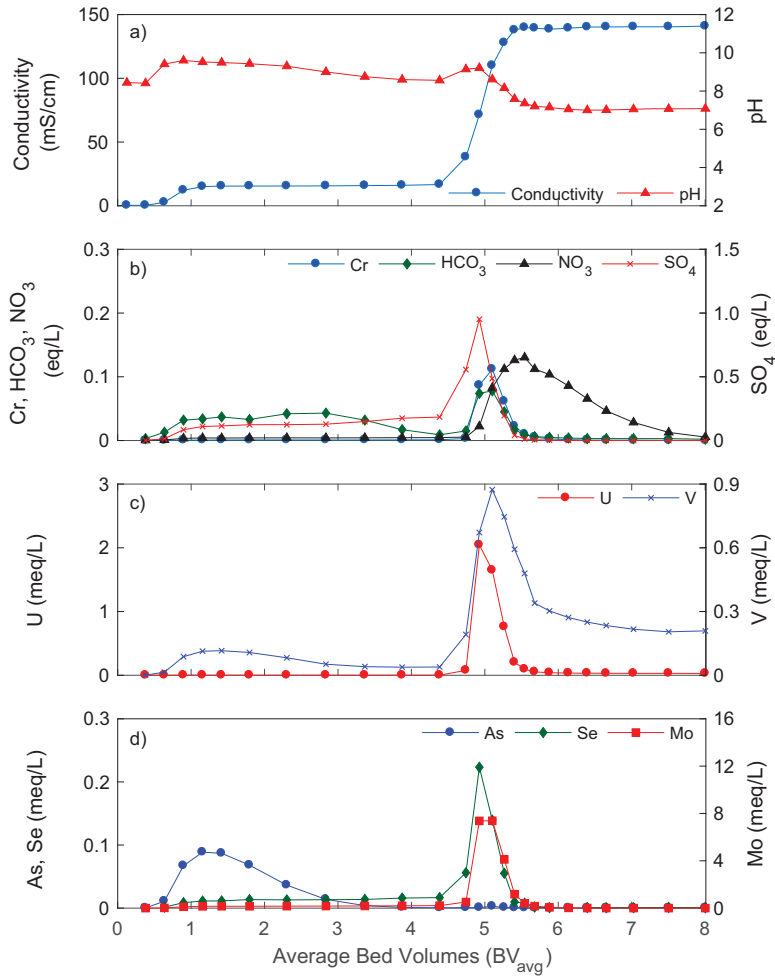


Figure A 4. Elution chromatograph for 2-Stage GW regeneration (R6) showing a) conductivity and pH, b) chromium, bicarbonate, nitrate and sulfate, c) uranium and vanadium, and d) arsenic, selenium and molybdenum concentration. Uranium concentrations below the MRL are plotted at MRL.

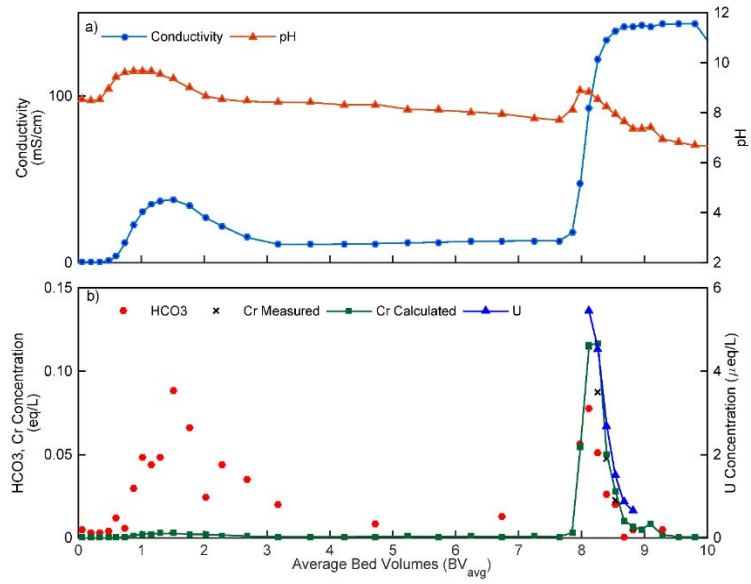


Figure A 5. Elution chromatograph for 2-Stage regeneration (R2) approach with a 0.8 N Stage followed by 0.1 N Stage and 2 N Stage presenting a) conductivity and pH, b) chromium, uranium and bicarbonate concentration. Calculated chromium concentrations are based on absorbance at 375 nm with measured verification samples.

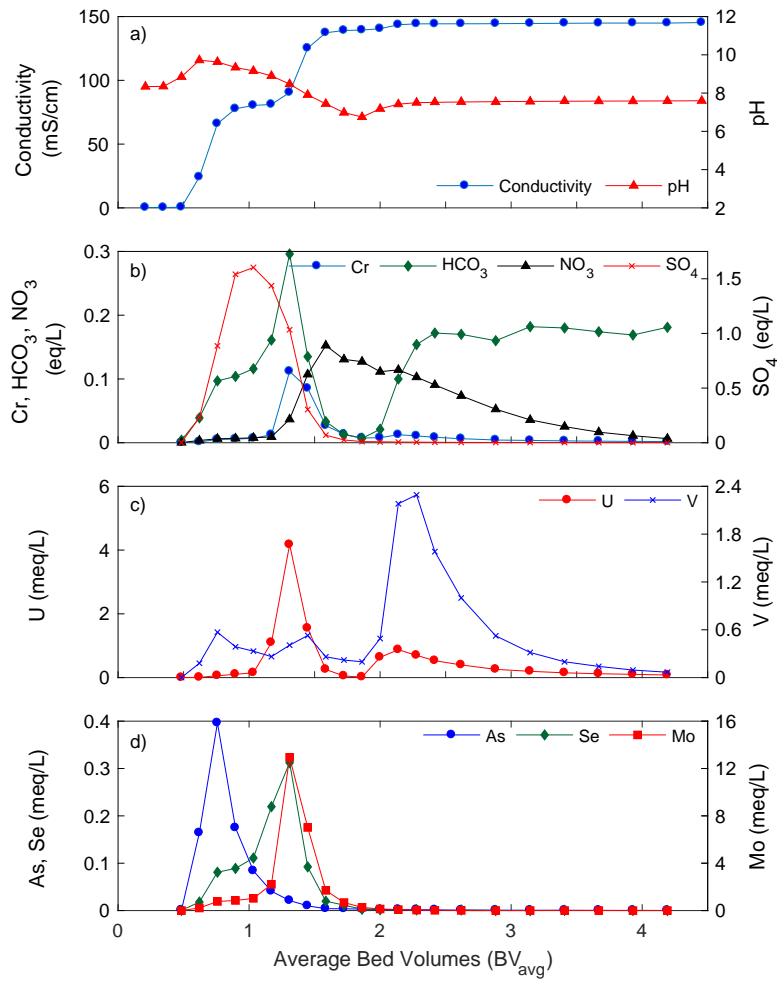


Figure A 6. Elution chromatograph for NaCl/NaHCO₃ regeneration (R5) showing a) conductivity and pH, b) chromium, bicarbonate, nitrate and sulfate, c) uranium and vanadium, and d) arsenic, selenium and molybdenum concentration.

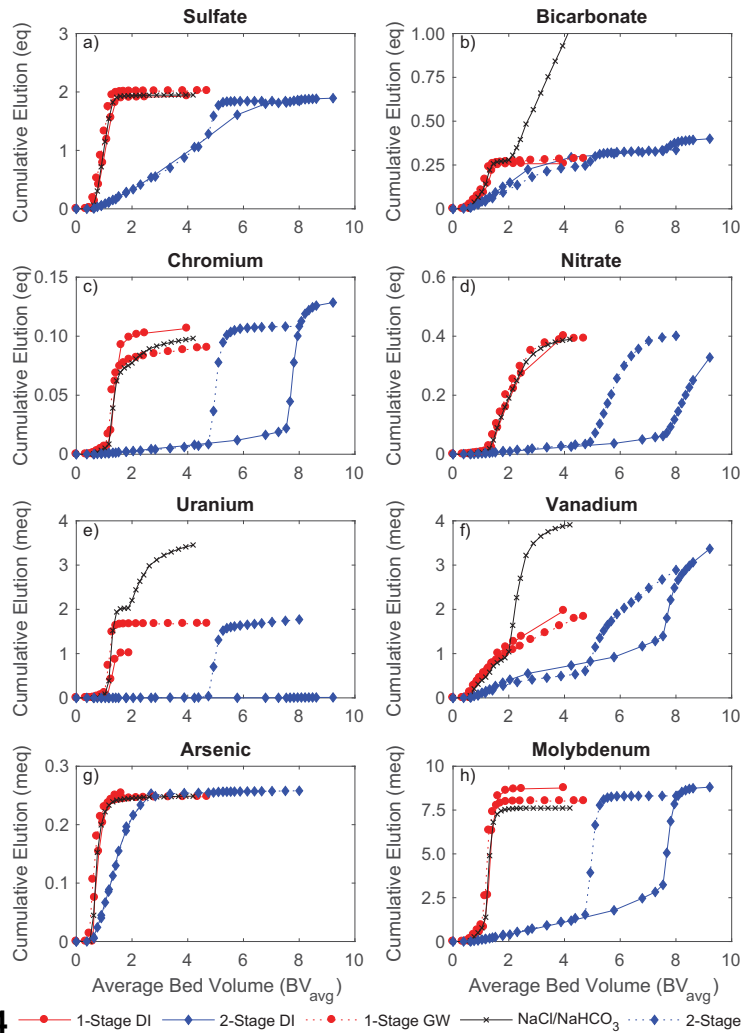


Figure A 7. Cumulative mass eluted as a function of regeneration bed volume for a) bicarbonate, b) nitrate, c) vanadium, d) molybdenum, e) arsenic and f) selenium.

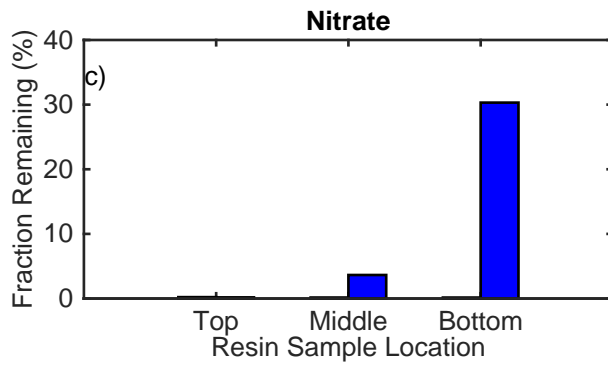
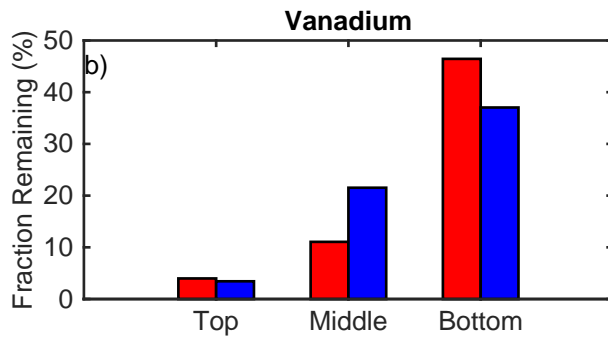
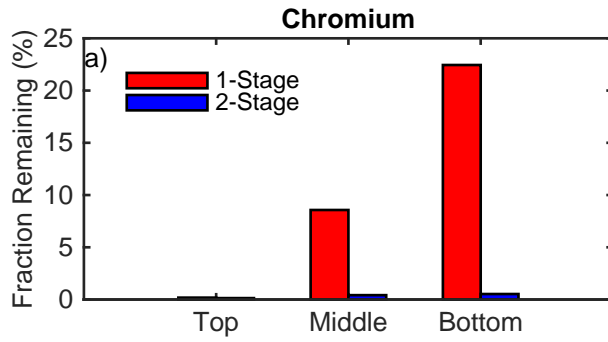


Figure A 8. Fraction of cc compared to pre-regener

**le (R1 and R3)
l c) nitrate.**

Table A 2. Cumulative elution of chromium, vanadium and uranium during regeneration for both loading cycles and during the acid wash after the second regeneration cycle. Cumulative elution values are separated by stage for the 2-Stage approaches (R3 and R6).

Background Water	Regen. Number	Approach	Stage	Cumulative Elution (meq)						Fraction Removed by Acid Wash ⁽¹⁾	
				Regeneration			Acid Wash			V	U
				Cr	V	U	Cr	V	U		
DI	R1	1-Stage DI	--	107	2.0	1.0	--	--	--	--	--
	R3	2-Stage DI	0.2 N	19	1.3	0.002	--	--	--	--	--
			2.0 N	110	2.1	0.008	--	--	--	--	--
			Total	129	3.4	0.010	--	--	--	--	--
Softened Well Water	R4	1-Stage GW	--	101	3.0	1.7	4.3	1.1	0.93	26%	35%
	R5	NaCl/NaHCO ₃	--	99	3.9	3.5	4.4	0.45	0.14	10%	4%
	R6	2-Stage GW	0.2 N	7.2	0.53	0.008	--	--	--	--	--
			2.0 N	101	2.5	1.8	--	--	--	--	--
			Total	109	3.1	1.8	1.7	1.3	1.3	29%	42%

Cumulative elution values are the total observed elution for the regenerations as shown in the Figures S-2 to S-7. Operational criteria to define waste fraction not applied.
⁽¹⁾Calculated as the mass of each element eluted during acid wash relative to the total mass eluted during both regeneration and acid wash

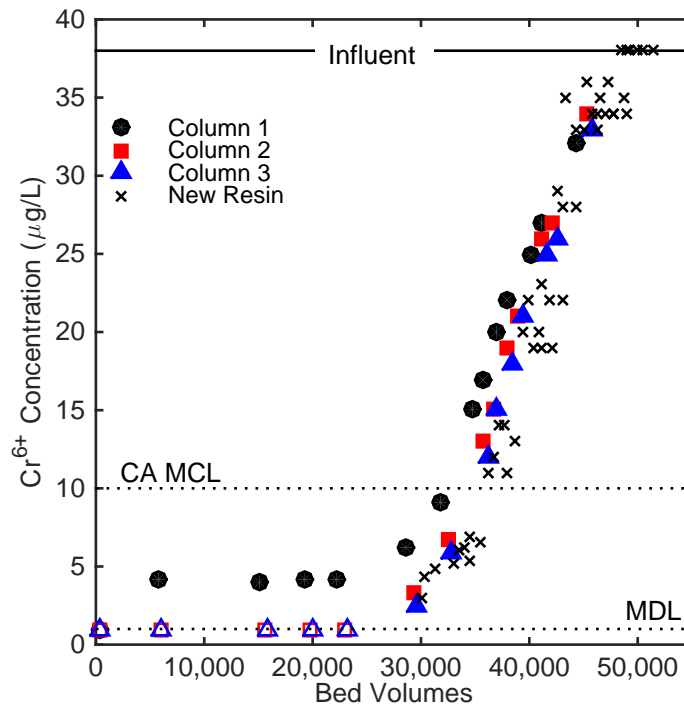


Figure A 9. Cr(VI) breakthrough during second loading cycle for columns subjected to different regeneration processes. Samples from first loading cycle indicated as New Resin.

Appendix B —Stannous Chloride Supplemental Information

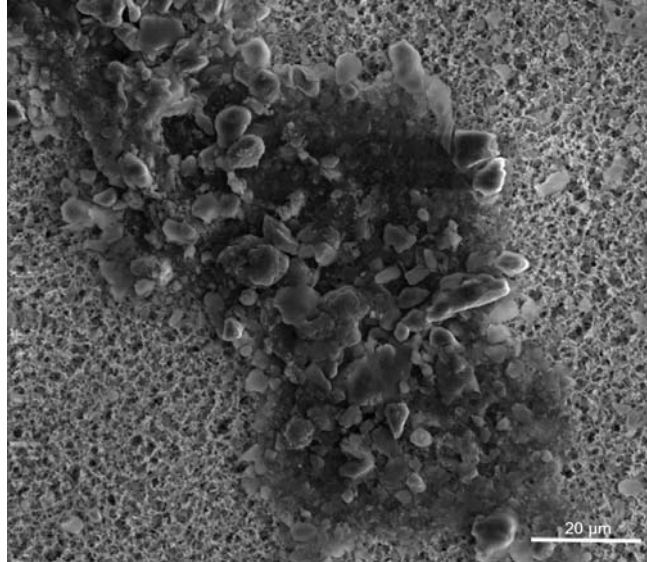


Figure B 1. SEM image of 0.45 µm filter used to filter raw OK.

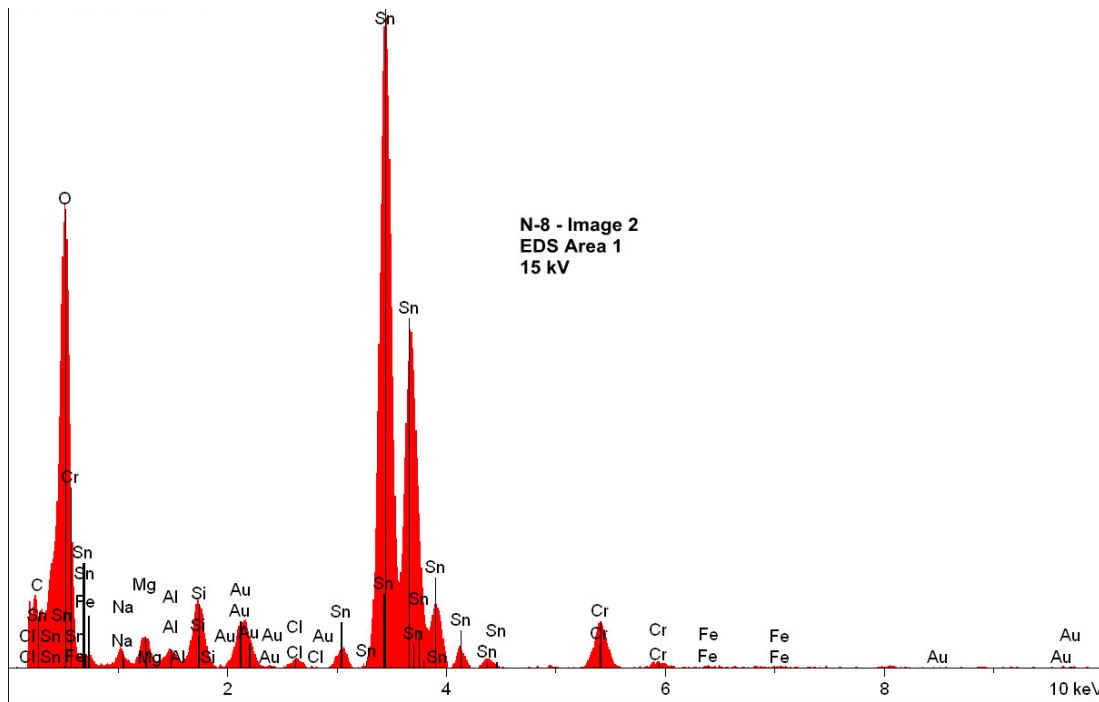


Figure B 2. EDS spectrum for solids depicted in Figure 4b and 4c in main manuscript.



Figure B 3. Cutout of a 20 µm PCF filter after testing with OK.



Figure B 4. Cutout of a 5 µm DCF filter after testing with CA-1.

Data Sets that Support the Final Report

Data files for the work completed at Joshua Basin Water District are located in the following folder:

Q:\Civil Engineering\8190\8190 Projects - Research (-)\Chrome (X9085 and FA280) - 2015-2018 (Arias-Paic)\

Data files for the stannous chloride work completed in Norman, Oklahoma are located in the following folder:

Q:\Civil Engineering\8190\8190 Projects - Research (-)\Norman Chromium - 2016 - (Arias-Paic)\

Point of contact: Miguel Arias-Paic, Ph.D., P.E., mariaspaic@usbr.gov, 303-445-2132